

**UNIVERSITY OF CRETE
DEPARTMENT OF CHEMISTRY**

**ISOLATION AND SYNTHESIS OF NATURAL PRODUCTS
WITH BIOLOGICAL ACTIVITY**



MASTER THESIS

**Design and Development of Innovative Nanoporous Covalent
Organic Frameworks**

BOSVELI D. ARTEMIS

**Master Thesis Supervisor:
Prof. Pantelis N. Trikalitis**

HERAKLION 2019

**ΠΑΝΕΠΙΣΤΗΜΙΟ ΚΡΗΤΗΣ
ΤΜΗΜΑ ΧΗΜΕΙΑΣ**

**ΑΠΟΜΟΝΩΣΗ ΚΑΙ ΣΥΝΘΕΣΗ ΦΥΣΙΚΩΝ ΠΡΟΙΟΝΤΩΝ ΜΕ
ΒΙΟΛΟΓΙΚΗ ΔΡΑΣΤΙΚΟΤΗΤΑ**



ΜΕΤΑΠΤΥΧΙΑΚΟ ΔΙΠΛΩΜΑ ΕΙΔΙΚΕΥΣΗΣ

**Σχεδιασμός και Ανάπτυξη Καινοτόμων Νανοπορωδών
Ομοιοπολικών Οργανικών Σκελετών**

ΜΠΟΣΒΕΛΗ Δ. ΑΡΤΕΜΙΣ

**Υπεύθυνος Καθηγητής:
Παντελής Ν. Τρικαλίτης**

ΗΡΑΚΛΕΙΟ 2019

*Στην μνήμη του πολυαγαπημένου μου
θείου Γιάννη*

THESIS COMMITTEE

Dr. Pantelis N. Trikalitis (Supervisor)

Professor, Department of Chemistry, University of Crete

Dr. Georgios E. Vassilikogiannakis

Professor, Department of Chemistry, University of Crete

Dr. Manolis Stratakis

Professor, Department of Chemistry, University of Crete

Ευχαριστίες

Η παρούσα εργασία εκπονήθηκε στο Εργαστήριο Χημείας Υλικών, του τομέα της Ανόργανης Χημείας του Τμήματος Χημείας του Πανεπιστημίου Κρήτης κατά τη χρονική περίοδο 2017-2019 στα πλαίσια του Προγράμματος Μεταπτυχιακών Σπουδών, Απομόνωσης και Σύνθεσης Φυσικών Προϊόντων με Βιολογική Δραστικότητα (ΑΣΦΔ).

Αρχικά θα ήθελα να ευχαριστήσω τον καθηγητή μου Παντελή Τρικαλίτη για το ενθαρρυντικό του πνεύμα, την εμπιστοσύνη που μου έδειξε και την αμείωτη προσπάθειά του για τη μετάδοση γνώσεων. Η συνεργασία μας ήταν εξαιρετικά εποικοδομητική και το ενδιαφέρον του για την πρόοδό μου συνεχόμενο.

Επίσης θα ήθελα να ευχαριστήσω θερμά τον καθηγητή κ. Στρατάκη και τον καθηγητή κ. Βασιλικογιαννάκη, που δεχτήκαν να γίνουν μέλη της επιτροπής αξιολόγησής μου και για το χρόνο που αφιέρωσαν στην διατριβή μου.

Επιπρόσθετα, θα ήθελα να ευχαριστήσω την Δρ. Γιασεμή Αγγελή και την μεταπτυχιακή φοιτήτρια Δανάη Μπατζάβαλη για την συνεργασία μας καθ' όλη την διάρκεια διεξαγωγής των πειραματικών διαδικασιών και όλους τους προπτυχιακούς φοιτητές του εργαστηρίου μας και ιδιαίτερα τον Νικόλα Γιακουμάκη και την Κατερίνα Μαυρονάσου και ιδιαίτερα τον προπτυχιακό φοιτητή Κωστή Φρουδά με τον οποίο δούλεψα μαζί στο μεγαλύτερο μέρος της διατριβής μου.

Τέλος θα ήθελα να ευχαριστήσω τους γονείς μου Ελένη Δαμιανίδου και Μπόσβελι Δαμιανό για την πολύπλευρη στήριξή τους σε κάθε μου προσπάθεια και βήμα.

Curriculum Vitae

ARTEMIS BOSVELI

Date of Birth: 22/04/1994
Nationality: Greek
E-mail: artemis_mposveli@yahoo.gr

EDUCATION

09/2017 - Today **University of Crete, Department of Chemistry** **Heraklion, Crete**
Master's Degree in Isolation and Synthesis of Natural Products with Biological Activity

09/2012 – 07/2017 **Aristotle University of Thessaloniki, Department of Chemistry** **Thessaloniki, Greece**
Bachelor Degree in Chemistry

09/2009 – 07/2012 **2nd High School of Kavala** **Kavala, Greece**

RESEARCH EXPERIENCE

11/2017 – Today **Masters Degree in Isolation and Synthesis of Natural Products with Biological Activity, under the supervisor of Prof. Pantelis N. Trikalitis.**

- a) Synthesis and characterization of new organic ligands
- b) Synthesis of new, porous covalent organic frameworks (COFs)
- c) Structural characterization using state-of-the-art equipment including PXRD, TEM, SEM and TGA.
- d) Advanced gas-sorption studies using various gases at different temperatures.

10/2016 – 03/2017 **Student Internship in Bayer AG, Wuppertal, Germany**
Department of Pharmaceutical Chemistry and Organic Synthesis

10/2015 - 06/2016 Undergraduate Research Thesis at Department of Chemistry, Aristotle University of Thessaloniki, under the supervision of Assistant Professor G. Gallios. Thesis title: Electrochemical oxidation degradation of dyeing waste.

SEMINARS/SESSIONS/CONFERENCES

17-19/05/2019	21st Conference of Postgraduate Students Department of Chemistry, (Presentation)	Heraklion, Greece
06/2018	20th Conference of Postgraduate Students Department of Chemistry	Heraklion, Greece
06/2017	Sustainable Water Treatment and Energy Transition	
12-13/10/2015	2nd Workshop on Water and Soil Clean-up from Mixed Contaminants and Autumn School on Advanced Adsorption and Oxidation Techniques for the Removal of Xenobiotics	Thessaloniki, Greece
10/2013 –01/2014	Production of Medicinal Plants and Essential Oils Aristotle University of Thessaloniki	Thessaloniki, Greece

LANGUAGES

Greek: Mother language
English: Certificate of Proficiency **C2** – University of Michigan
German: Goethe-Zertifikat **B2**

SKILLS

ECDL- European Computer Driving Licence (Microsoft Office: Word, Excel, PowerPoint, Concepts of IT, Information and Communication)

Βιογραφικό Σημείωμα

ΑΡΤΕΜΙΣ ΜΠΟΣΒΕΛΗ

Ημερομηνία Γέννησης: 22 Απριλίου 1994
Εθνικότητα: Ελληνική
E-mail: artemis_mposveli@yahoo.gr

ΕΚΠΑΙΔΕΥΣΗ

09/2017 - Σήμερα **Πανεπιστήμιο Κρήτης** **Ηράκλειο, Ελλάδα**
Απομόνωση και Σύνθεση Φυσικών Προϊόντων με Βιολογική Δραστικότητα Μεταπτυχιακές Σπουδές,
Σχολή Θετικών Επιστημών, Τμήμα Χημείας

09/2012 – 07/2017 **Αριστοτέλειο Πανεπιστήμιο Θεσσαλονίκης, Bsc** **Θεσσαλονίκη, Ελλάδα**
Σχολή Θετικών Επιστημών, Τμήμα Χημείας

09/2009 – 07/2012 **2^ο Λύκειο Καβάλας** **Καβάλα, Ελλάδα**

ΕΡΕΥΝΗΤΙΚΗ/ΕΠΑΓΓΕΛΜΑΤΙΚΗ ΔΡΑΣΤΗΡΙΟΤΗΤΑ

11/2017 – Σήμερα **Μεταπτυχιακό Δίπλωμα Ειδίκευσης στο Πανεπιστήμιο Κρήτης, υπό την επίβλεψη του Καθηγητή κ. Παντελή Ν. Τρικαλίτη.**

- 1) Σύνθεση και χαρακτηρισμό νέων οργανικών υποκαταστατών
- 2) Σύνθεση νέων πορωδών οργανικών ομοιοπολικών σκελετών
- 3) Δομικός χαρακτηρισμός των υλικών χρησιμοποιώντας οργανολογία και μεθόδους αιχμής
- 4) Μελέτη προσρόφησης αερίων σε διάφορες θερμοκρασίες

10/2016 – 03/2017 **Πρακτική Άσκηση στην Bayer AG, Βούπερταλ, Γερμανίας**
Τμήμα Φαρμακευτικής Χημείας και Οργανικής Σύνθεσης

10/2015 - 06/2016 **Πτυχιακή εργασία στο Αριστοτέλειο Πανεπιστήμιο
Θεσσαλονίκης, υπό την επίβλεψη του κ. Γεώργιου Γάλλιου**
Αποικοδόμηση αποβλήτων βαφείου με ηλεκτροχημική οξείδωση.

ΣΕΜΙΝΑΡΙΑ/ΗΜΕΡΙΑΔΕΣ/ΣΥΝΕΔΡΙΑ

17-19/05/2019 **21^ο Συνέδριο Μεταπτυχιακών Φοιτητών Χημείας,** **Ηράκλειο,**
Ηράκλειο Κρήτης (Παρουσίαση) **Ελλάδα**

06/2018 **20^ο Συνέδριο Μεταπτυχιακών Φοιτητών** **Ηράκλειο,**
Χημείας, **Ελλάδα**
Ηράκλειο Κρήτης

06/2017 **Sustainable Water Treatment and Energy
Transition**

12-13/10/2015 **2nd Workshop on Water and Soil Clean-up from** **Θεσσαλονίκη,**
Mixed Contaminants and Autumn School on **Ελλάδα**
Advanced Adsorption and Oxidation Techniques
for the Removal of Xenobiotics

10/2013 –01/2014 **Παρακολούθηση Δια Βίου Προγράμματος** **Θεσσαλονίκη,**
Μάθησης του Αριστοτελείου Πανεπιστημίου, **Ελλάδα**
Παραγωγή Φαρμακευτικών Φυτών και Αιθέριων
Ελαίων

ΞΕΝΕΣ ΓΛΩΣΣΕΣ

Ελληνική Μητρική

Αγγλική Certificate of Proficiency **C2**– University
of Michigan

Γερμανική Goethe-Zertifikat **B2**

ΓΝΩΣΕΙΣ Η/Υ

ECDL- European Computer Driving Licence (Microsoft
Office: Word, Excel, PowerPoint, Concepts of IT,
Information and Communication)

Abstract

Covalent Organic Frameworks (COFs) are a novel class of crystalline porous materials that allows the atomically precise integration of organic units into extended structures with periodic skeletons and ordered nanopores. COF architectures offer confined molecular spaces for the interplay of photons, electrons, holes, ions and guest molecules, thereby exhibiting unique properties and functions, such as gas storage and separation.

The objective of this work was the design, synthesis and characterization of novel organic linkers and their successful implementation for the development of new porous organic materials. The targeted ligands were symmetric aldehydes and one hexagonal amine which were used for the synthesis of new imine-based COFs. In total five (5) new COFs were synthesized, presenting various topologies. In addition to the typical solvothermal reaction used for the development of COFs and for comparison purposes, we explored the use of aniline as a modulator at ambient conditions, towards the synthesis of single crystalline COFs. All of the materials were structurally characterized using powder X-ray diffraction experiments, transmission electron microscopy (TEM), scanning electron microscopy (SEM) and thermogravimetric analysis (TGA). Gas sorption studies were carried out for the new materials. The new COFs were obtained in polycrystalline form, however only some of them could be activated successfully. Their porosity along with gas sorption properties were studied in detail, providing important findings.

In particular, COF 1a, COF 4 and COF 5 were found to present high CO₂ uptake with high selectivity at 1 bar and at 273, 283 298 K. The corresponding data place these solids among the best COF-type materials for CO₂ uptake, with high isosteric heat of adsorption at zero coverage (Q_{st}^0 for COF 1a is 29.5 kJ mol⁻¹).

The results of the present Thesis provide important information for the targeted synthesis of novel COFs based on imine bonds, using reticular chemistry rules. Our findings help to better understand how these system forms and the evaluation of their gas sorption properties provide important knowledge towards understanding the underlying structure-property relationship.

Key words: COFs, porous materials, gas sorption

Περίληψη

Οι ομοιοπολικοί οργανικοί σκελετοί (Covalent Organic Frameworks, COFs) είναι μια νέα οικογένεια πορωδών υλικών με πιθανές σημαντικές εφαρμογές λόγω των εξαιρετικών ιδιοτήτων τους, προερχόμενες από το ελεγχόμενο πορώδες σε συνδυασμό με τις ιδιότητες του οργανικού σκελετού και την εξαιρετική τους σταθερότητα. Η σύνθεσή τους βασίζεται στους ισχυρούς ομοιοπολικούς δεσμούς μεταξύ χημικών στοιχείων όπως C, Si, B, N και O προς το σχηματισμό δικτύων ποικίλων γεωμετριών με προσβάσιμους πόρους. Τα υλικά αυτά έχουν μεγάλη σταθερότητα σε υψηλές θερμοκρασίες και σε έναν μεγάλο αριθμό οργανικών διαλυτών, ιδιότητες που ώθησαν την επιστημονική κοινότητα να εξετάσει την απόδοση των COFs για πολύ σημαντικές εφαρμογές όπως η προσρόφηση και ο διαχωρισμός αερίων και η κατάλυση.

Στα πλαίσια της παρούσας εργασίας σχεδιάσαμε και συνθέσαμε επιτυχώς νέα COFs βασισμένα σε ιμινικούς δεσμούς χρησιμοποιώντας ως μονομερή νέες αλδεΐδες και μια αμίνη διαφορετικών γεωμετριών. Κάθε υλικό συντέθηκε είτε με την χρήση ανιλίνης, ως ρυθμιστή σε θερμοκρασία περιβάλλοντος είτε χωρίς σύμφωνα με γνωστές διαλυτοθερμικές αντιδράσεις. Τα υλικά χαρακτηρίστηκαν με σύγχρονες τεχνικές συμπεριλαμβανομένων, την περίθλαση ακτίνων-X σε δείγμα σκόνης (PXRD), την ηλεκτρονική μικροσκοπία διέλευσης (TEM), την ηλεκτρονική μικροσκοπία σάρωσης (SEM) και τη θερμοσταθμική ανάλυση (TGA).

Ορισμένα από αυτά τα υλικά ενεργοποιήθηκαν επιτυχώς και οι προσροφητικές τους ιδιότητες μελετήθηκαν εκτενώς ως προς τα αέρια CO₂, Ar και N₂ σε διάφορες θερμοκρασίες και σε χαμηλές πιέσεις χρησιμοποιώντας εμπορικό σύστημα τελευταίας τεχνολογίας. Συγκεκριμένα, τα COF 1a, COF 4 και COF 5 βρέθηκε ότι παρουσιάζουν υψηλή πρόσληψη CO₂ με υψηλή εκλεκτικότητα σε 1 bar στους 273, 283 298 K. Επίσης παρουσιάζουν υψηλή ενθαλπία προσρόφησης (Q_{st}^0 για το COF 1a είναι 29,5 kJ mol⁻¹).

Τα αποτελέσματα της παρούσας εργασίας παρέχουν σημαντικές πληροφορίες για την στοχευμένη σύνθεση νέων COF βασισμένων σε δεσμούς ιμίνης και μας βοηθούν στην καλύτερη κατανόηση του τρόπου σχηματισμού αυτών των συστημάτων καθώς η αξιολόγηση των ιδιοτήτων προσρόφησης των αερίων παρέχουν σημαντική γνώση για την κατανόηση της βασικής σχέσης δομής-ιδιοτήτων.

Λέξεις Κλειδιά: COFs, πορώδη υλικά, προσρόφηση αερίων

ΠΕΡΙΕΧΟΜΕΝΑ

Ευχαριστίες.....	V
Curriculum Vitae	VI
Βιογραφικό Σημείωμα	VIII
Abstract.....	XI
Περίληψη	XII
1. Introduction.....	1
1.1 Porous Materials	1
1.2 Covalent Organic Frameworks.....	2
<i>1.2.1 Reticular chemistry, Design and Topologies of COFs</i>	<i>4</i>
1.3 Types of COFs	7
<i>1.3.1. Boron-containing COFs</i>	<i>7</i>
<i>1.3.2. Triazine-based COFs (CTFs).....</i>	<i>7</i>
<i>1.3.3. Imide-linked COFs</i>	<i>7</i>
<i>1.3.4. Imine-linked COFs</i>	<i>8</i>
1.4. Synthetic Procedures	10
<i>1.4.1 Solvothermal Conditions</i>	<i>10</i>
<i>1.4.2 Crystallization of single crystal COFs at ambient temperature using modulator</i>	<i>11</i>
1.5 Properties and Applications of COFs.....	13
<i>1.5.1 Catalysis</i>	<i>14</i>
<i>1.5.2 Energy storage.....</i>	<i>14</i>
<i>1.5.3 Gas storage.....</i>	<i>14</i>
Bibliography	18
2. Synthetic Procedures of 2D COFs with Honeycomb Structure	22
2.1 Synthesis of COF 1a	23
<i>2.1.1 Structural Characterization of COF 1a</i>	<i>26</i>
<i>2.1.2 Gas sorption properties</i>	<i>27</i>
2.2 Synthesis of COF 1b.....	31
<i>2.2.1 Structural Characterization of COF 1b</i>	<i>33</i>
2.3 Synthesis of COF 2a	35
<i>2.3.1 Structural Characterization of COF 2a</i>	<i>37</i>
2.4 Synthesis of COF 2b.....	40
<i>2.4.1 Structural Characterization of COF 2b</i>	<i>41</i>

2.4.2 <i>Gas sorption properties</i>	41
3. Synthetic Procedures of COFs with tetratopic and hexagonal building units	42
3.1 Synthesis of COF 3a	44
3.1.1 <i>Structural Characterization of COF 3a</i>	45
3.1.2 <i>Gas sorption properties</i>	46
3.2 Synthesis of COF 3b	47
3.2.1 <i>Structural Characterization of COF 3b</i>	48
3.3 Synthesis of COF 4	49
3.3.1 <i>Structural Characterization of COF 4</i>	50
3.3.2 <i>Gas sorption properties</i>	51
3.4 Synthesis of COF 5	53
3.4.1 <i>Structural Characterization of COF 5</i>	54
3.4.2 <i>Gas sorption properties</i>	54
Bibliography	58
4. Conclusions and outlook	60
Appendix 1	62
Appendix 2	86

1. Introduction

1.1 Porous Materials

Porous materials are characterized in their structure by the presence of cavities, which confer some unique properties to these solids. They became the subject of scientific experiments, not until the 18th century, when Cronstedt in 1756 first described a zeolite, Scheele in 1773, Priestley in 1775 and Fontana in 1777 investigated the adsorptive capacity of charcoal [1].

More recently the progress in chemistry and materials science has given rise to several distinct classes of porous material, such as metal organic frameworks (MOFs), porous organic polymers and covalent organic frameworks (COFs). These materials are characterized by general trends in structural evolution: from inorganic to organic components, from small to large pores, from rigid frameworks to soft dynamic skeleton, and from 2D to 3D architectures [2]. As we can understand the need to create uniformity within the pore size, shape and volume has steadily increased over recent years because it can lead to superior applications properties [3]. But in order to find for this kind of materials greater use at an industrial scale, it is necessary to optimize multiple functions in addition to pore structure and surface area, such as stability, sorption kinetics, mechanical properties, and thermal properties.


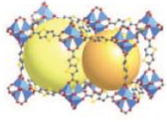


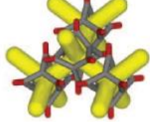
	Zeolites	Metal-organic frameworks¹	Covalent-organic frameworks	Porous organic polymers	Porous molecular solids
					
Porosity	Microporous or mesoporous ² ; narrow pore size distributions	Can be ultraporous ³ /mesoporous; narrow pore size distributions	Can be ultraporous/mesoporous; narrow pore size distributions	Can be ultraporous/mostly microporous; broader pore sizes	Can be ultraporous/mesoporous, but this is rare so far
Crystallinity	Typically high; can also be amorphous	Typically high	Modest to high	Amorphous	High, but amorphous examples, too

Figure 1. Classes of porous solids and selected functions [5].

The range of applications of these fascinating crystalline porous materials is though huge such as catalysis, gas storage, gas separation, ionic conductors, energy storage and production, smart sensors and optoelectronics [4]. This rapid development in this area expands the interest from scientific researchers in the fields of materials, organic synthesis,

and diverse applications, too. MOFs, COFs as well as other related materials could arguably be superior to currently existing options owing to some features that are not present in classical materials, standing above all the possibility of chemical design [5].

1.2 Covalent Organic Frameworks

Covalent Organic Frameworks are the results of the ground-breaking work of Yaghi and co-workers in 2005. COFs are a class of porous polymers in which organic building blocks are precisely integrated into extended structures with periodic skeletons and ordered pores [2]. These porous materials are lightweight ingeniously formed by strong covalent linkages between C, Si, B, N, and O. The porous architectures can be either two-dimensional (2D) or three dimensional (3D). COFs also follow reticular chemistry protocols similar to that of metal–organic frameworks (MOFs) [6].

Covalent bonds connect atoms to form molecules and then further link these molecules to giant covalent structures and then to covalent frameworks. Diamond, boron nitride and silicon carbide are the hardest materials on Earth and they are covalently bonded solids [7]. But to be able to construct new covalent bonded materials it is obligatory to understand the nature of this covalent bond formation. Organic synthesis researchers achieved to control extremely efficient covalent bond in zero dimension. Simultaneously the covalent chemistry in one dimension has been extended explored by polymers chemists. But, according to the famous Nobel winner Roald Hoffmann “in two or three dimensions it’s a synthetic wasteland” [8].

The error correction and the fact of self-healing during the crystallization are due to the reversibility in bond formation. This is the reason why direct crystallization cannot be occurred to the best of our knowledge. It is absolutely necessary to be applied in reaction the conditions of reversibility. Doing this it is prevented the formation of amorphous disordered kinetic products. The system can repair all the unpleasant and unwanted bond formations through back reaction and bond reformation. The final goal is to be able to be isolated a crystalline thermodynamic product with the lowest free energy [9].

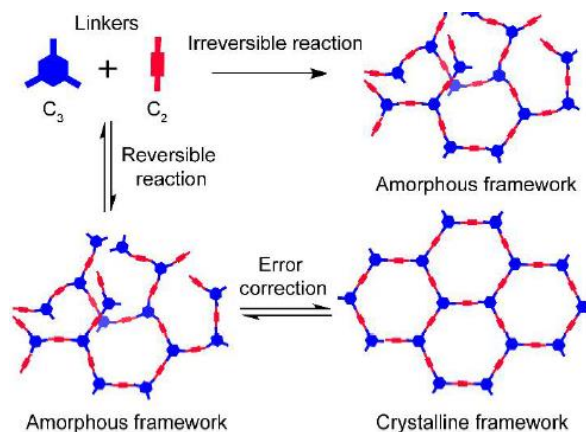


Figure 2. Schematic representation of crystalline and amorphous COF formation by reversible and irreversible reactions [8].

The crystallinity is inevitable from the fact that these ordered structures lead to crystalline frameworks. On the contrary, despite the fact that most of these materials have high porosity, which can be used as an additional proof that the correct structure has been obtained, some COFs are not porous due to interpenetration, staggered stacking or the presence of bulky functional groups that completely fill the pores.

In past years crystalline materials based on the covalent bond were synthesized by the groups of Wuest [10] and King [11]. These single crystals of 2D covalent networks though were unable to give neither permanent porosity nor thermal stability. Lack of those properties makes this kind of polymers unsuitable for practical applications.

In Figure 3 below can be explained in details the exact idea of the structural design of covalent organic frameworks. The chemical structures have been simplified so that the building blocks are described as geometric shapes which can be linked through the vertices. In the picture is illustrated some reactive groups oriented in a suitable manner so upon bonding they will create an infinite, periodic and ordered network of covalently bound atoms [12].

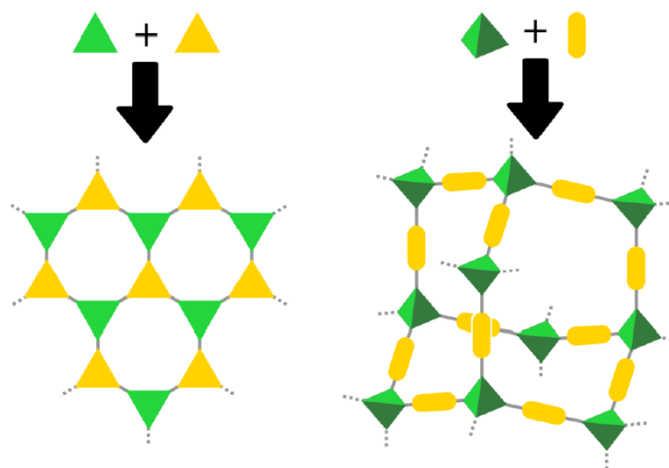


Figure 3. Schematic representation of COF networks generated by the bonding of two triangular building blocks (left) and a tetrahedral with a linear building block (right) [13].

1.2.1 Reticular Chemistry, Design and Topologies of COFs

Reticular chemistry is a term that describes the ability of designing and synthesizing materials like MOFs and COFs in a rational way from molecular building blocks. These building units have different shape, connectivity and size and aim to the development of robust frameworks with specific properties like dimensionality.

The directionality of covalent bonds provides means of controlling how building units come together into predesigned structures. The skeletons and pores of COFs can be designed using a topology diagram (Figure 4). The most common topologies that these materials give are hexagonal, tetragonal, rhombic and trigonal. The diversity of building blocks makes COFs an emerging materials platform for structural control and functional design. The fact that the building units used in the assembly of COFs maintain their geometry during the reaction makes it possible to predict the structure of the resulting solid [13].

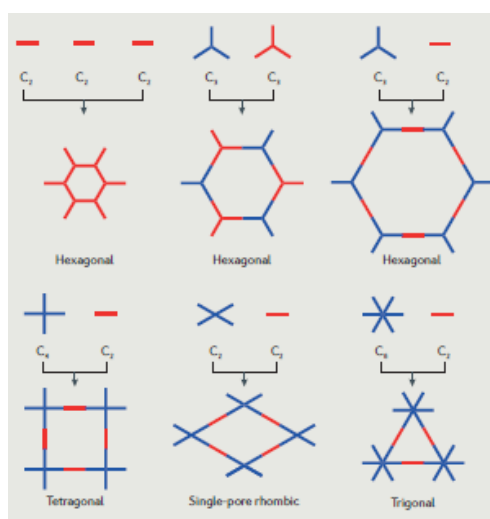


Figure 4. The COF polygon shapes that have been developed thus far include hexagonal, tetragonal, rhombic [2]. and trigonal structures, and the building blocks that can be classified as C2-, C3-, C4- and C6-symmetric units based on the directional symmetry of the reactive groups [2].

COFs can be classified as either two-dimensional (2D) COFs (Figure 5) or three-dimensional (3D) COFs (Figure 6), based on the dimensionality of the covalent connectivity.

Networks that propagate only in two dimensions consequently restrict covalent bonds to be in a plane, resulting in the formation of layers. These layers do not remain isolated and have a strong tendency to form a layered material in which the integrity of the layers is maintained by strong covalent bonds while weaker intermolecular interactions, frequently π - π stacking, hold the different layers together.

In contrast, 3D COFs are synthesized from non-planar (typically tetrahedral) building blocks to form highly porous networks. Three-dimensional (3D) topologies allow the formation of covalent bonds in all directions [14].

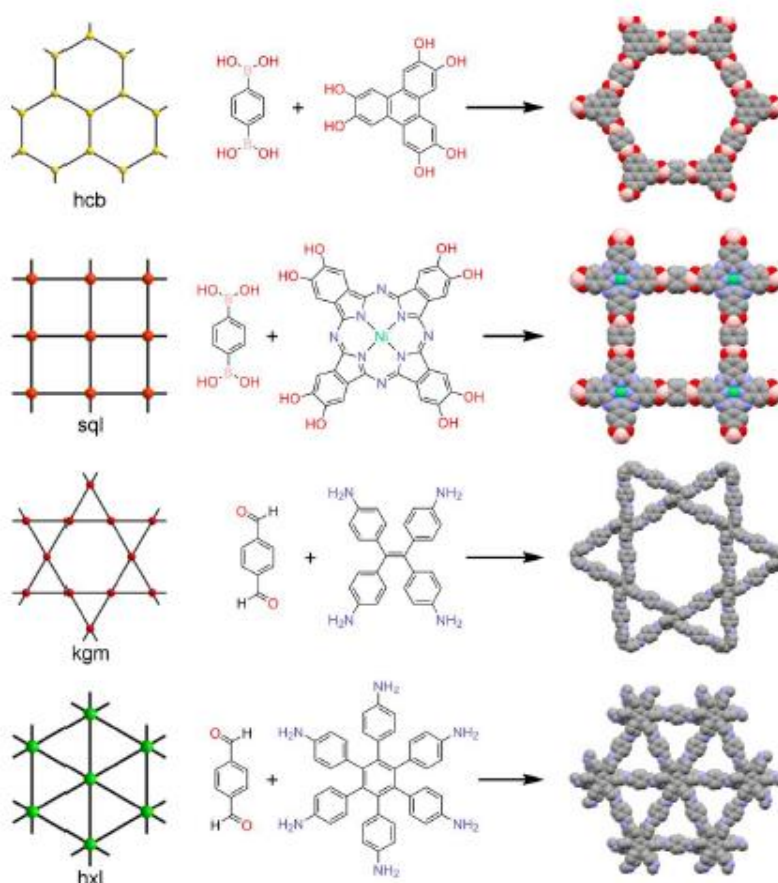


Figure 5. Representation of all the 2D topologies (left) found in reported COFs and examples of synthesized structures corresponding to each topology (space filling model, C: grey, B: pink, O: red, N: blue, Ni: green, H omitted for clarity) [13].

In some cases it is reported the use of flexible building blocks to form a covalently bonded network. The high number of degrees of freedom adds an extra difficulty since many conformations will not provide a suitable orientation for the linkages, thus leading to a disordered structure. Size is also another important factor when selecting building blocks. It is especially attractive if there are linear linkers, since their length will determine the diameter of the pores and allows obtaining families of isorecticular COFs that differ only in the size of the cavities [15].

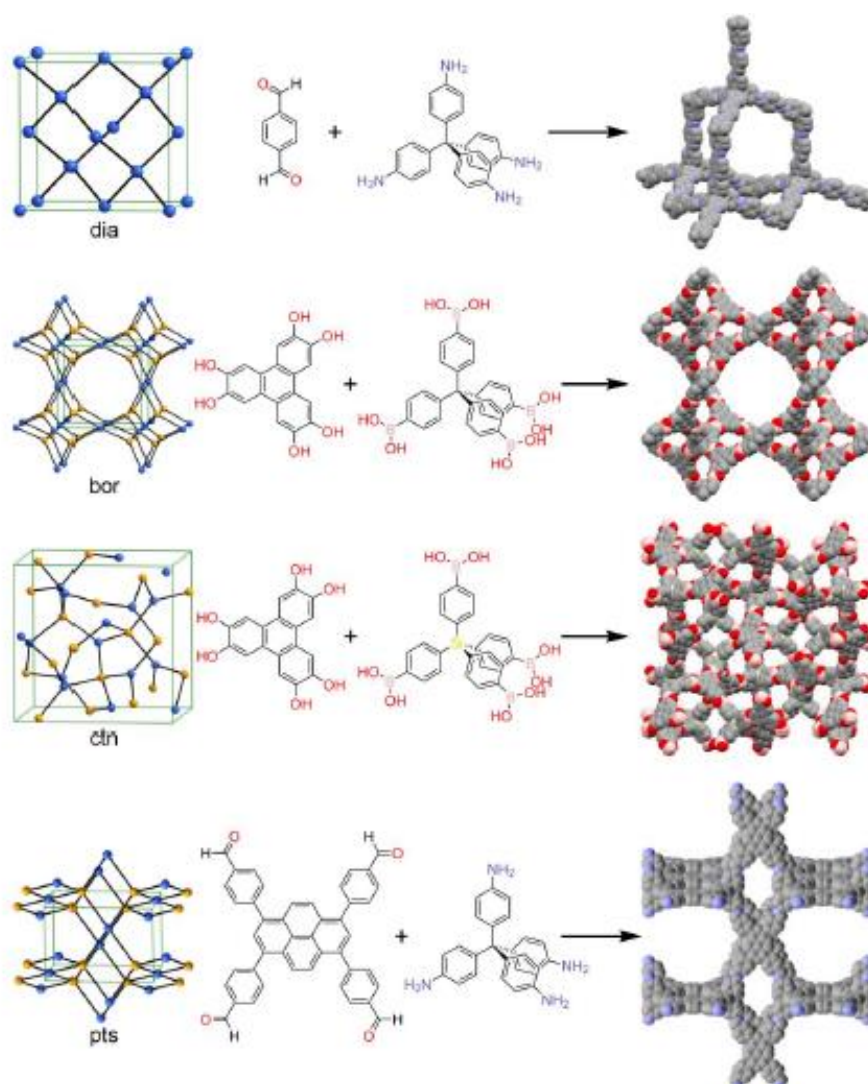


Figure 6. Representation of all the 3D topologies (left) found in reported COFs and examples of synthesized structures corresponding to each topology (space filling model, C: grey, B: pink, O: red, N: blue, Si: yellow, H omitted for clarity) [13].

1.3 Types of COFs

After deciding the shape of the building blocks, it is necessary to choose which reaction is going to be used to join them. At present, COFs basically can be classified into four main categories: boron-containing, triazine-based, imide-linked, and imine-based COFs. These kinds of COFs according to their different properties can be used in various applications in industrial point of view.

1.3.1. Boron-containing COFs

The self-condensation of boronic acids to form boroxine rings and the formation of boronic esters from boronic acids and catechols were the reactions first used in the synthesis of COFs. COF-1 and COF-5 were prepared and first reported by Yaghi and coworkers in 2005. However, most of the boron-containing COFs have a fatal shortcoming, they are not stable in moist air or in water [16].

1.3.2. Triazine-based COFs (CTFs)

The second type of COF is triazine-based COFs. The first CTF (CTF-1) was prepared by Thomas and co-workers in 2008 and it was based on the cyclotrimerisation of nitrile building units in the presence of ZnCl_2 at 400 °C. The harsh preparation conditions, including high reaction temperature and purification in acid solution, bring about the destruction of the ordered structure. That is the reason why CTFs often have lower crystallinity and small porosity. The harsh high reaction temperature makes it also very difficult to find monomers that can be used to the synthesis of CTFs, which does not benefit further development and practical large-scale production [17].

1.3.3. Imide-linked COFs

Yan's group reported for the first time in 2014 imide-linked COFs. These are synthesized through the imidization reaction. These COFs exhibited high surface area and had great potential for loading dye molecules and drug delivery. Also this kind of COFs showed high thermal stability up to 520 °C. Most of the synthetic procedures that are used are simple, green and environmentally friendly. But the reaction temperature was up to 345

°C which may be a hindrance. However, despite the excellent stability and high porosity of this series of new COFs, there are still few reports about them in comparison with other kinds of COFs after the work of Yan's group [18].

1.3.4. Imine-linked COFs

The first imine-based COF (COF-300) was developed by Yaghi and co-workers in 2009, through the co-condensation reaction of aldehyde and amine [19]. Such COFs compared with that of boronate ester-linked COFs have enhanced chemical stability in the presence of water, acids and alcohols. Various aldehydes and amines with different geometries have been explored for the synthesis of imine-based COFs. These building blocks cover a broad range of organic π units with discrete sizes and different functions, ranging from simple arenes to heterocyclic molecules, extended π systems, coordinated strings and large macrocycles, providing a rich range of skeletons [20].

According to literature more and more reactions are used in the synthesis of COFs the last years. The choose of the linkage is very important because from the nearly infinite possibilities offered by organic chemistry to create bonds, only reversible reactions yield crystalline networks (Figure 7).

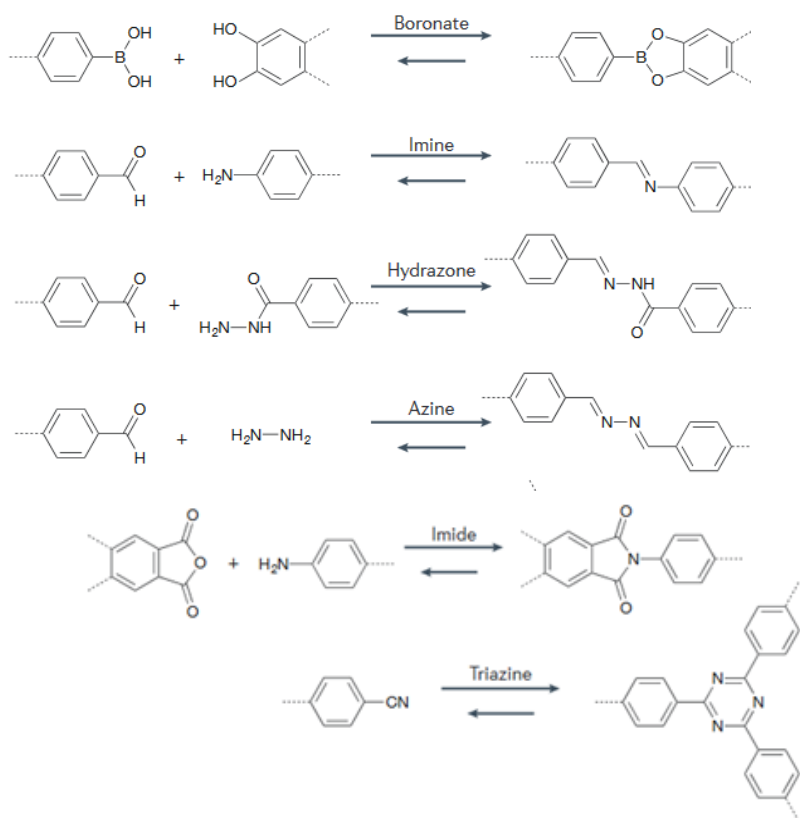


Figure 7. Diversity of linkages for the formation of COFs [2].

As mentioned before, the advantages of this reaction are the relatively high thermal and chemical stability of the final product while being very tolerant with different reaction conditions that range from room temperature reactions to solvothermal syntheses conditions. All of these make probably the imine-based COFs the most favored strategy for the synthesis of such crystalline porous materials.

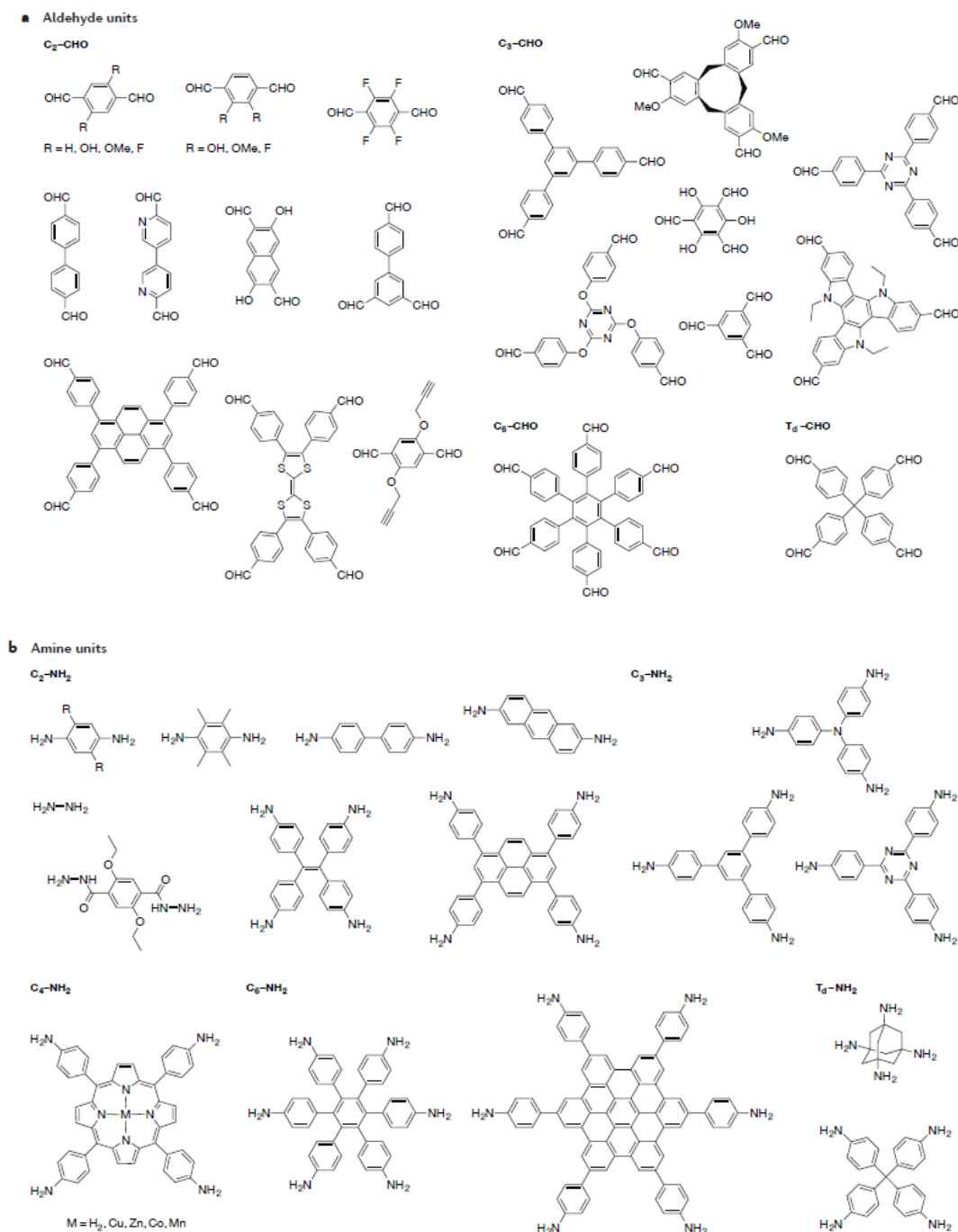


Figure 8. Typical building blocks used to form imine-linked COFs. Building blocks bearing aldehyde (panel a) and amine (panel b) units [2].

1.4. Synthetic Procedures

1.4.1 Solvothermal Conditions

The experimental approach to conduct most of the COFs is fairly similar. The great majority of the reported procedures are carried out in sealed Pyrex tubes. These tubes consist the building blocks in a suitable mixture of solvents, which is not capable of dissolving the monomers in many cases. Then the necessary catalyst is added before evacuating and sealing the tube. The mixture is heated under solvothermal conditions for several days, after which the solid is recovered, washed and dried [21].

In imine-based COFs cases, the reaction most commonly carried out in 1,4-dioxane or 1,4-dioxane:mesitylene mixture using aqueous acetic acid as catalyst at temperatures close to 120 °C over several days in a sealed tube. Quite frequent is the use of mixtures such as *o*-dichlorobenzene with *n*-butanol as well.

After the addition of the catalyst an amorphous precipitate is observed most of the times. This rapid initial formation of an amorphous network subsequently crystallizes into the layered 2D network. Reported experiments provide the first mechanistic insight into the mechanism of imine-linked 2D COF formation [22].

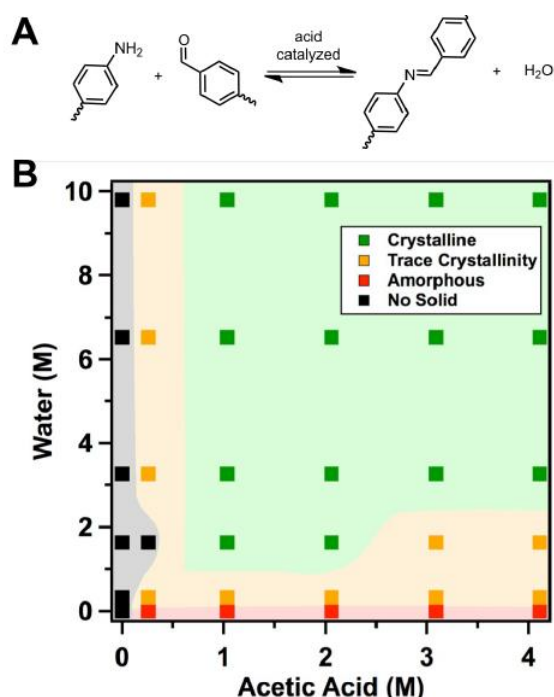


Figure 9. (A) Linkage equilibrium controlling imine network formation (B) COF formation as a function of water and acetic acid concentration in the growth solution [22].

In the absence of acetic acid no precipitate is observed, even after heating the solution to 70 °C for 5 days. In contrast, the addition of glacial acetic acid 0.25 – 4.1 M in the absence of additional water induces the immediate precipitation of an amorphous polymer network. After heating the mixtures at 70 °C for 3 days, yields of the amorphous solid are >90% or greater, however no evidence of crystallinity is observed. The addition of both water and acetic acid is necessary to generate the COF, where concentrations ≥ 3.3 M water and ≥ 1 M acetic acid reliably induce crystallinity and maintain high yields (Figure 10).

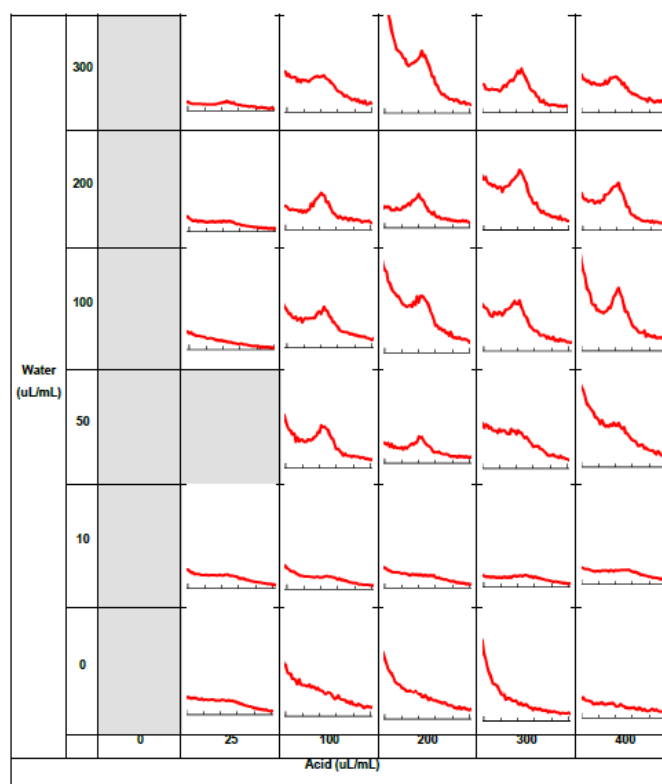


Figure 10. Powder X-ray diffraction pattern of TAPB-PDA COF in the low angle 2θ region, synthesized in the presence of water and/or glacial acetic acid, added to 1mL of stock. Reaction conditions: 70 °C, 72 h. Conditions in gray yielded no solid [22].

1.4.2 Crystallization of single crystal COFs at ambient temperature

In 2018 Yaghi and coworkers have developed a general procedure to grow large single crystals of three-dimensional imine-based COFs (COF-300, hydrated form of COF-300, COF-303, LZU-79, and LZU-111) with the use of a modulator [24]. The high quality of

the crystals allowed collection of single crystal X-ray diffraction data for the first time in the history of this kind of materials.

This general approach involves the use of aniline as a modulator to grow high-quality large single crystals of 3D porous COFs held together by strong imine bonds. Aniline has reactivity similar to that of COF monomers, but it is mono-functional and acts as an inhibitor to nucleation, and thus changes the crystallization process. Such reaction conditions should be designed to allow the covalent linkage (imines) between the building blocks to be reversible and slow enough for efficient self-correction of defects.

In a typical imine COF synthesis, the formation of amorphous solid is initially observed, and over time this material transforms into a crystalline phase through an error-correction mechanism [23]. Thus, immediate precipitation causes the COF solid to be invariably amorphous or polycrystalline rather than single crystalline.

In order the reversibility of imine bond formation to be increased and to slow down the kinetics of imine bond formation, a large excess of aniline was added to the reaction mixture (Figure 11).

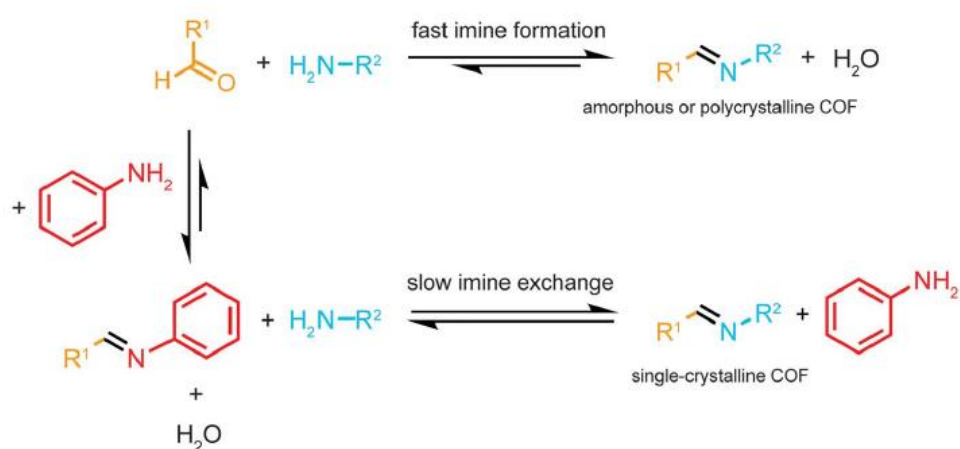


Figure 11. Crystal growth of large imine-based COFs modulated by aniline [24].

In the absence of aniline, amorphous or polycrystalline COFs are produced, whose formation is governed by fast nucleation and limited crystal growth. Aniline on the other hand acts as a competitive modulator with the multifunctional amine-based building units. Also, aniline is an amine and the imine bonds are more susceptible to nucleophilic attack by amines rather than by water.

The crystal size of single crystalline COFs was controlled by adjusting the amount of aniline. The reaction parameters such as time, temperature, pH, solvent, and concentration

played also important role to the formation of single crystal COFs. The building blocks that were used were tetratopic and ditopic amines and aldehydes (Figure 12).

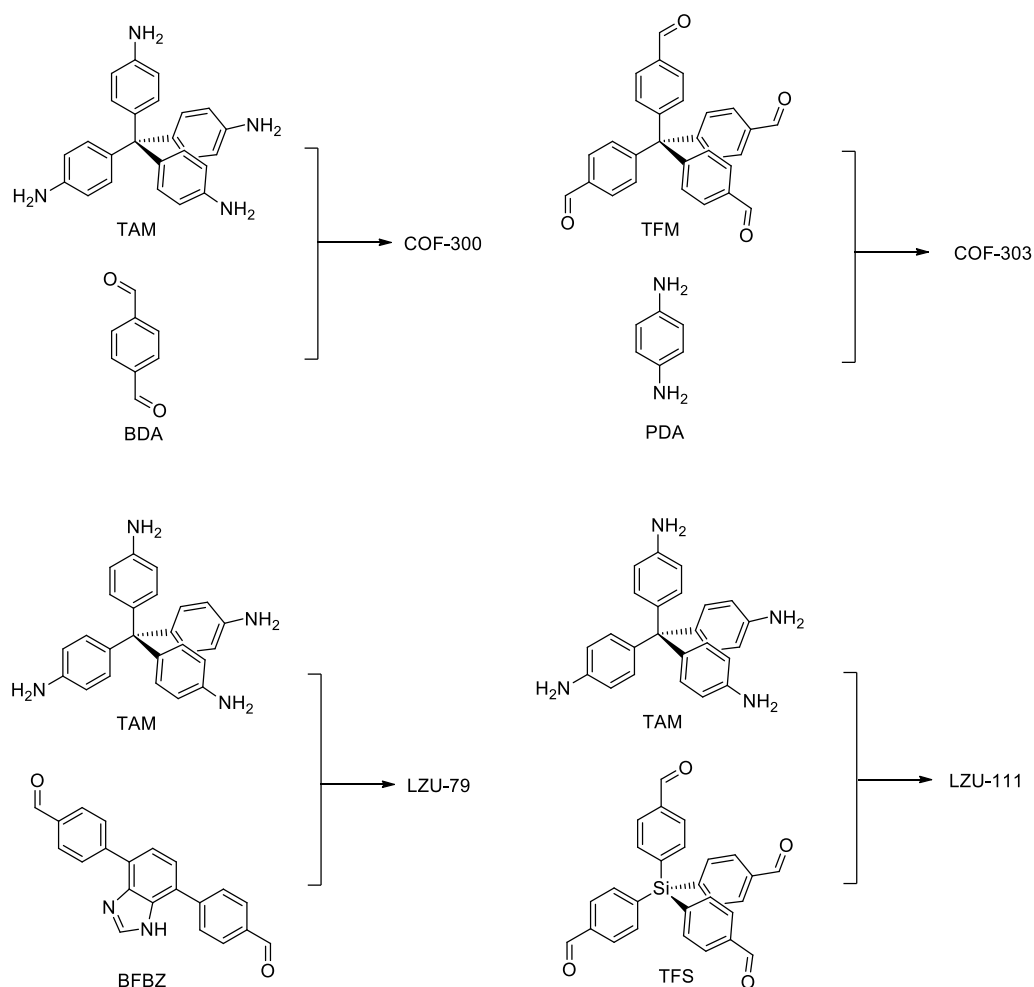


Figure 12. Building blocks of single crystalline COF-300, COF-303, LZU-79, LZU-111 [24].

According to Yaghi's report, the excess of aniline that was used to obtain large single crystals was between 15 and 80 equivalents. The size of these crystals was from 15 up to 100 μm and the time reaction at ambient temperature was within 15 to 80 days [24].

1.5 Properties and Applications of COFs

One of the most important aspects of COFs, despite the ability of predesigning their structure is their properties. The distinctive physical and chemical features of these materials make them outstanding candidates for a plethora of applications. The well-defined crystalline porous structures together with tailored functionalities have offered the COF materials

superior potential in diverse applications, such as gas storage, adsorption, energy storage, drug delivery and catalysis. The fact that COFs can be made exclusively out of light elements such as boron, carbon, nitrogen and hydrogen give the potential of achieving very low densities, property important for energy storage, gas storage and separation [25]. The high strength and stability of covalent bonds provides COFs also with high thermal and chemical stability [26].

1.5.1 Catalysis

As the cases of other porous solids, suitable COF candidates for catalytic applications incorporate robust catalytic sites and possess high stability to thermal treatments, water, and most of the organic solvents. Furthermore, the easy accessibility to the catalytic sites and the efficient mass transport inside the porous catalyst should also be guaranteed for the ideal catalytic performance.

A series of 2D COFs were prepared as supports of heterogeneous hybrid catalysts for various reactions, including nitrophenol reduction [27], water oxidation [28], reduction of CO₂ to CO [29], reduction of N-methylpyrrole [30], etc. In addition, Yan's group presented two 3D imine-based COFs, showing excellent recyclability, remarkable conversion and high size selectivity in Knoevenagel condensation reactions [31]. Also, COFs have been applied in the field of organocatalysis. Xu *et al.* reported a stable and crystalline COF, and synthesized chiral organocatalysts with high crystallinity and porosity [32].

1.5.2 Energy storage

Due to their high surface area, extended π conjugated systems, tunable pore size and ability to organize redox active groups, COFs are considered as candidate materials for energy storage devices. Dichtel's group firstly reported COFs that were studied in this area [33]. Mulzer *et al.* reported also polymer-modified COFs that showed superior volumetric energy and power densities comparable with other porous carbon-based electrode [34].

1.5.3 Gas storage

In order to have access to the porosity of this kind of materials a proper activation procedure should be occurred. In fact, activation of the pores is a step that should not be

overlooked, since the final performance of the material is highly dependent on it. The reported strategies range from solvent exchange and evacuation at high temperature under reduced pressure, to drying with supercritical carbon dioxide. The porosity of COFs is commonly confirmed by nitrogen adsorption at 77 K or by argon at 87. COFs can be excellent adsorbents for gas storage applications including carbon dioxide, hydrogen and methane.

Excessive CO₂ emission derived from population expansion and industrial development is the main reason for the “Greenhouse Effect”, which is one of the greatest global issues currently confronting us [35]. Recent studies on the impact of a further temperature rise of 1.5 °C revealed that it would result in a series of crucial problems on ecosystem, plants, and environments, causing global warming and climate change. Solutions for reducing CO₂ emission from various sources and removing CO₂ from air are urgent to be found. Porous materials, such as zeolites, MOFs, porous carbons and COFs, have been considered as potential candidates to solve this serious problem [36].

COFs possess advantages, such as large CO₂ capture capacity, high CO₂ selectivity, good recyclability, easy pore functionalization, uniform pore size and good stability. COFs as mentioned before are built from the condensation of organic units with various shapes and geometries and their structures and linkages affect the CO₂ capture.

As shown in Figure 13, a higher degree of functionalisation with alkyne and alkane chain reduces the CO₂ uptake ability of the material due to the weak interaction of these groups with the gas. The reduction in surface area and pore volume derived from the space occupied by these chains. However, when other groups are introduced, the capacity of the material increases as a consequence of dipole interactions or even the formation of stronger acid-base pairs with amines, which was corroborated by the trend in the values of the isosteric heat of adsorption.

Adsorption enthalpy, represented by the isosteric heat of adsorption (Q_{st}), is related to the affinity between COFs and CO₂. The highest Q_{st} values reported are of TFPB-TAPB-COF, TFPA-TAPB-COF, BTMA-TAPACOF, and TFPA-TAPA-COF. They are 17.7, 21.1, 24.6, and 28.4 kJ mol⁻¹ respectively (Figure 14).

Among various linkages, the azine (N=N) linkage is effective to enhance the capacity owing to the interactions of CO₂ with the linkages through the nitrogen lone pairs. For examples, ACOF- 1, HEX-COF-1, and COF-JLU2 [37] (Figure 15) are excellent adsorbents with high capacities of 17.7, 20, and 21.7 wt % at 273 K and 1 bar, respectively.

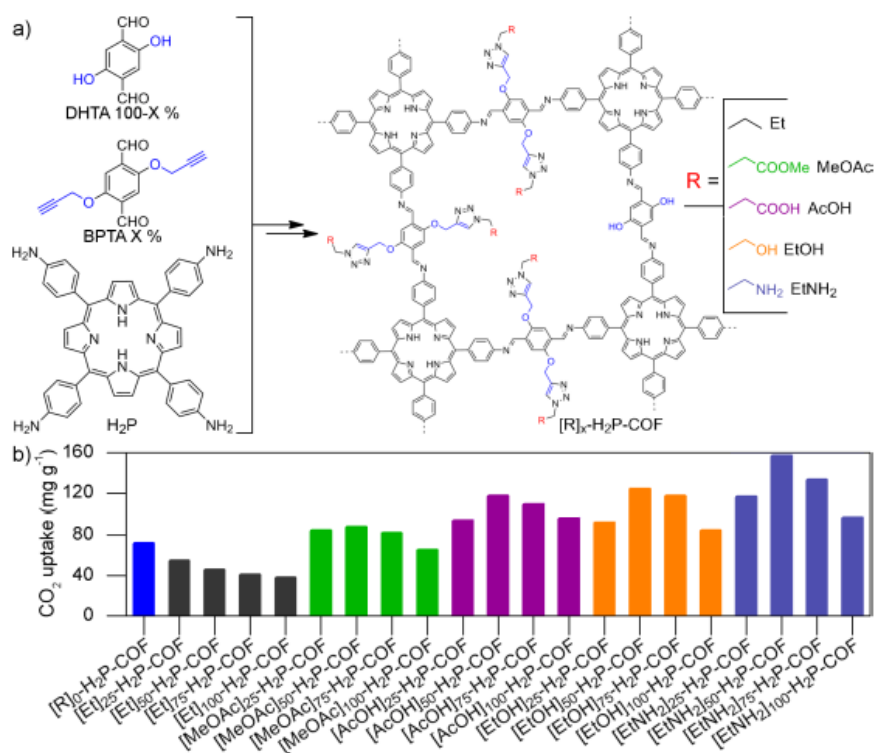


Figure 13. a) Post-functionalised COFs studied for CO₂ uptake. The X in the formula indicates the percentage of hydroxyl groups that are substituted by the corresponding functional group. b) CO₂ uptakes measured at 273 K of the COFs.

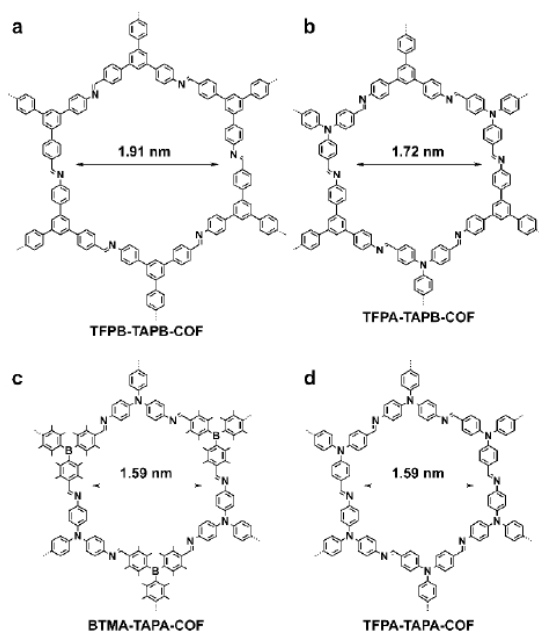


Figure 14. COFs for CO₂ adsorption [38].

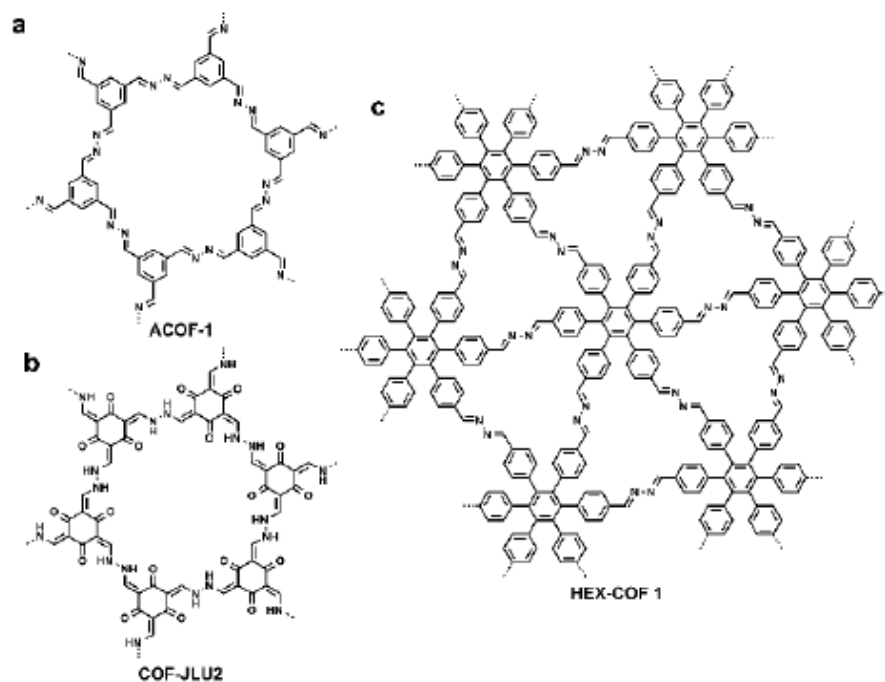


Figure 15. COFs for CO₂ adsorption [39].

Hydrogen has been pursued as an ideal substitute for traditional fossil fuels, especially in the automotive applications, due to its clean combustion and high chemical energy density [40]. In general, COFs with larger surface areas possess higher hydrogen uptake capacities when measured under the same conditions. For example, COF-18E with a BET surface area of 1263 m² g⁻¹ shows the highest hydrogen uptake (1.55 wt% at 1 bar, 77 K) among similar 2D COFs with different alkyl chain lengths. In contrast, COF-11E with a surface area of 105 m² g⁻¹ shows a hydrogen uptake of 1.22 wt% at 1 bar and 77 K [41].

On the other hand, a recent report by Zheng and co-workers suggests that the capacity of hydrogen storage can be enhanced by incorporating undulated macrocyclic cyclotricatechylene into 2D COFs. The obtained CTC-COF shows higher hydrogen uptake (1.12 wt %) at low pressure (1.05 bar) than those of 2D COFs with similar structures [42].

As the main component of natural gas, methane is abundant and inexpensive in comparison with conventional fossil fuels. In order to put methane into driving automobiles in a practical manner, effective and safe storage systems need to be developed. Accordingly, the capability of methane storage in certain COF materials has been examined. Analogous to the cases of hydrogen storage, the capacities of methane storage in 3D COFs are higher than those of 2D COFs [43].

Bibliography

- [1] Wright, P. A. The Royal Society of Chemistry, Cambridge, UK, **2007**.
- [2] Huang, N.; Wang, P.; Jiang, D. *Nat. Rev. Mater.* **2016**, *1*(10), 16068.
- [3] Davis, E. M. *Nature* **2002**, *417*, 813-821.
- [4] Zhang, J.; Han, X.; Wu, X.; Liu, Y.; Cui, Y. *J. Am. Chem. Soc.* **2017**, *139* (24), 8277-8285.
- [5] Slater, G. A.; Cooper, I. A. *Science* **2015**, *348*, 6238.
- [6] Chandra, S.; Kandambeth, S.; Biswal, B. P.; Lukose, B.; Kunjir, S.M.; Chaudhary, M.; Babarao, R.; Heine, T.; Banerjee, R. *J. Am. Chem. Soc.* **2013**, *135* (47), 17853-61.
- [7] Wentorf, R. H.; Devries, R. C.; Bundy, F. P. *Science* **1980**, *208*(4446), 873-80.
- [8] Kandambeth, S.; Dey, K.; Banerjee, R. *J. Am. Chem. Soc.* **2018**, *141*(5), 1807-1822.
- [9] Jin, Y.; Yu, C.; Denman, R. J. *Chem. Soc. Rev.* **2013**, *42*, 6634-6654.
- [10] Beaudoin, D.; Maris, T.; Wuest, J. D. *Nat. Chem.* **2013**, *5* (10), 830-4.
- [11] Kissel, P.; Murray, D. J.; Wulftange, W. J.; Catalano, V. J.; King, B. T. *Nat. Chem.* **2014**, *6*, 774-778.
- [12] Côté, A. P.; Benin, A. I.; Ockwig, N. W.; O’Keeffe, M.; Matzger, A. J.; Yaghi, O. M. *Science* **2005**, *310* (5751), 1166–1170.
- [13] Diercks, C. S.; Yaghi, O. M. *Science* **2017**, *355*, 6328.
- [14] Biswal, B. P.; Chandra, S.; Kandambeth, S.; Lukose, B.; Heine, T.; Banerjee, R. *J. Am. Chem. Soc.* **2013**, *135* (14), 5328–5331.
- [15] Jiang, D.; Chen, X.; Geng, K.; Liu, R.; Tan, K. T.; Gong, Y.; Li, Z.; Tao, S.; Jiang, Q. *Angew. Chem. Int. Ed.* **2019**, *10*, n. pag.
- [16] Lanni, L. M.; Tilford, R. W.; Bharathy, M.; Lavigne, J. J. *J. Am. Chem. Soc.* **2011**, *133*, 13975–13983.
- [17] Kuhn, P.; Antonietti, M.; Thomas, A., *Angew. Chem.* **2008**, *Int. Ed.*, *47*, 3450–3453.
- [18] Fang, Q.; Wang, J.; Gu, S.; Kaspar, R. B.; Zhuang, Z.; Zheng, J.; Guo, H.; Qiu, S.; Yan, Y. *J. Am. Chem. Soc.* **2015**, *137*, 8352–8355.
- [19] Uribe-Romo, F. J.; Hunt, J. R.; Furukawa, H.; Klöck, C.; O’Keeffe, M.; Yaghi, O. M., *J. Am. Chem. Soc.* **2009**, *131*, 4570–4571.
- [20] Segura, J. L.; Mancheno, M. J.; Zamora, F. *Chem. Soc. Rev.* **2016**, *45*, 5635-5671.
- [21] Smith, B. J.; Dichtel, W. R. *J. Am. Chem. Soc.* **2014**, *136* (24), 8783–8789.

- [22] Smith, B. J.; Overholts, A. C.; Hwang, N.; Dichtel, W. R. *Chem. Commun.* **2016**, *52*, 3690-3693.
- [23] Zhao, Y.; Guo, L.; Gándara, F.; Ma, Y.; Liu, Z.; Zhu, C.; Lyu, H.; Trickett, C. A.; Kapustin, E. A.; Terasaki, O.; Yaghi, O. M. *J. Am. Chem. Soc.* **2017**, *139*, 13166–13172.
- [24] Ma, T.; Kapustin, E. A.; Yin, S. X.; Liang, X.; Zhou, Z.; Niu, J.; Li, L.; Wang, Y.; Su, J.; Li, J.; Wang, X.; Wang, W. D.; Wang, W.; Sun, S.; Yaghi, O. M., *Science* **2018**, *361*(6397), 48-52.
- [25] El-Kaderi, H. M.; Hunt, J. R.; Mendoza-Cortés, J. L.; Côté, A. P.; Taylor, R. E.; O’Keeffe, M.; Yaghi, O. M. *Science* **2007**, *316* (5822), 268–272.
- [26] Ding, S.Y.; Wang, W. *Chem. Soc. Rev.* **2013**, *42*, 548-568.
- [27] Pachfule, P.; Kandambeth, S.; Díaz, D. D.; Banerjee, R. *Chem. Commun.* **2014**, *50*, 3169–3172.
- [28] Aiyappa, H. B.; Thote, J.; Shinde, D. B.; Banerjee, R.; Kurungot, S. *Chem. Mater.* **2016**, *28*, 4375–4379.
- [29] Margalit, Y.; Zhou, Z.; Machluf, S.; Rohrllich, D.; Japha, Y.; Folman, R. *Science* **2015**, *349*, 1205–1208.
- [30] He, T.; Liu, L.; Wu, G.; Chen, P. J. *Mater. Chem. A* **2015**, *3*, 16235–16241.
- [31] Fang, Q.; Gu, S.; Zheng, J.; Zhuang, Z.; Qiu, S.; Yan, Y. *Angew. Chem., Int. Ed.* **2014**, *53*, 2878–2882,
- [32] Xu, H.; Gao, J.; Jiang, D. *Nat. Chem.* **2015**, *7*, 905–912.
- [33] DeBlase, C. R.; Silberstein, K. E.; Truong, T.; Abruña, H. D.; Dichtel, W. R. *J. Am. Chem. Soc.* **2013**, *135*, 16821–16824.
- [34] Mulzer, C. R.; Shen, L.; Bisbey, R. P.; McKone, J. R.; Zhang, N.; Abruña, H. D.; Dichtel, W. R. *ACS Cent. Sci.* **2016**, *2*, 667–673.
- [35] Foster, G. L.; Royer, D. L.; Lunt, D. J. *Nat. Commun.* **2017**, *8*, 14845.
- [36] D'Alessandro, D. M.; Smit, B.; Long, J. R. *Angew. Chem. Int. Ed.* **2010**, *49*, 6058–6082.
- [37] Li, Z.; Zhi, Y.; Feng, X.; Ding, X.; Zou, Y.; Liu, X.; Mu, Y. *Chem. - Eur. J.* **2015**, *21*, 12079-12084.
- [38] Alahakoon, S. B.; Thompson, C. M.; Occhialini, G. and Smaldone, R. A. *ChemSusChem*, **2017**, *10*, 2116-2129.
- [39] Huang, N.; Xu, H.; Chen, Q. and Jiang, D. *Chem. Commun.*, **2017**, *53*, 4242-4245.
- [40] Schlappbach, L.; Züttel, A. *Nature* **2001**, *414*, 353.

- [41] Han, S. S.; Furukawa, H.; Yaghi, O. M.; Goddard III, W. A. *J. Am. Chem. Soc.* **2008**, *130*, 11580.
- [42] Yu, J. T.; Chen, Z.; Sun, J.; Huang, Z. T.; Zheng, Q. Y. *J. Mater. Chem.* **2012**, *22*, 5369.
- [43] Wu, H.; Gong, Q.; Olson, D. H.; Li J., *Chem. Rev.* **2012**, *112*, 836.

Thesis aim and objectives

The purpose of this work is the synthesis of new novel symmetric organic ligands in order to explore and design interesting covalent organic frameworks (COFs) with new topologies for potential applications in gas sorption. However, it is important to note that the application of a particular COF is dictated by its structure, pore characteristics and functionalities.

The choice and design of the organic linkers was crucial for the execution of this work. The synthesis of novel COFs is based on the successful condensation reactions between different organic building units. The shapes and geometries of the organic linkers play significant role because during the reaction COFs maintain these geometries. That is why it is possible to predict the structure of the resulting frameworks. These solids have also diverse pore architectures and very important properties. We synthesized organic building blocks with triangular, rectangular and hexagonal shapes.

Our point of interest was the imine-based COFs, formed by the condensation of an aldehyde and an amine, in the presence of acetic acid as a catalyst. This type of COFs is the most promising because they have good chemical stability in most organic solvents, acids, alcohols or water compared with boron-containing COFs. Also, they have higher crystallinity and porosity in comparison with triazine-based COFs. The new COFs were synthesized under solvothermal reaction conditions, with or without aniline (modulator).

The presence of extensive aromatic systems in the linkers that we designed and synthesized is expected to enhance the interaction of these materials with gases of environmental and/or energy interest such as CO₂. Finally, their adsorption properties were extensively studied.

2. Synthetic Procedures of 2D COFs with Honeycomb Structure

In this chapter, we present the synthesis and the characterization of two new 2D COFs with honeycomb structure. In order to synthesize these materials triangular, hexagonal and linear organic linkers were combined in the presence of acetic acid. Under controlled reaction conditions, good quality crystalline materials were produced. Taking into consideration the significance of the organic linkers, in terms of linking connectivity in directing the overall framework topology, we designed and successfully synthesized one triangular and one hexagonal organic ligand (Figure 16).

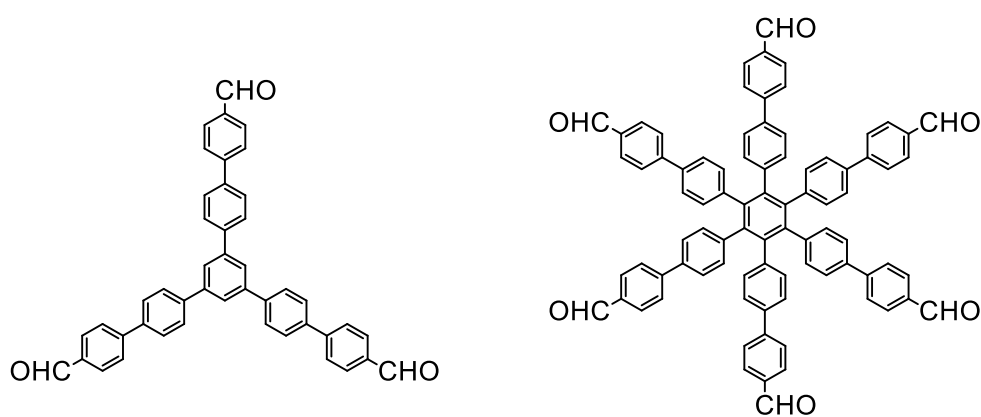


Figure 16. The 3-connected triangular and the 6-connected hexagonal organic linker.

In COF literature, none of these two linkers have been reported up to date. There are few examples of two-dimensional (2D) COFs with smaller or reduced amine building blocks (Figure 17). [1], [2] Our goal was to synthesize expanded organic units to create novel COFs with increased aromaticity and porosity. [3]

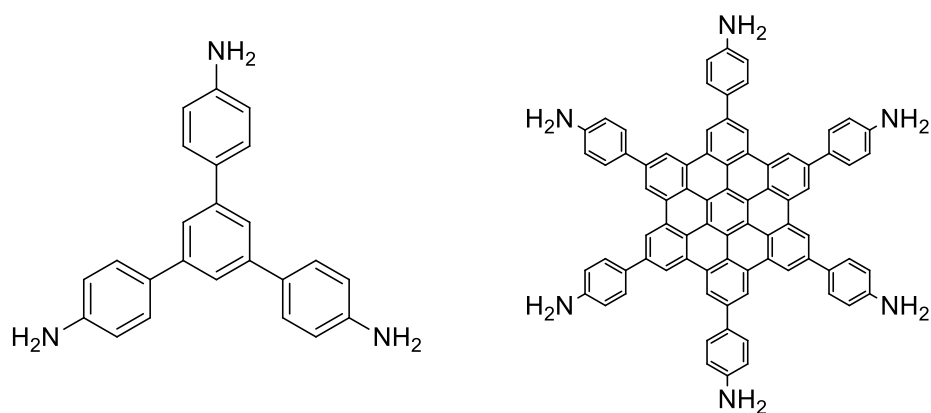


Figure 17. The building blocks of the TAPB-PDA COF (right) and the HBC-COF (left).

General methods

All the as-made materials, immediately isolated after the completion of the reaction, showed no Bragg peaks. Surprisingly when the solids were immersed in tetrahydrofuran (THF) to fully exchange the 1,4-dioxane molecules, powder X-ray diffraction (PXRD) patterns show the presence of a strong, low angle Bragg peak, suggesting the presence of a large periodicity (large d-spacings), originating from a regular pore arrangement. Apart from the 1,4-dioxane exchange, THF dissolves and removes any remaining starting materials. This THF soaking period varies from five days to two months, depending on the material. The results suggest that this kind of treatment provides to the individual layers the necessary time (kinetic effect) to be arranged in a periodic fashion by maximizing favorable π - π stacking interactions.

After the PXRD structural characterization of the materials, a suitable activation procedure was applied and evaluation of gas sorption properties was executed. It was observed that in contrast to THF treatment, when the solids were immersed in dimethylformamide (DMF), the supernatant liquid was turned into dark reddish color, indicating that DMF is capable in removing unreacted starting materials (the aldehyde and amine are colored). This can be attributed to the higher polarity of DMF versus THF and also to a possible swelling effect that expand the layers and provide access to any trapped unreacted organic molecules. Daily exchange of the THF took place with 3 ml DMF (3 exchanges per day). The copious exchanges were stopped only when the supernatant liquid was colorless, indicating the complete removal of all unreacted molecules. For the final activation step which requires the removal of all solvent molecules via vacuum with or without heating, it is important to exchange DMF with a more volatile solvent, in order to minimize framework-solvent interactions and in this way avoid possible structural deformation or even collapse of the porous network. For this reason, daily exchange of the DMF took place with 3 ml THF (3 exchanges per day). After the removal of the THF some samples were activated under dynamic vacuum at room temperature, at 80 °C or 120 °C, for 20 hours.

Interestingly, only with these two solvents our materials could be properly activated. We tried also other solvents, such as ethanol, 1,4-dioxane, chloroform and acetonitrile but none of them was successful.

2.1 Synthesis of COF 1a

For a given system, bearing one kind of aldehyde and one kind of amine as reagents, two different syntheses were executed, with and without aniline. The reason was to explore the effect of the modulator on the quality of the final product, in terms of the degree of crystallinity.

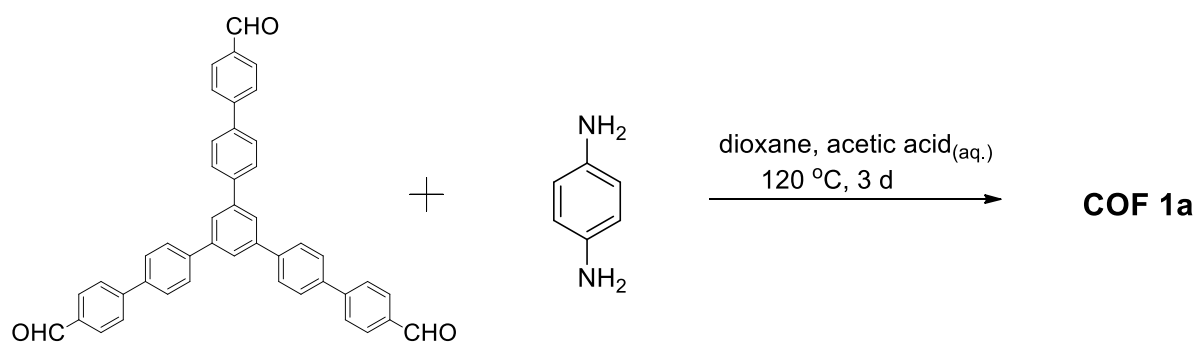


Figure 18. The synthesis of COF 1a without aniline.

Under argon atmosphere, trialdehyde (80 mg, 0.129 mmol) and p-Phenylenediamine (20.9 mg, 0.1935 mmol) were added into a two-neck flask with 5.2 mL 1,4-dioxane. The mixture was sonicated for 10 min and 3 M AcOH_(aq.) (1.04 mL) was added. The reaction mixture was stirred and refluxed at 120 °C for 3 days to afford a yellow solid (Figure 18).

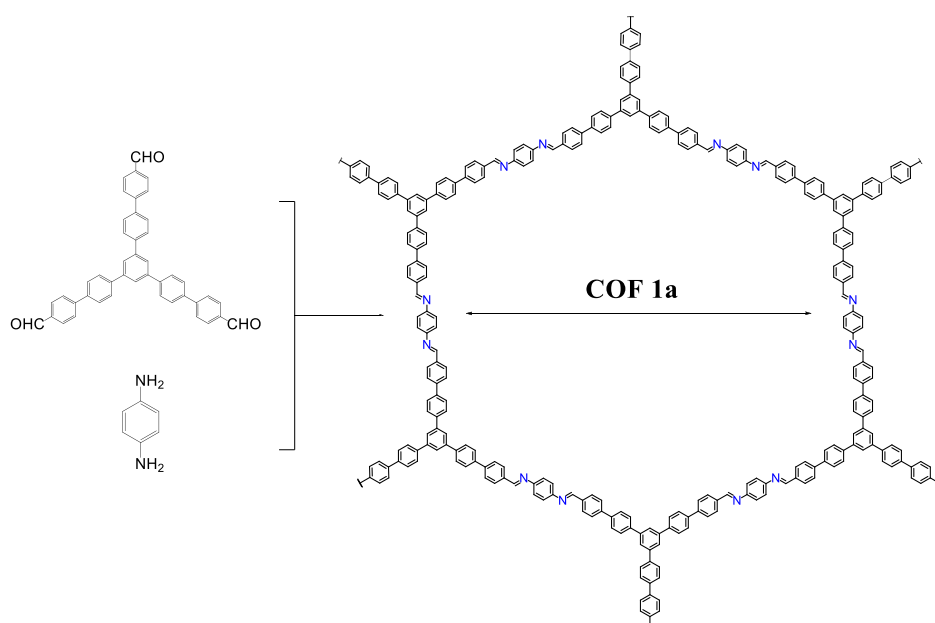


Figure 19. Schematic representation of the synthesis of imine-linked COF 1a

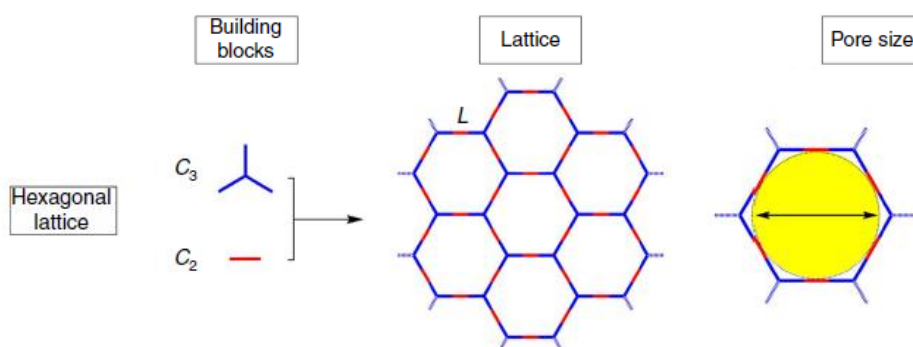


Figure 20. Topology diagram for COFs with hexagonal lattice and their pore size [2].

The morphology of the final product was studied with scanning electron microscopy (SEM). The figures that follow reveal the formation of relatively uniform, small, irregularly shaped, spongy particles, of size approximately 1 μM (Figure 21). The variation of the morphology between the particles is typical of the reported SEM images of COFs.

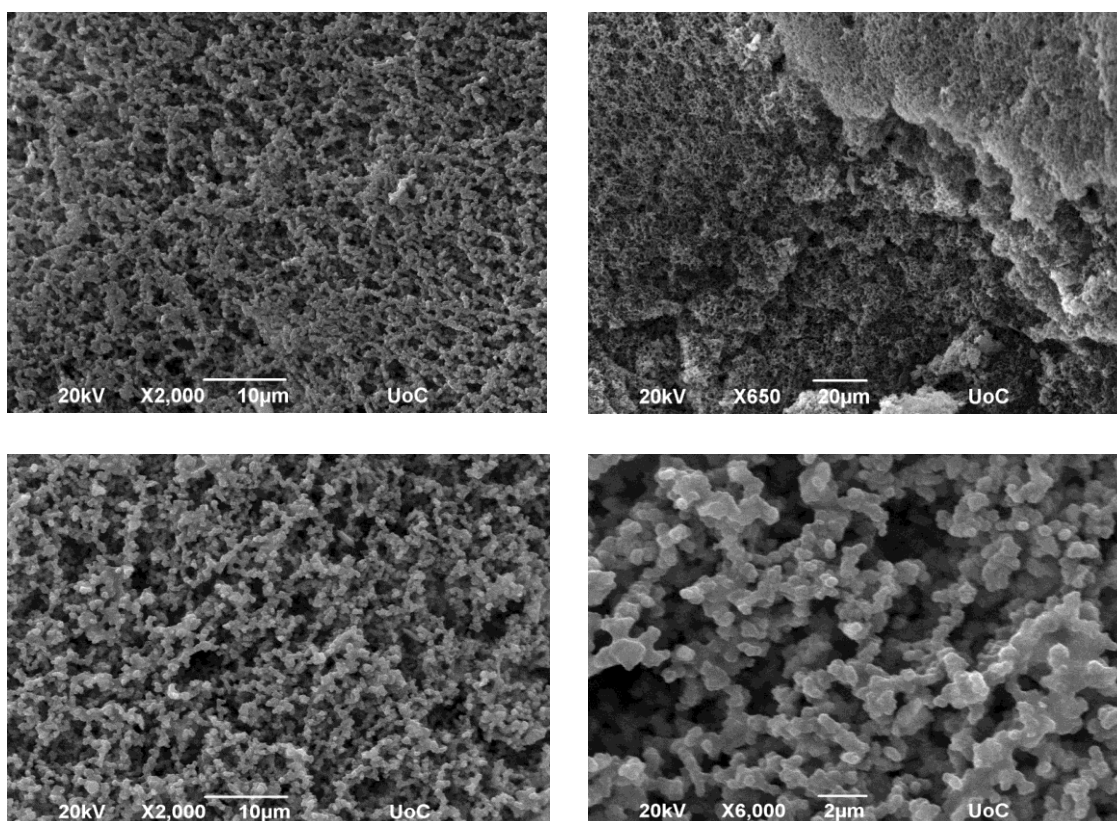


Figure 21. SEM images of COF 1a

2.1.1 Structural Characterization of COF 1a

According to general methods the solid was immersed in tetrahydrofuran for 5 days to fully exchange the 1,4-dioxane molecules. PXRD pattern (Figure 22), shows the presence of strong, low angle Bragg peak at 2.13° 2θ degrees (41.6 \AA), followed by two weak but clearly visible peaks centered at 3.6° (24.6 \AA) and 4.2° (21.1 \AA) 2θ angles, respectively. The observed Bragg peaks are indexed into a hexagonal lattice with a unit cell size of 49.6 \AA . This pattern suggests the presence of pores with hexagonal periodicity. No Bragg peaks were observed at high angles, indicating that the framework is atomically amorphous.

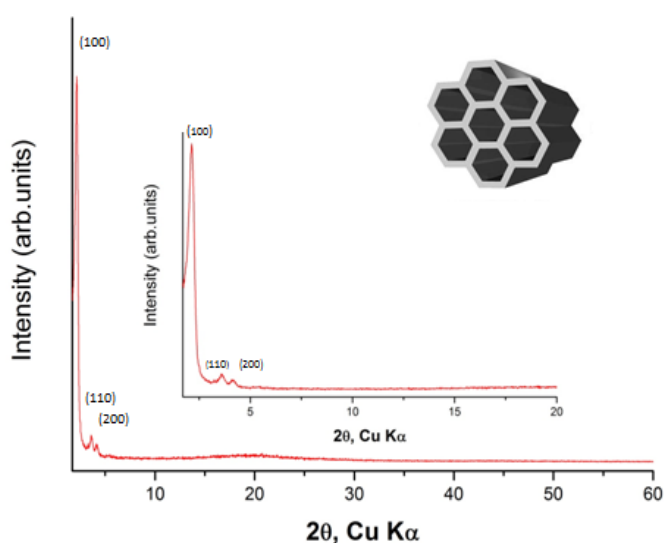


Figure 22. Experimental PXRD pattern of the COF 1a.

The thermal stability of this material was studied using a thermogravimetric analyzer (TGA). Accordingly, few milligrams of the sample was placed on a quartz pan and heated up to 600°C with a heating rate of 5°C min^{-1} , under nitrogen atmosphere. No significant weight loss was observed up to 450°C demonstrating the high thermal stability of the organic framework.

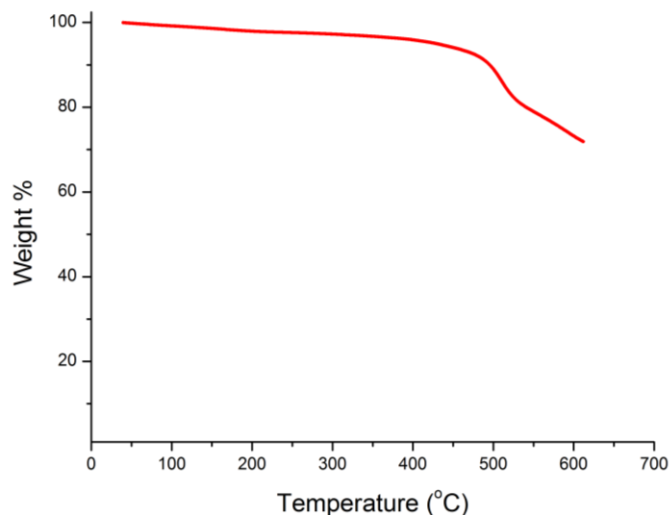


Figure 23. TGA of COF 1a under nitrogen atmosphere.

FT-IR spectroscopy of the COF 1a exhibited a stretching vibration band at $\sim 1600\text{ cm}^{-1}$ which can be assigned to C=N bond based on previously reported COFs. [1]

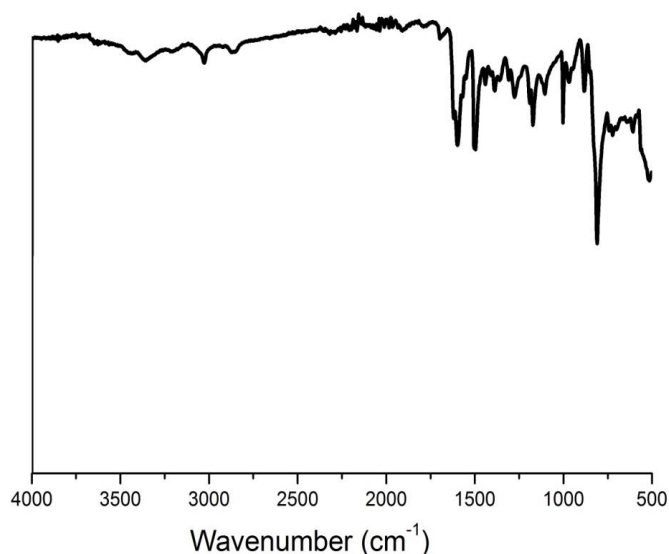


Figure 24. FT-IR spectra of COF 1a.

2.1.2 Gas sorption properties

After the successful characterization, a suitable activation procedure was applied and evaluation of gas sorption properties was executed. Argon sorption measurements at 87 K confirmed the permanent porosity of COF 1a. Accordingly, the calculated BET surface area, using consistency criteria, was estimated to be $250\text{ m}^2\text{ g}^{-1}$ (Figure 25). The pore size

distribution curve revealed one peak centered at 40 Å (Figure 26). The experimental total pore volume is 0.23 cm³ g⁻¹ at 0.99 p/p₀.

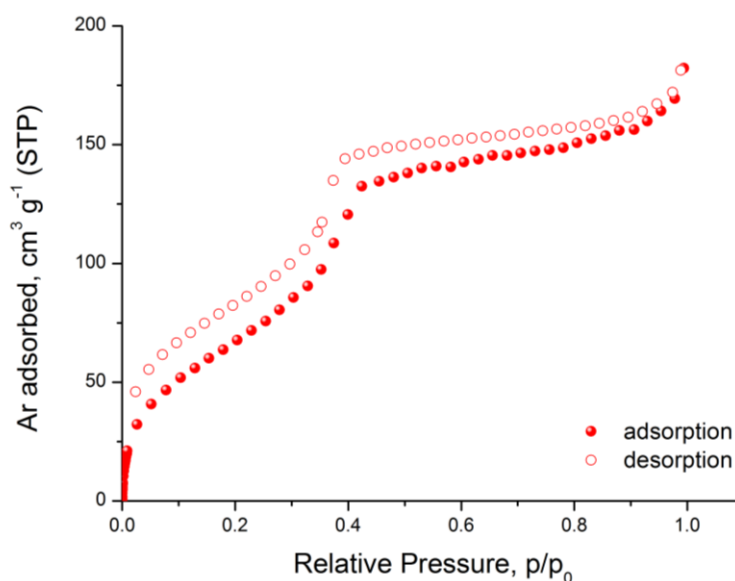


Figure 25. Argon sorption isotherm of the COF 1a recorded at 87 K.

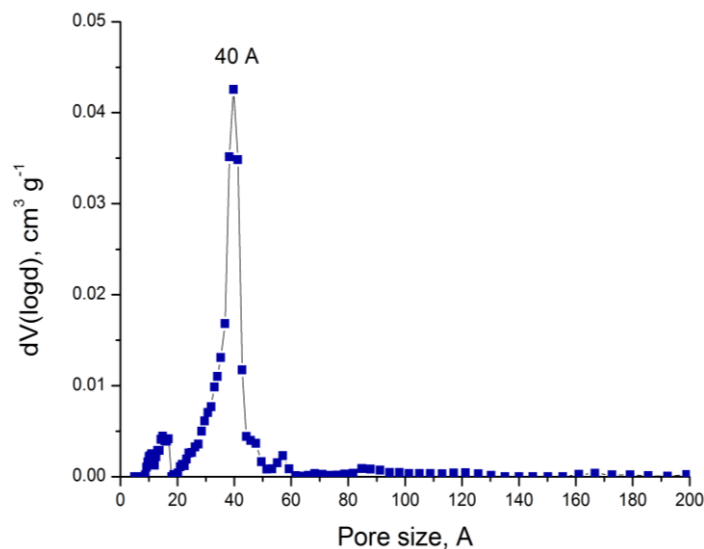


Figure 26. Pore size distribution.

Furthermore, in order to evaluate the gas sorption properties of this COF we performed CO₂ sorption measurements. Accordingly, CO₂ adsorption isotherms at 273 K and 298 K up to 1 bar were measured (Figure 27), from which the Q_{st} was calculated using a Virial type equation as well as the Clausius-Clapeyron equation, for comparison (Figure 28). At zero coverage (Q_{st}⁰) the corresponding value was found to be 29.5 kJ mol⁻¹.

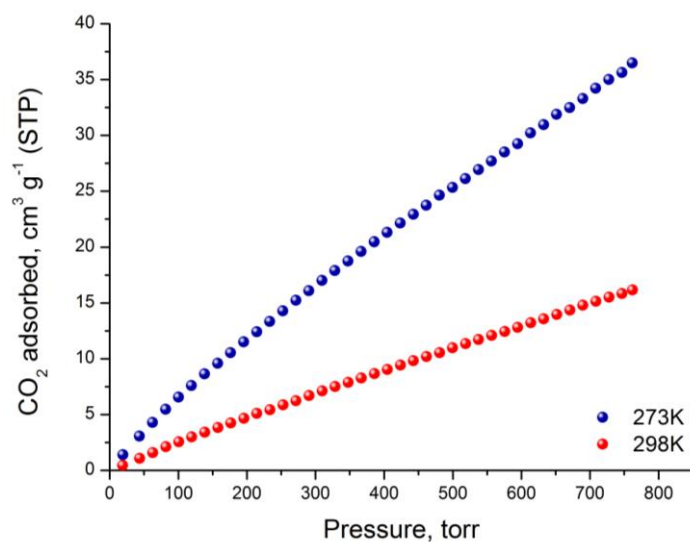


Figure 27. CO₂ sorption isotherms of COF 1a at the indicated temperatures, up to 1 bar.

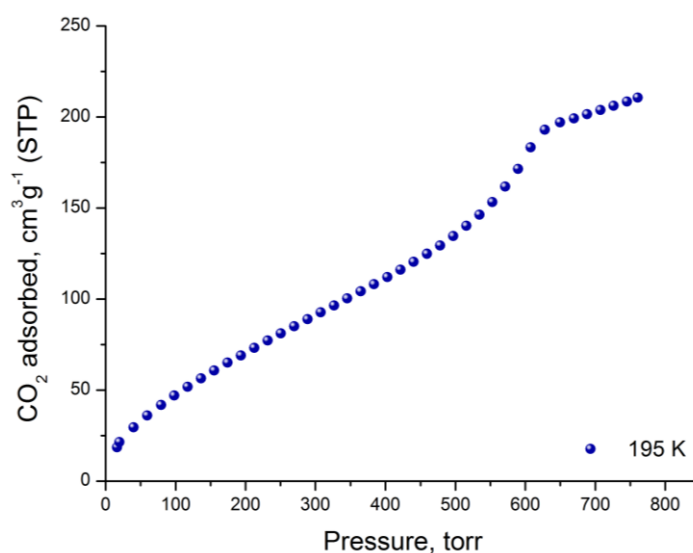


Figure 28. CO₂ sorption isotherm of COF 1a at 195 K.

Carbon dioxide adsorption isotherm was also measured at 195 K up to 1 bar (Figure 28), in order to probe the pore system of this COF. The isotherm shows a gradual increase in uptake with increasing pressure up to 500 torr, followed by a relatively steep increase between 550 and 650 torr and finally reaching a semi-plateau at 700 torr. The step increase in uptake is attributed to the “solidification” of CO₂ inside the mesopores. The corresponding total pore volume is 0.4 cm³ g⁻¹, which is very close to the value obtained from the Ar isotherm, indicating that the pore system is fully accessible by CO₂ molecules.

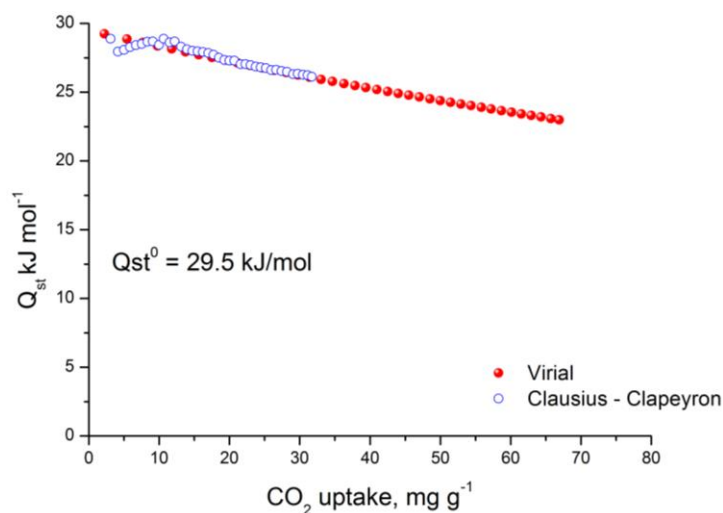


Figure 29. Calculated isosteric heat of adsorption for CO₂.

The observed Q_{st}^0 of CO₂ for COF 1a is among the best for imine-based COFs [4] [5] [6]. The CO₂ uptake at 273 K, 298 K and 1 bar is 36.5 cm³ g⁻¹ and 16.2 cm³ g⁻¹ respectively and compares well with reported COFs if we take into account the surface area and pore size. For example ACOF-1 has similar monomers as our COF 1a (Figure 30) shows a BET area of 1176 m² g⁻¹, with pore size of 9.4 Å. The CO₂ isotherm of ACOF-1 at 273 K and 1 bar, shows 180 cm³ g⁻¹ of CO₂ uptake (Figure 31). The corresponding isosteric heat of adsorption at zero coverage is 27.6 kJ mol⁻¹, which is one of the highest reported values for COFs with imine-linked organic cages. [4]

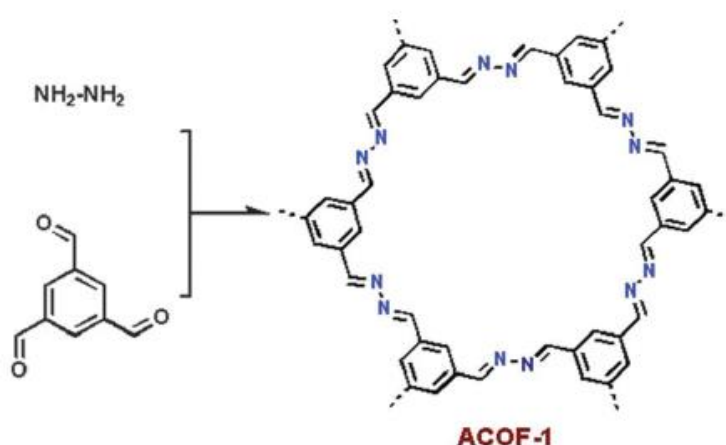


Figure 30. Schematic representation of the synthesis of ACOF-1 [4].

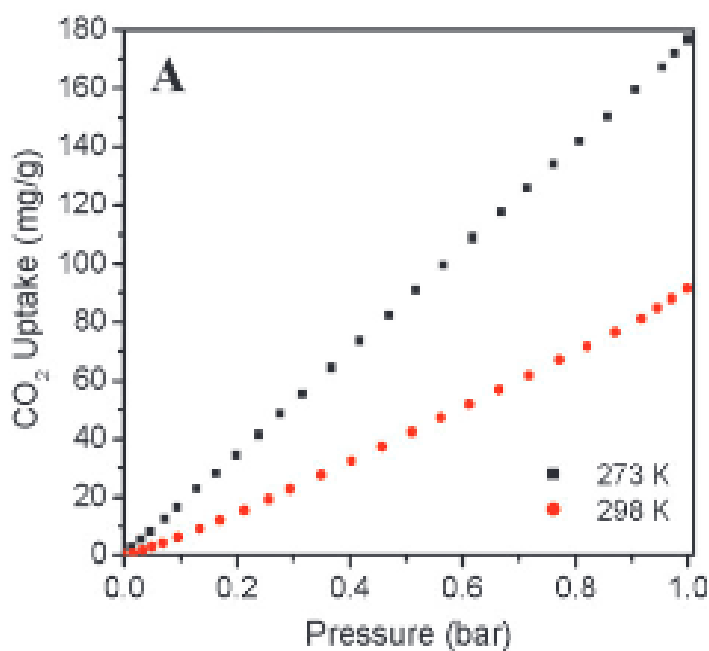


Figure 31. CO₂ sorption isotherms of ACOF-1 at the indicated temperatures, up to 1 bar. [4].

2.2 Synthesis of COF 1b

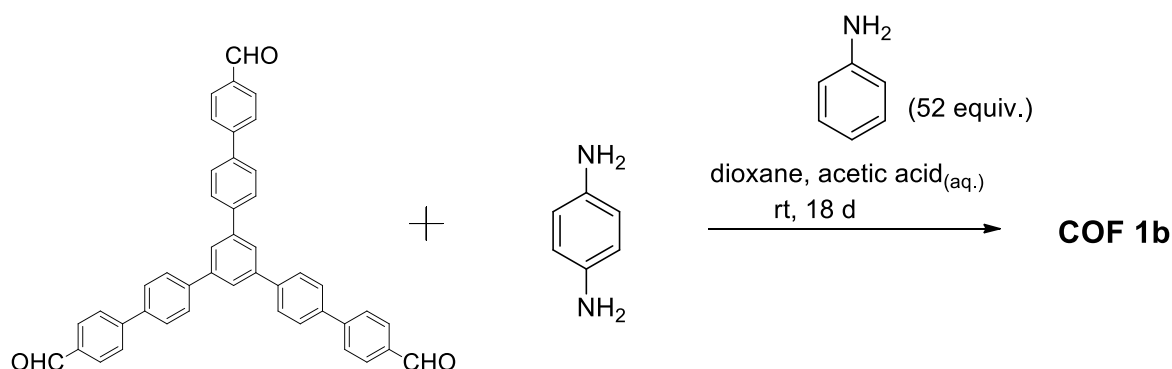


Figure 32. The synthesis of COF 1b with aniline.

A vial was charged with trialdehyde (17 mg, 0.027 mmol), aniline (0.12 mL, 52 eq) and 0.5 mL of 1,4-dioxane, then 0.2 mL of aqueous acetic acid (6 M) was added to the solution. p-Phenylenediamine (4.5 mg, 0.042 mmol) dissolved in 1,4-dioxane (0.5 mL) was then added. The mixture was allowed to stand further at ambient temperature and the COF 1b was slowly crystallized. After 18 days a yellow solid was obtained (Figure 32).

The morphology of the final product was studied with SEM (Figure 33). Interestingly, this COF is made of relatively large (>20 μm) flake-like particles with sharp facets and edges. The shape of some of them resembles the shape of a hexagonal unit cell

(angles of 60 and 120 degrees). This kind of particles morphology is in marked contrast compared to the particles obtained using the same monomers but without aniline. The origin of this differentiation is currently under investigation.

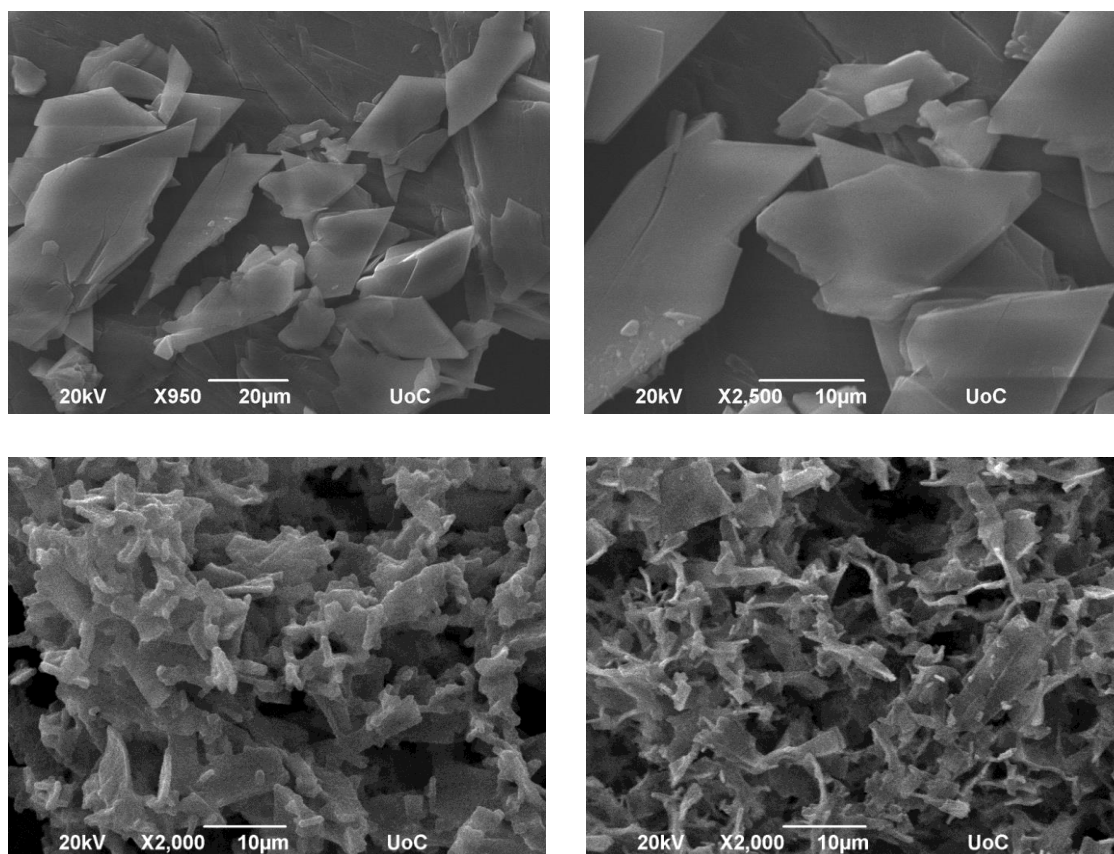


Figure 33. SEM images of COF 1b.

The morphology of the COF 1b was also studied with the use of transmission electron microscopy (TEM) (Figure 34). A representative high resolution TEM image is shown in figure 34 where lattice fringes with periodicity $\sim 12 \text{ \AA}$ are observed. The observed atomic periodicity could be associated with the mean layer-to-layer distance within the COF structure.

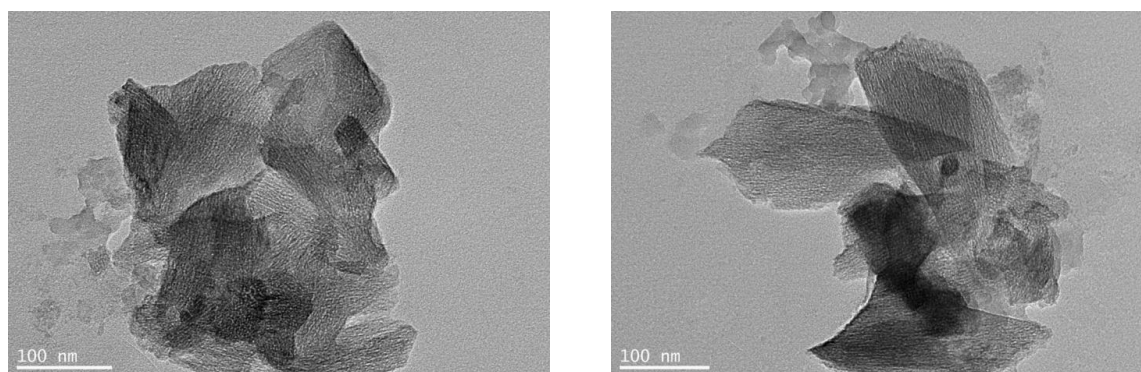
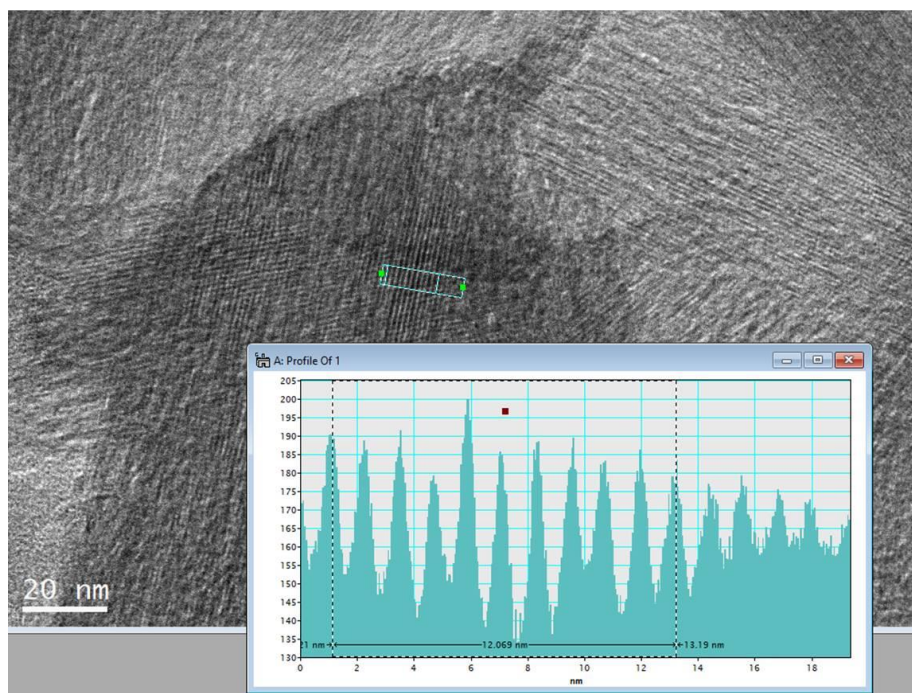


Figure 34. Representative high resolution TEM images of COF 1b.

2.2.1 Structural Characterization of COF 1b

The material was kept for 2 months in THF and further characterized by PXRD. This time, the pattern shows sharp diffraction peaks at 2.38° (36.9 \AA), 4.7° (18.6 \AA), 7.1° (12.4 \AA), 14.7° (6.0 \AA) and 23.9° (3.7 \AA) from which the first three suggest the formation of a lamellar (layered) structure, consistent with miller indices (100), (200) and (300) while the other two could be assigned to in-plane reflections (Figure 35). To our surprise, the use of aniline at ambient temperature in the same system resulted in a different material.

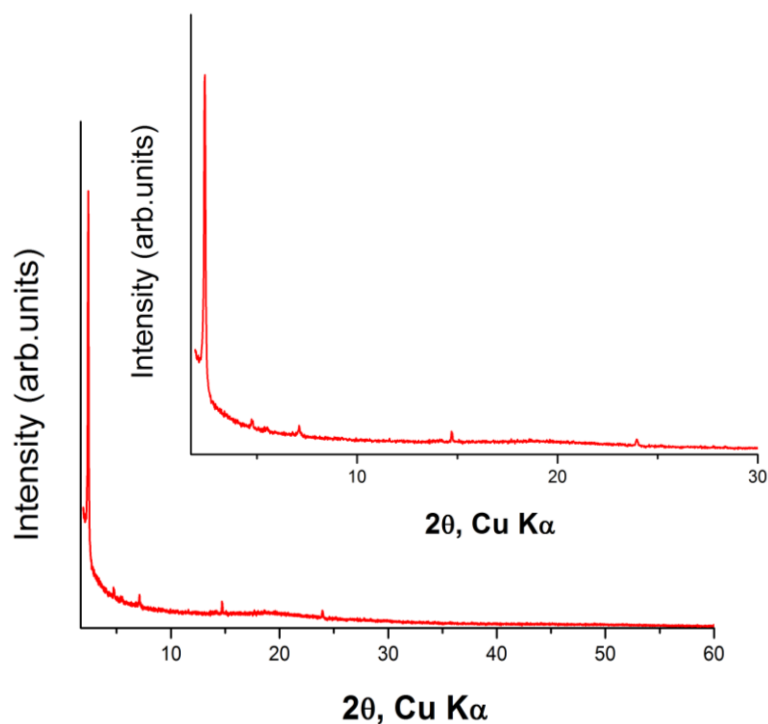


Figure 35. Experimental PXRD pattern of the COF 1b.

After the general procedure that we follow and the removal of the THF the sample was not activated under dynamic vacuum at room temperature for 20 hours. We tried also to activate the COF under dynamic vacuum for 20 hours at 80 °C and 120 °C, but unfortunately it was not possible the activation as well.

Comparing the two different synthetic methods applied in COF 1, we come to the conclusion that under solvothermal reaction conditions in only three days reaction time without the use of aniline, it was much easier and successful the characterization and activation of this COF. It is entirely possible that the aniline-based synthesis results in a COF that contains some bound aniline in the framework causing a disruption of the 2D network that in turn leads to loss of porosity and periodicity. In any case, questions are open and further experimentation is needed.

2.3 Synthesis of COF 2a

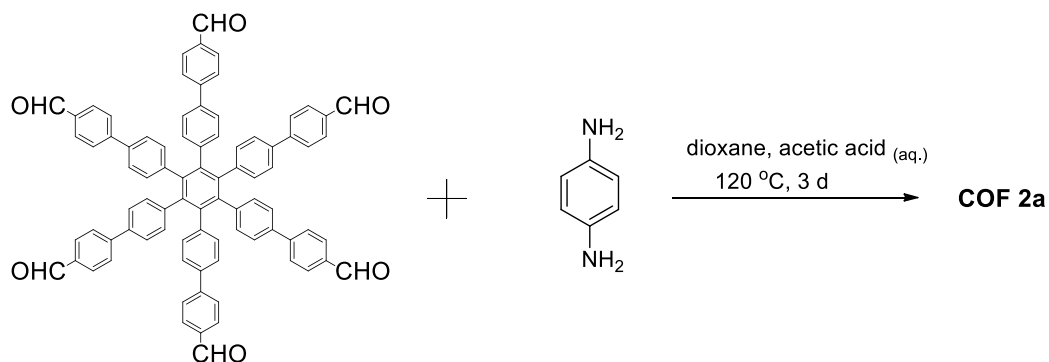


Figure 36. Synthesis of COF 2a without aniline.

Under argon atmosphere, hexaldehyde (13 mg, 0.011 mmol) and p-Phenylenediamine (3.64 mg, 0.033 mmol) were added into a two-neck flask with 2 mL 1,4-dioxane. The mixture was sonicated for 10 min and 3M AcOH_(aq) (0.4 mL) was added. The reaction mixture was stirred and refluxed at 120 °C for 3 days to obtain a yellow solid (Figure 36).

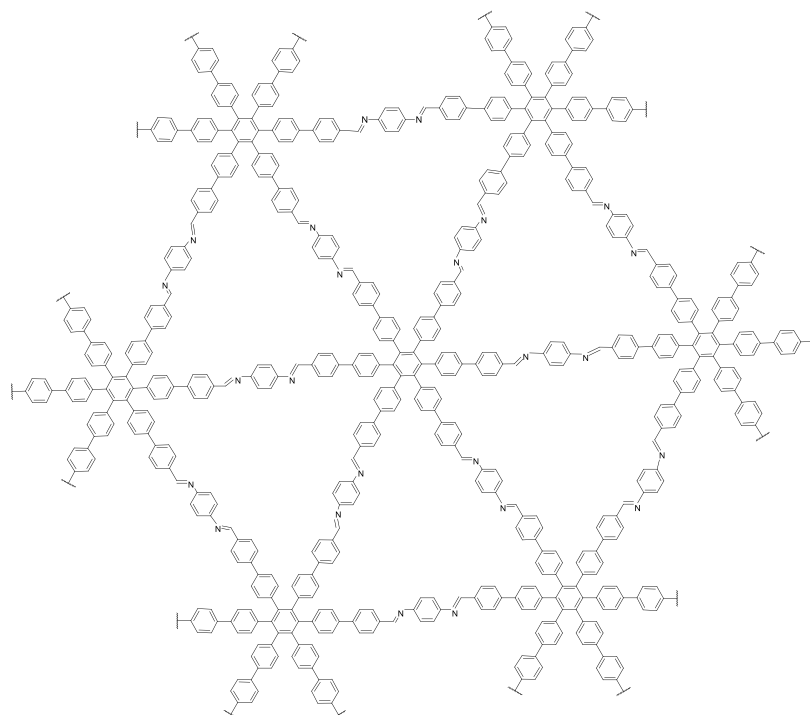


Figure 37. Schematic representation of the synthesis of imine-linked COF 2a.

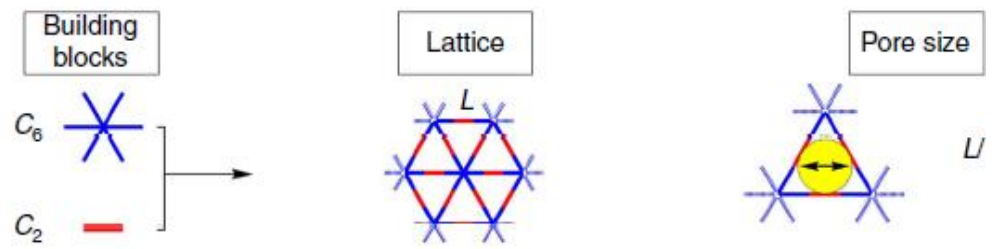


Figure 38. Topology diagrams for this kind of COFs and their pore size [2].

The morphology of the final product was studied with (SEM) (Figure 39). Interestingly, this COF is made of very large ($>500\ \mu\text{m}$) flake-like particles with sharp facets and edges. The shape of some of them resembles the shape of a hexagonal unit cell (angles of 60 and 120 degrees).

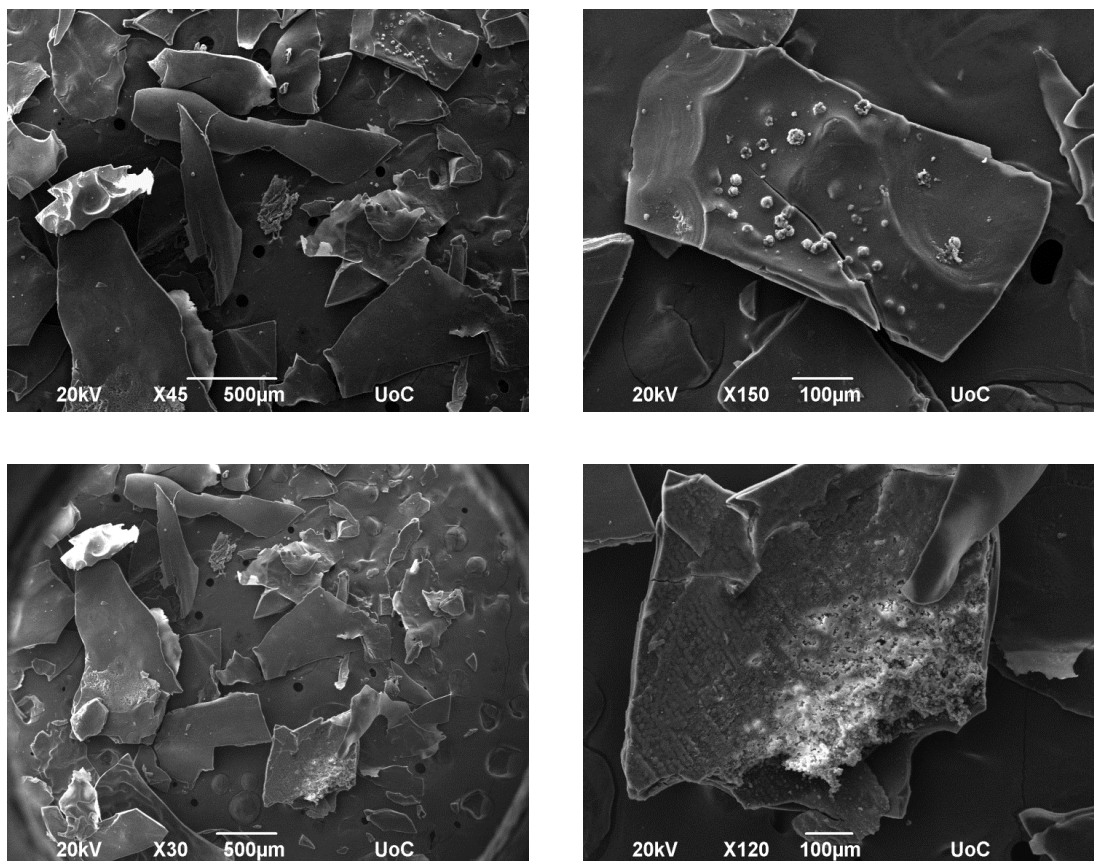


Figure 39. SEM images of COF 2a.

2.3.1 Structural Characterization of COF 2a

The solid was immersed in THF for six weeks. After that treatment the corresponding PXRD pattern shows the presence of a strong Bragg peak at 2.38° (37 \AA) angle followed by weaker peaks at 4.7° (18.7 \AA), 7.1° (12.4 \AA) and 29.5° (3 \AA) 2θ position, from which the first three suggest the formation of a lamellar (layered) structure, consistent with miller indices (100), (200) and (300) while the last one could be assigned to an in-plane reflections, similar to COF 1b (Figure 40). The formation of a layered structure without the use of aniline as modulator is in marked contrast with the case of COF -1.

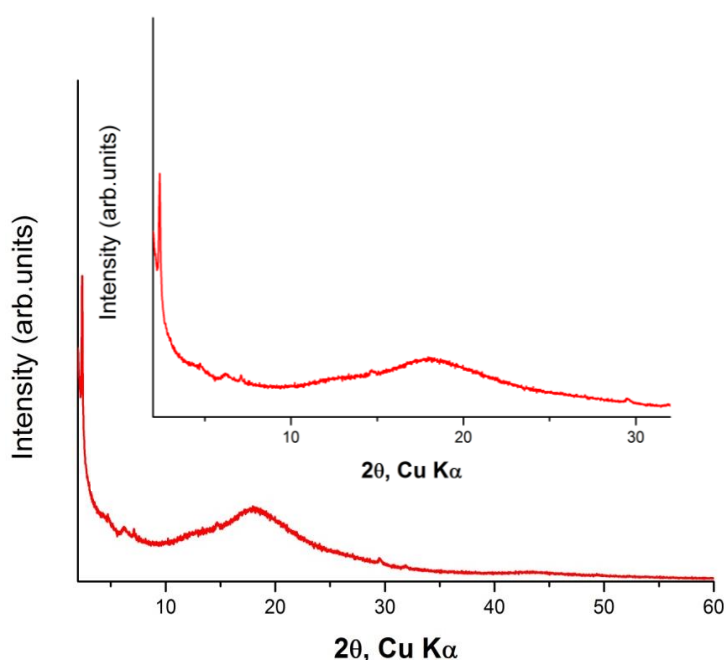


Figure 40. Experimental PXRD pattern of the COF 2a.

The thermal stability of this material was studied using a thermogravimetric analyzer (TGA). Accordingly, few milligrams of the sample was placed on a quartz pan and heated up to 600°C with a heating rate of 5°C min^{-1} , under nitrogen atmosphere. A relatively steep weight loss was observed between 110°C and 200°C , which is attributed to the presence of DMF. Between 200°C and 400°C a gradual decrease in weight is observed which could be attributed to some strongly bound DMF molecules and/or unreacted molecules. Above 400°C , the observed steep decrease is attributed to framework decomposition (Figure 41).

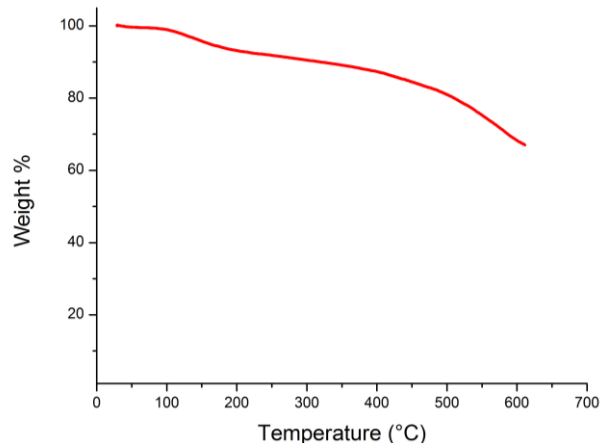


Figure 41. TGA of COF 2a under a nitrogen atmosphere.

FT-IR spectroscopy of the COF 2a exhibited a stretching vibration band at $\sim 1600\text{ cm}^{-1}$ which can be assigned to C=N bond based on previously reported imine-based COFs.

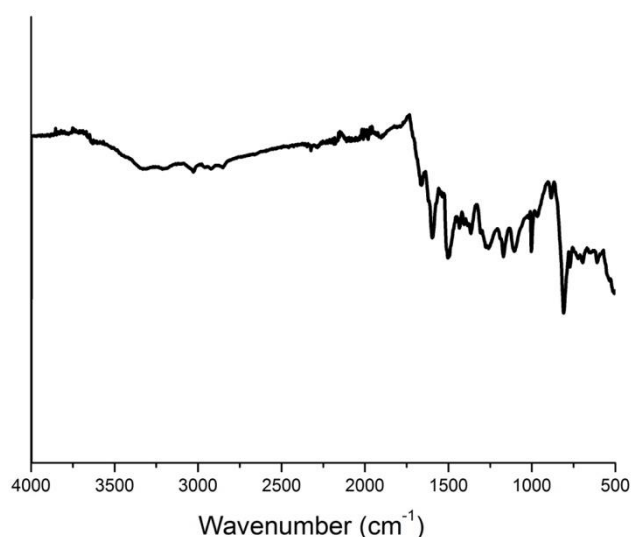


Figure 42. FT-IR spectra of COF 2a.

The material was not possible to be activated despite the copious exchanges of the solvents, according to general methods that we followed. After the removal of the THF the sample was evacuated under dynamic vacuum at room temperature for 20 hours. The nitrogen adsorption isotherm recorded at 77 K showed that this material is not porous. We tried also to activate the COF under dynamic vacuum for 20 hours at 80 °C and 120 °C but unfortunately it was not possible as well.

As far as the literature results are concerned, nitrogen sorption isotherm was measured at 77 K for HPB-COF (Figure 43). HPB-COF is an imine-linked COF, which was

synthesized without the use of aniline according to the typical solvothermal conditions. This reported COF has a similar but smaller monomeric aldehyde as building block, as ours (Figure 44). [2] Therefore, the fact that our material is not becoming porous after removal of solvent molecules, could be attributed to the fact that HPB-COF and COF 2a have different structures, being hexagonal and lamellar, respectively. In particular, the results suggest that the lamellar structure provides no accessible space between neighboring layers, as the hexagonal structure does. In the later, favorable π - π stacking interactions keep the layers in a eclipsed position (one of the top of the other) creating in this way pores with hexagonal periodicity. However, in case of the larger monomer in COF 2a, the relative positioning of the phenyl rings could result to reduced π - π interactions, causing the formation of a staggered arrangement with no accessible porosity.

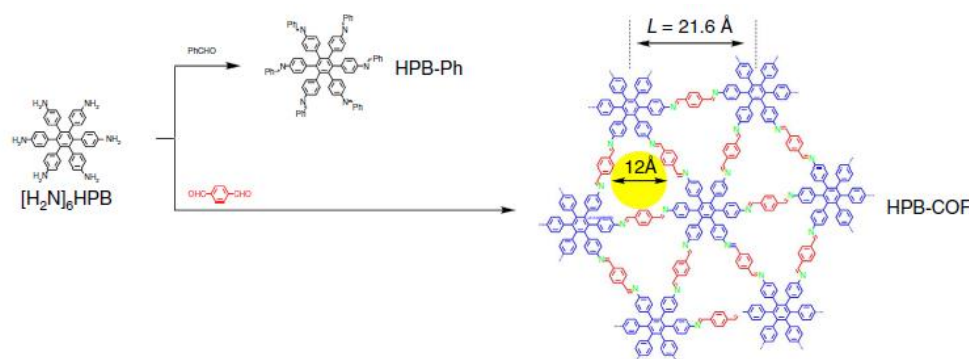


Figure 43. Schematic representation of the synthesis of imine-linked HPB-COF [2].

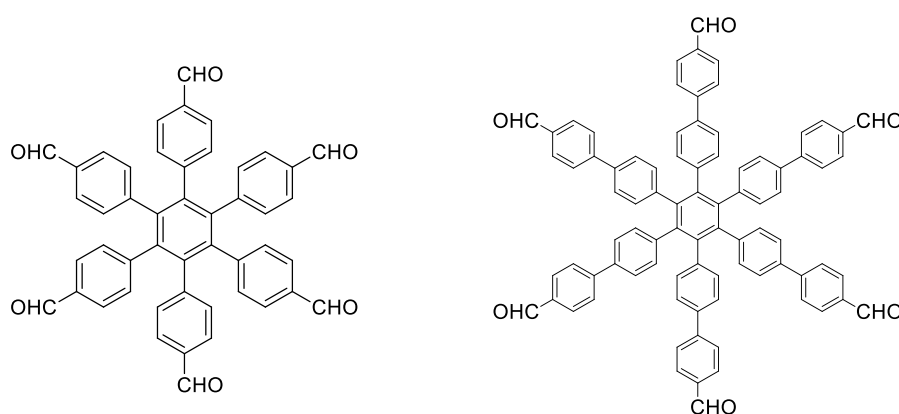


Figure 44. The 6-connected organic linker of HPB-COF (left) and the 6-connected organic linker of COF 2a (right).

2.4 Synthesis of COF 2b

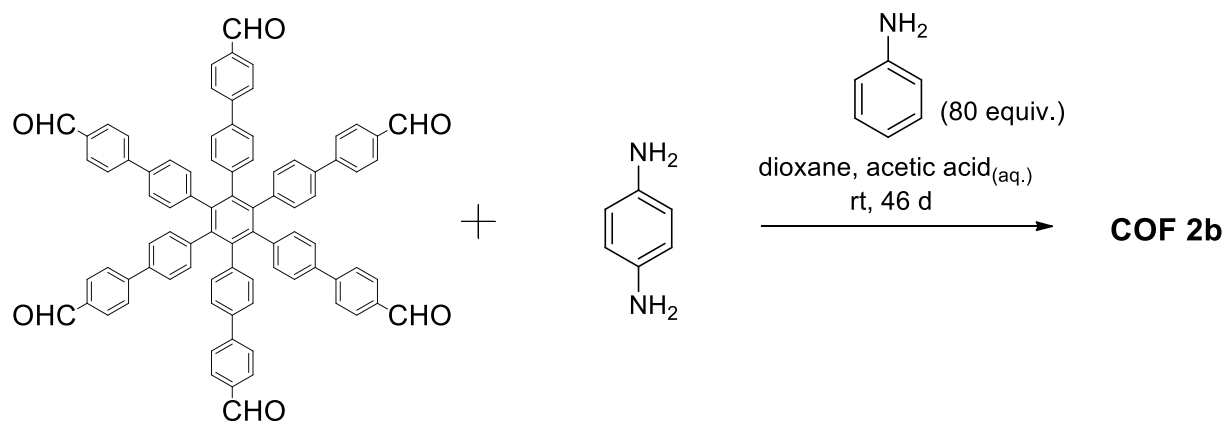
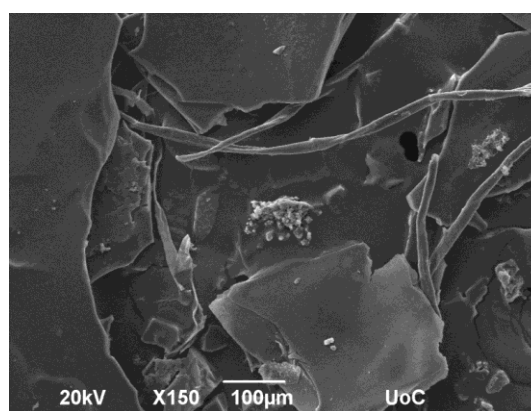
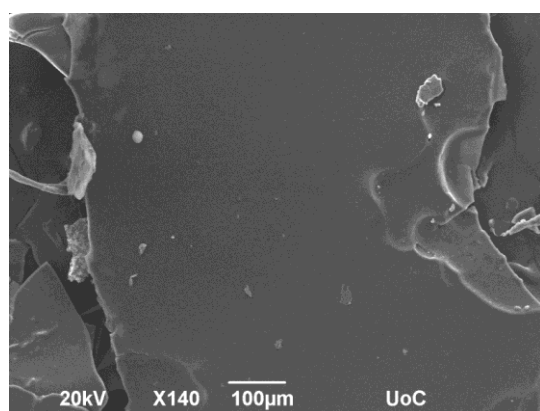


Figure 45. The synthesis of COF 2b with aniline.

A vial was charged with hexaldehyde (10 mg, 0.008 mmol), aniline (58 μ L, 80 eq) and 1 mL of 1,4-dioxane. Then, 0.2 mL of aqueous acetic acid (6 M) was added to the solution. Finally, p-Phenylenediamine (2.7 mg, 0.026 mmol) dissolved in 1,4-dioxane (1 mL) was added. The mixture was allowed to further stand at ambient temperature where the COF 2b was slowly precipitated. After 46 days a yellow product was obtained (Figure 45).

The morphology of the final product was studied with the use of SEM (Figure 46). This COF is also made of very large (>500 μ m) flake-like particles with sharp facets and edges. This kind of particles morphology is almost identical to the particles obtained using the same monomers but without aniline. This similarity is probably due to the large size of the monomer.



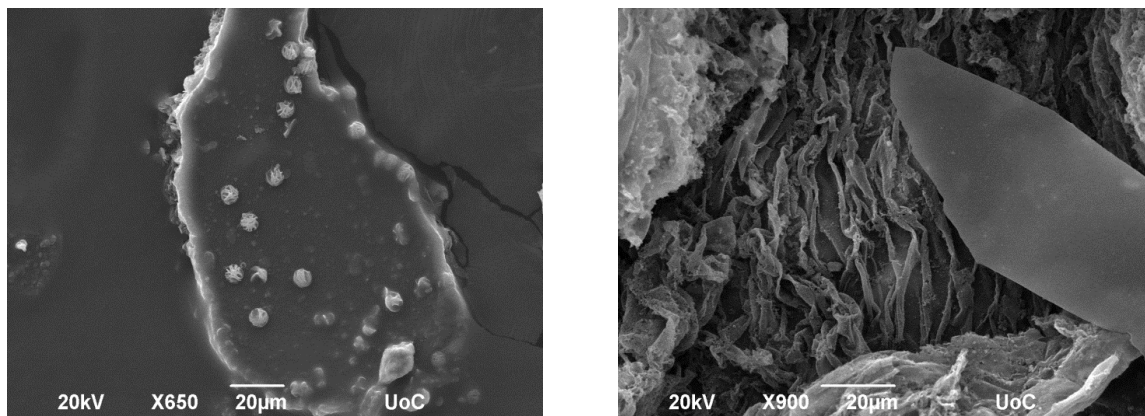


Figure 46. SEM images of COF 2b.

2.4.1 Structural Characterization of COF 2b

The solid was immersed in THF for four weeks. After that treatment the corresponding PXRD pattern shows the presence of a strong Bragg peak at 2.4° ($d=36.6 \text{ \AA}$) angle followed by a very weak peak at 7.1° ($d=12.5 \text{ \AA}$) 2θ position (Figure 47).

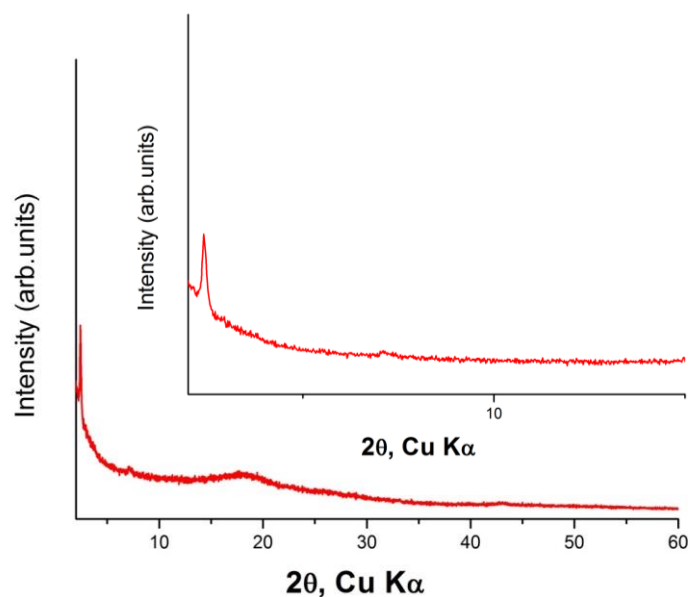


Figure 47. Experimental PXRD pattern of the COF 2b.

2.4.2 Gas sorption properties

The material was activated after the copious exchanges of the solvents according to general procedures. The activation was occurred under dynamic vacuum at 120°C for 20 hours. To evaluate the permanent porosity, a nitrogen sorption isotherm was recorded at 77 K

(Figure 48). The calculated BET surface area, using consistency criteria, was estimated to be $105 \text{ m}^2 \text{ g}^{-1}$ and the experimental total pore volume is $0.14 \text{ cm}^3 \text{ g}^{-1}$ at 0.99 p/po.

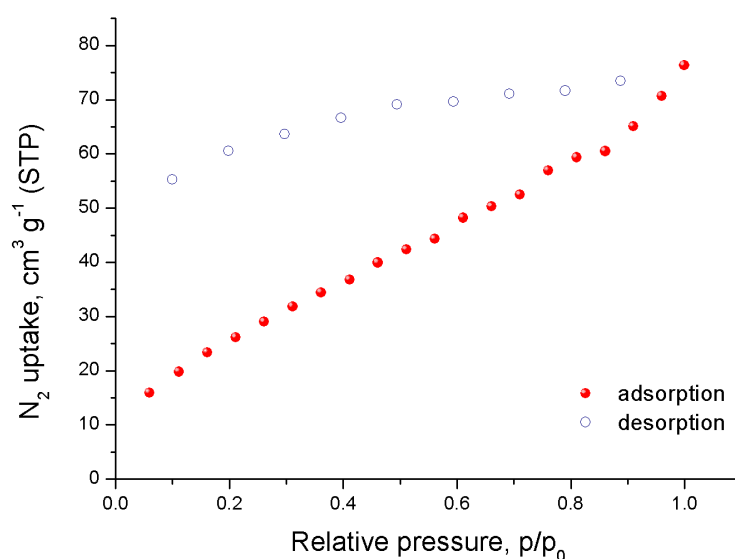


Figure 48. Nitrogen sorption isotherm of COF 2b recorded at 77 K.

The adsorption isotherm shows an almost steady increase in N₂ uptake, reaching $75 \text{ cm}^3 \text{ g}^{-1}$ (STP) at 1 bar. Interestingly, the desorption isotherm shows a large hysteresis that goes down at very low relative pressures. This behavior could be explained by the presence of a highly flexible structure. These results need to be further confirmed and therefore additional experiments are required.

Comparing the two synthetic methods of COF 2, the results suggest that in contrast with COF 1a, the use of aniline as a modulator indeed provides a material with some porosity.

3. Synthetic Procedures of COFs with tetratopic and hexagonal building units

In this chapter, we present the synthesis and the characterization of three novel COFs with new topologies. In order to synthesize these materials, suitable organic linkers with rectangular and hexagonal connectivity were designed and synthesized (Figure 49). The new COFs were obtained by combining the amine with aldehyde precursors in the presence of acetic acid, under controlled reaction conditions.

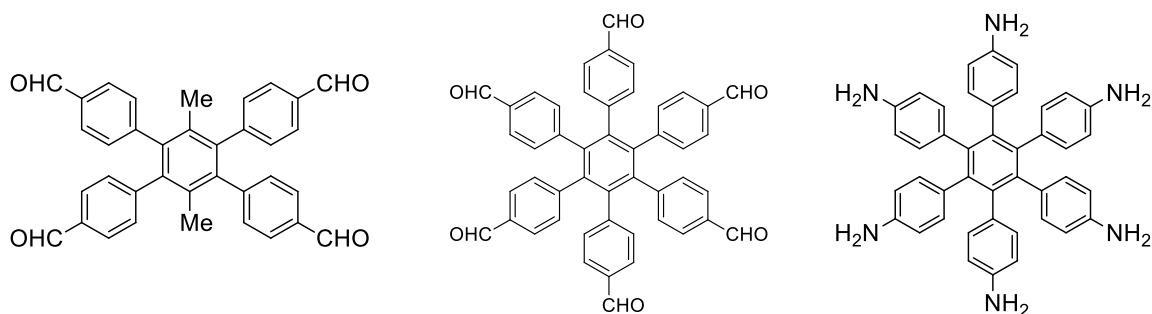


Figure 49. The 4-connected rectangular and the 6-connected hexagonal organic linkers that were synthesized.

It is noted that in literature, very limited imine-based COF have been reported based on similar organic linkers. The $[H_2N]_6$ HPB bearing six amino groups and the hexaldehyde with six-fold symmetry (Figure 50) are building blocks that are used in the past as monomers of HPB-COF and HEX-COF 1. [2] [7] HEX-based COFs with this type of structure are interesting due to their high π -density and extremely small pore size. To the best of our knowledge, the CO_2 sorption properties for HEX-based COFs, have not been reported up to date.

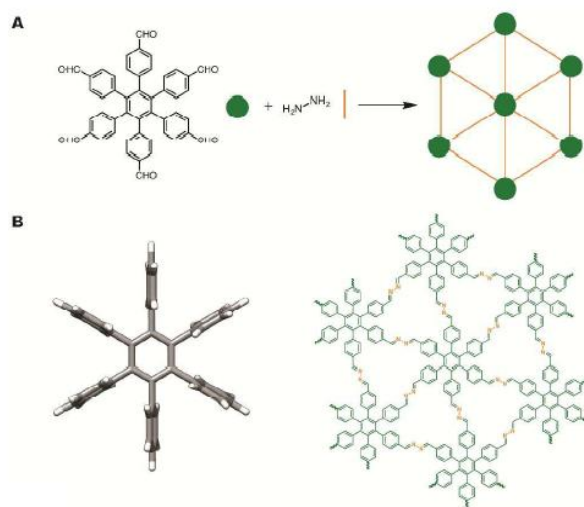


Figure 50. (A) Synthesis of a COF using a six fold symmetric HEX monomer containing aldehyde groups and hydrazine. (B) HEX-based monomers are non-planar as a result of the steric hindrance between the phenyl rings. Resultant COFs have topologically planar 2D structures despite the lack of planarity in the monomers [7].

3.1 Synthesis of COF 3a

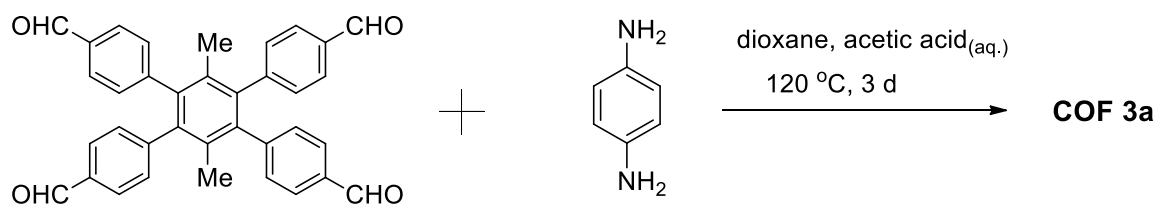


Figure 51. The synthesis of COF 3a without aniline.

Under argon atmosphere tetraldehyde (40 mg, 0.077 mmol) and p-Phenylenediamine (12.4 mg, 0.115 mmol) were added into a two-neck flask with 3 mL 1,4-dioxane. The mixture was sonicated for 10 min and 3 M AcOH (0.6 mL) was added. The reaction mixture was stirred and refluxed at 120 °C for 3 days to obtain a yellow precipitate (Figure 51).

The morphology of the final product was studied with the use of SEM (Figure 52). The figures that follow reveal the formation of small and chunky particles.

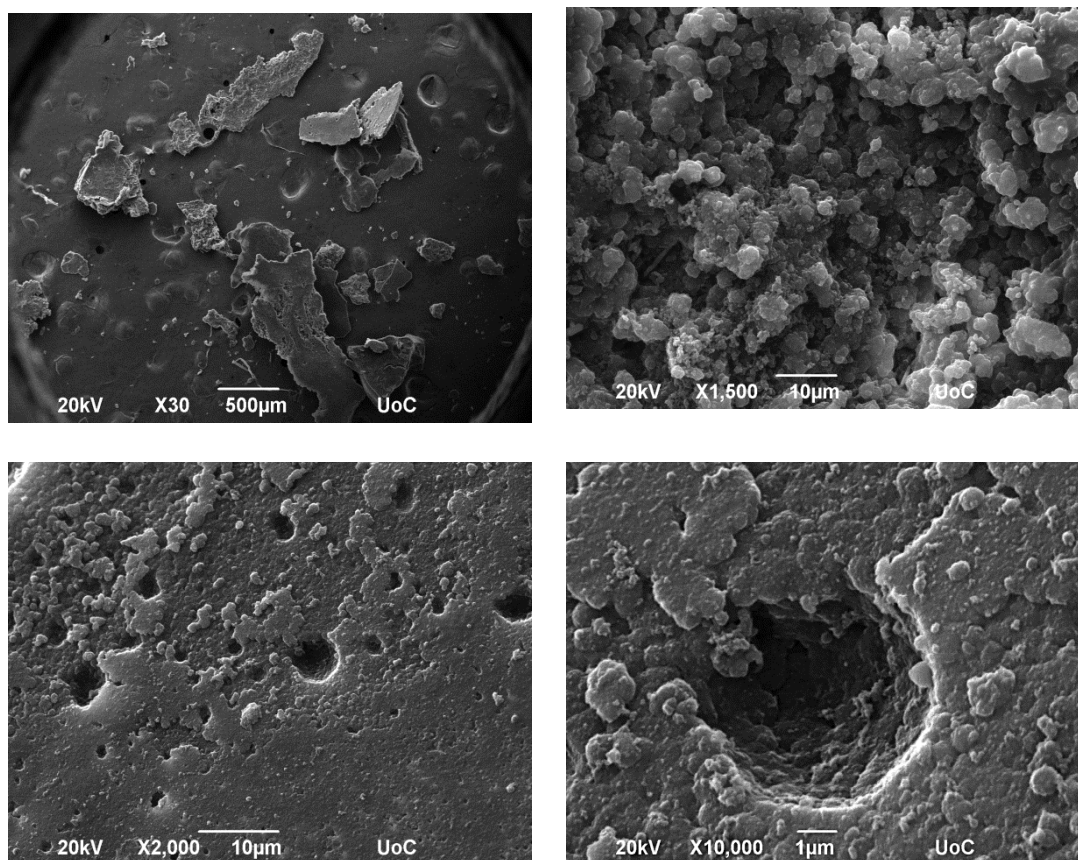


Figure 52. SEM images of COF 3a.

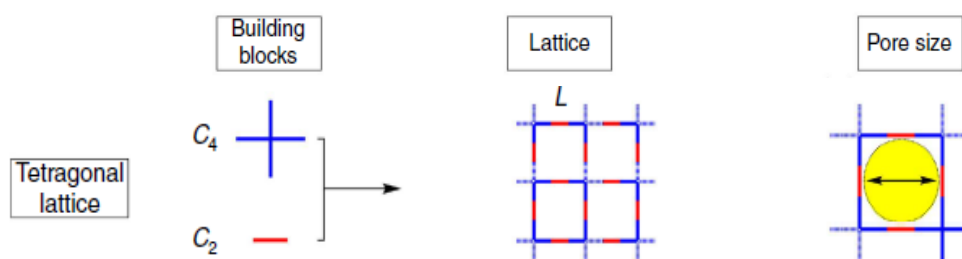


Figure 53. Topology diagrams for COFs based on a tetragonal and a linear building block and their pore size [2].

3.1.1 Structural Characterization of COF 3a

After the usual treatment the product was isolated and the corresponding PXRD pattern shows several broad Bragg peaks at low and high angle regions. This kind of PXRD patterns is quite unusual and suggests the formation of a COF with pore and atomic periodicity due to the presence of low and high angle Bragg peaks, respectively (Figure 54). Further investigation is required in order to understand the nature of the observed periodicities and the atomic structure of this novel COF.

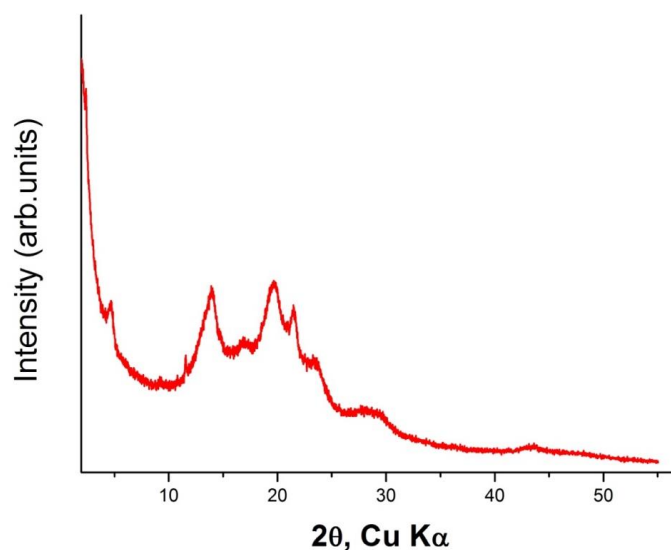


Figure 54. Experimental PXRD pattern of the COF 3a.

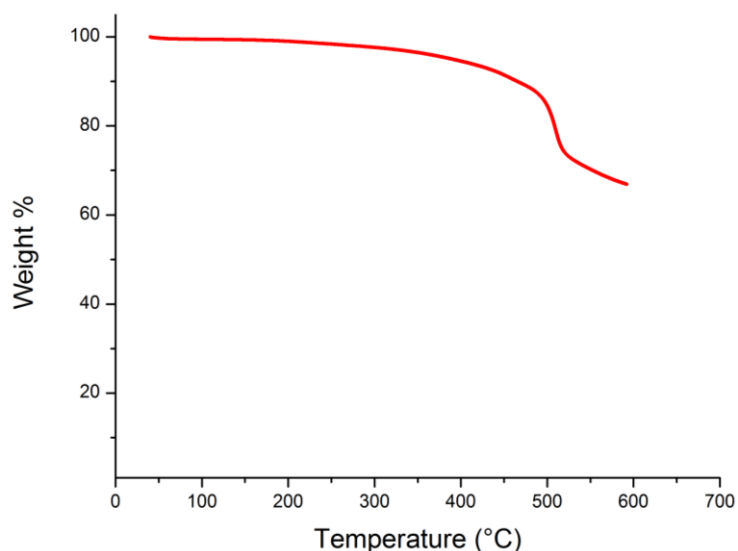


Figure 55. TGA of COF 3a under a nitrogen atmosphere.

The thermal stability of this material was studied using a thermogravimetric analyzer (TGA). Accordingly, few milligrams of the sample was placed on a quartz pan and heated up 600 °C with a heating rate of 5 °C min⁻¹, under nitrogen atmosphere. No significant weight loss was occurred up to 400 °C demonstrating the high thermal stability of the organic framework. The sample was run on a thermal gravimetric analyzer with samples held in a platinum pan under nitrogen atmosphere using a 5 °C min⁻¹ ramp rate (Figure 55).

3.1.2 Gas sorption properties

The material was activated after the copious exchanges of the solvents according to general procedures. The activation was occurred under dynamic vacuum at 80 °C for 20 hours. To evaluate the permanent porosity, a nitrogen sorption isotherm was recorded at 77 K (Figure 55).

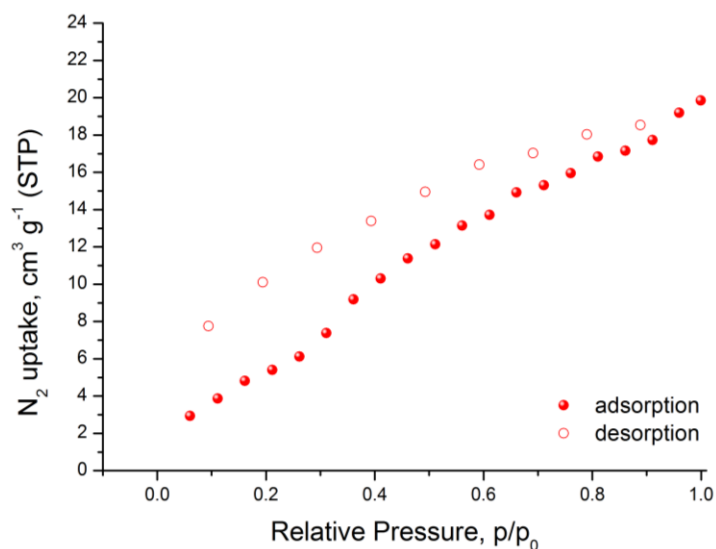


Figure 55. Nitrogen sorption isotherm of COF 3a recorded at 77 K.

3.2 Synthesis of COF 3b

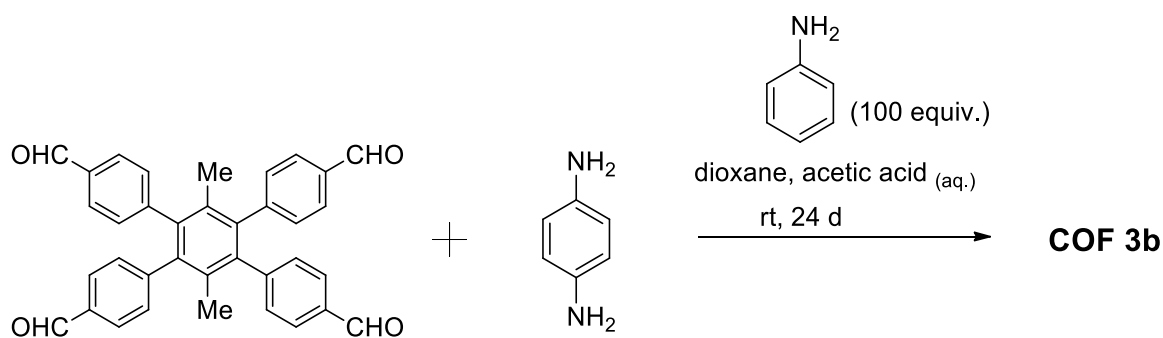


Figure 56. Synthesis of COF 3b with aniline.

A vial was charged with tetraldehyde (6 mg, 0.011 mmol), aniline (0.1 mL, 100 eq) and 0.5 mL of 1,4-dioxane, then 0.2 mL of aqueous acetic acid (6 M) was added to the solution. p-Phenylenediamine (2.5 mg, 0.022 mmol) dissolved in 1,4-dioxane (1.5 mL) was then added. Then the mixture was allowed to further stand at ambient temperature for 24 days to obtain a yellow precipitate (Figure 56).

The morphology of the final product was studied with the use of SEM (Figure 57). The figures that follow reveal the formation of chunky particles. These particles are smaller than particles of COF 3a.

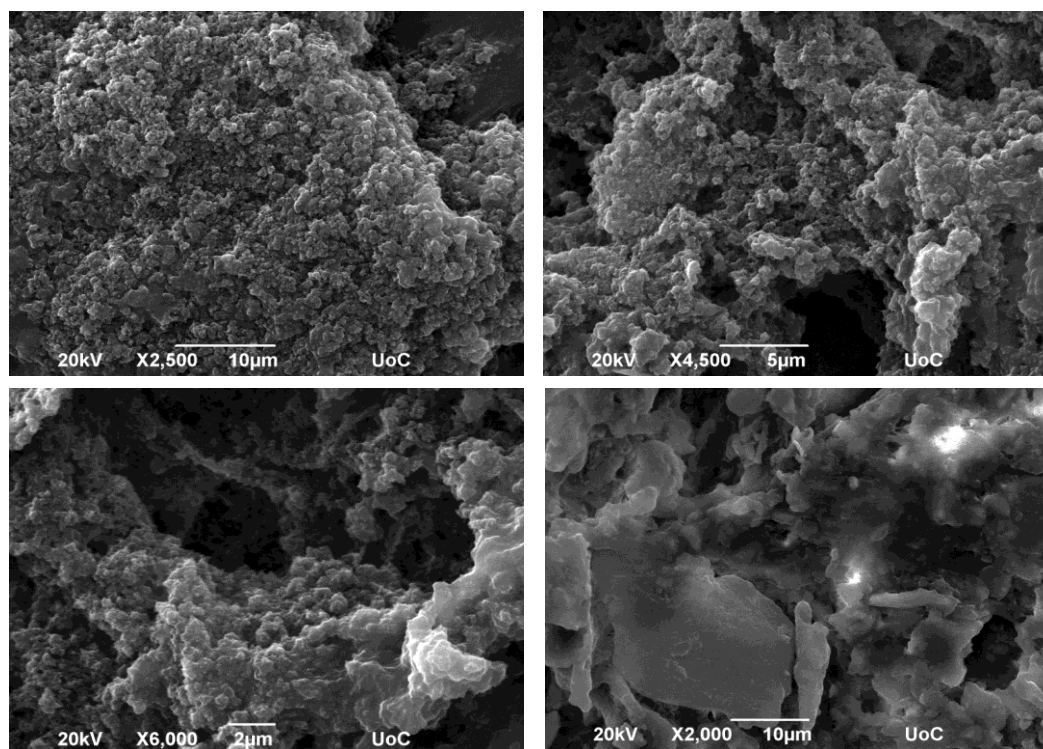


Figure 57. SEM images of COF 3b.

3.2.1 Structural Characterization of COF 3b

The solid was immersed in THF for four weeks. After that treatment the corresponding PXRD pattern shows the presence of a strong Bragg peak at 2.4° (36.6 \AA) angle followed by a weaker peak at 7.1° (12.3 \AA) 2θ position (Figure 58). Interestingly, this pattern is almost identical with the pattern of COF 3a, without aniline.

The material was kept two months in THF and the procedure was followed according to general methods. After the removal of the THF the sample was not activated under dynamic vacuum at room temperature for 20 hours. We tried also to activate the COF under dynamic vacuum for 20 hours at 80°C and 120°C , but unfortunately it was not possible as well.

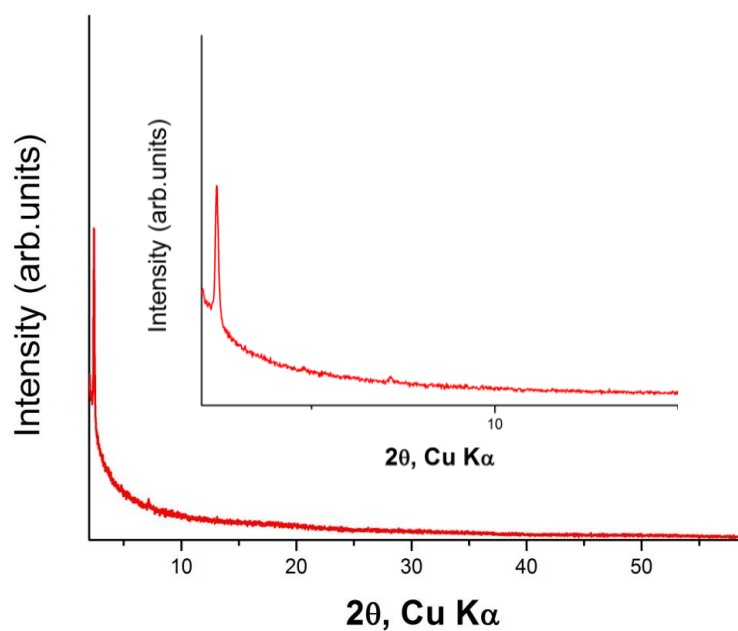


Figure 58. Experimental PXRD pattern of the COF 3b.

3.3 Synthesis of COF 4

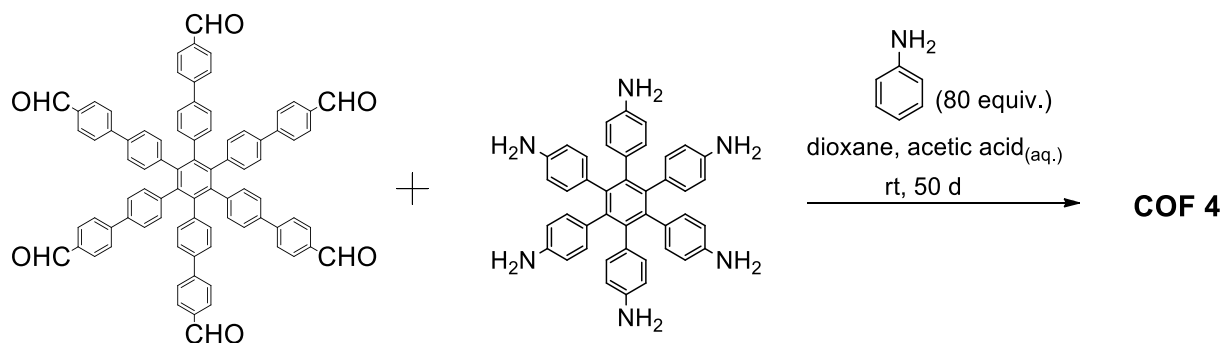


Figure 59. Synthesis of COF 4 with aniline.

A vial was charged with hexaldehyde (10 mg, 0.008 mmol), aniline (58 μ L, 80 eq) and 1 mL of 1,4-dioxane, then 0.2 mL of aqueous acetic acid (6 M) was added to the solution. $[H_2N]_6HPB$ (5 mg, 0.008 mmol) dissolved in 1,4-dioxane (2 mL) was then added. The mixture was allowed to further stand at ambient temperature for 50 days to obtain a yellow precipitate (Figure 59).

The morphology of the final product was studied with the use of SEM (Figure 60). The figures that follow reveal the formation of relatively uniform, small, irregularly shaped, spongy particles, of size approximately 1 μ M.

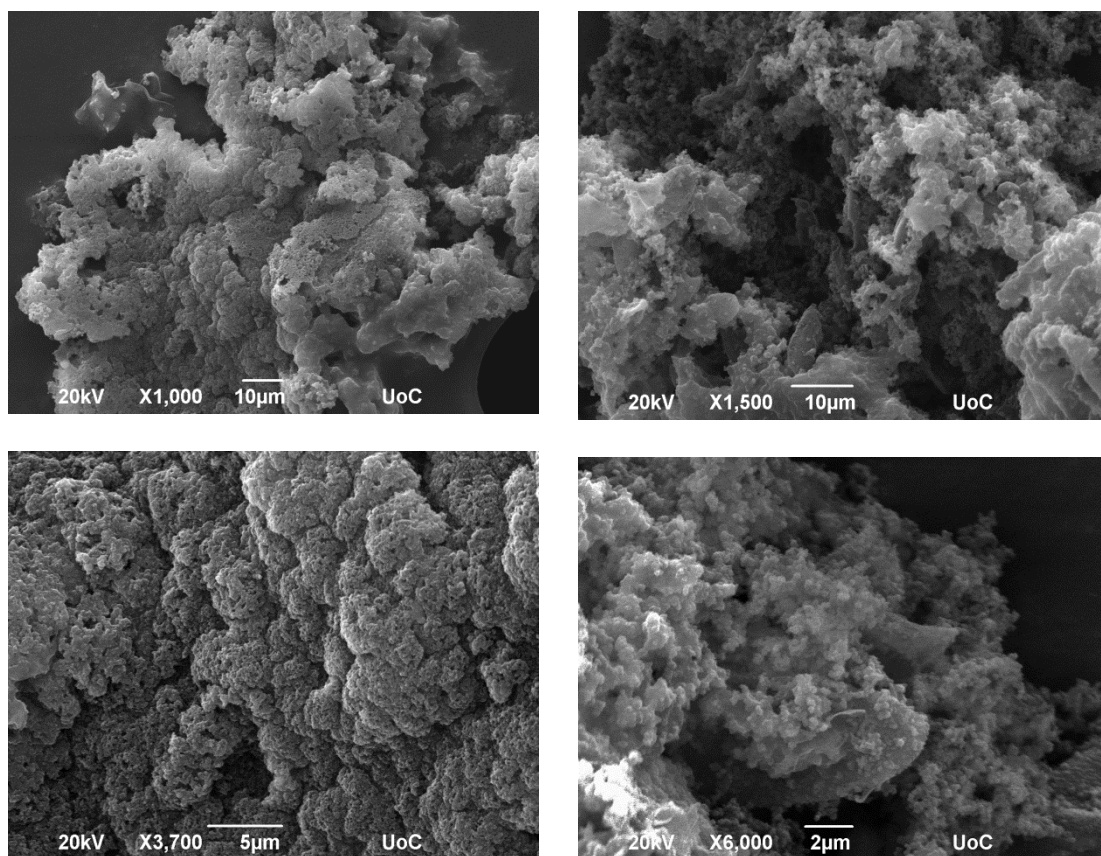


Figure 60. SEM images of COF 4.

3.3.1 Structural Characterization of COF 4

The solid was immersed in THF for six weeks. After that treatment the corresponding PXRD pattern shows the presence of a strong Bragg peak at 2.4° (36.6 \AA) angle. No other Bragg peaks were observed at higher angles, indicating that the framework is atomically amorphous (Figure 40). This pattern suggests the presence of pores with no periodicity.

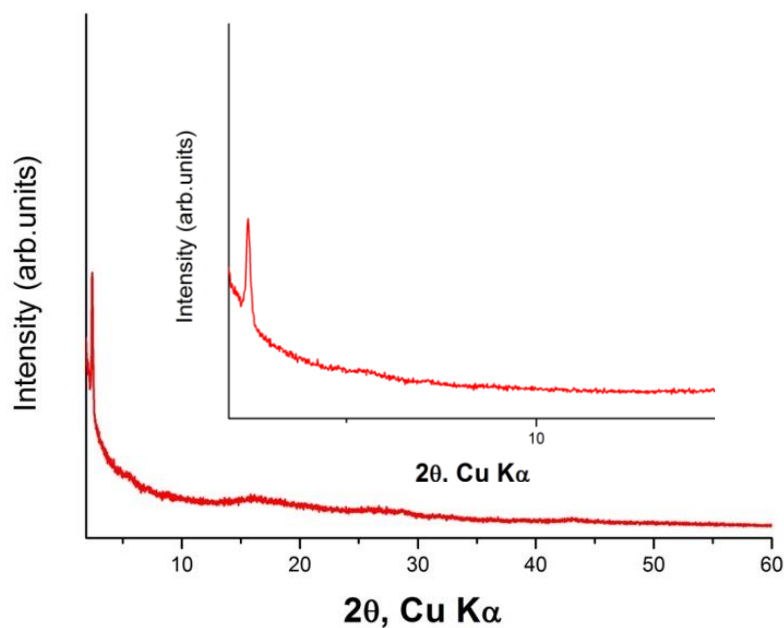


Figure 61. Experimental PXRD pattern of the COF 4.

3.3.2 Gas sorption properties

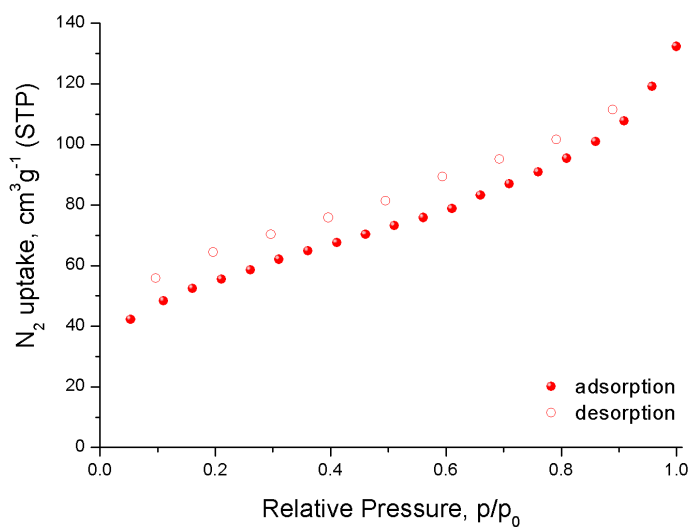


Figure 62. Nitrogen sorption isotherm of COF 4 recorded at 77 K.

The material was activated after the copious exchanges of the solvents according to general procedures. The sample was activated under dynamic vacuum at 80 °C for 20 hours. Nitrogen sorption measurements at 77 K confirmed the permanent porosity of COF 4 (Figure 62). In particular, the BET area is 190 m² g⁻¹ and the total pore volume 0.2 cm³ g⁻¹ at p/p₀ 0.99.

Furthermore, in order to evaluate the gas sorption properties of this COF we performed CO₂ sorption measurements at 273 K and 298 K up to 1 bar (Figure 63). The corresponding Q_{st} was calculated using both a Virial type and the Clausius-Clapeyron equation (Figure 64) and at zero coverage (Q_{st}⁰) is 6 kJ mol⁻¹. The CO₂ uptake at 273 K, 298 K and 1 bar is 84.5 cm³ g⁻¹ and 75.8 cm³ g⁻¹ respectively. The observed uptake is high compared to other COFs and is attributed to the presence of a large number of aromatic units originating from the organic molecular building blocks.

These experiments should be verified in order to have conclusive results because the amount of the sample was limited.

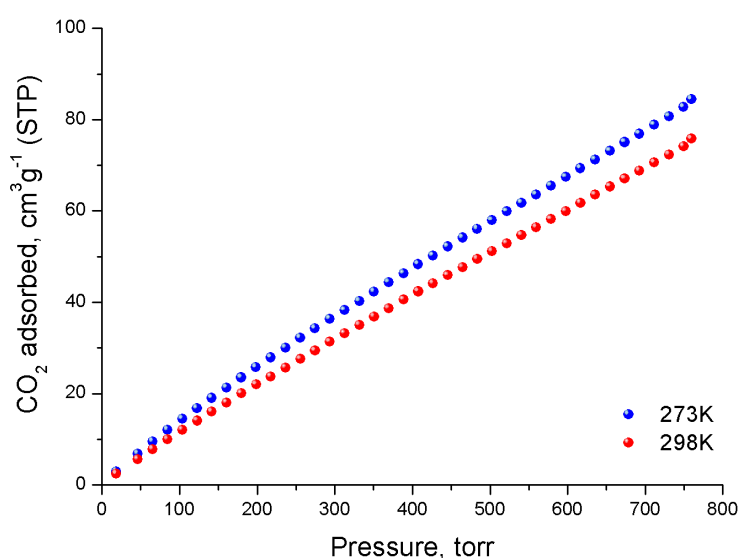


Figure 63. CO₂ sorption isotherms of COF 4 at the indicated temperatures, up to 1 bar.

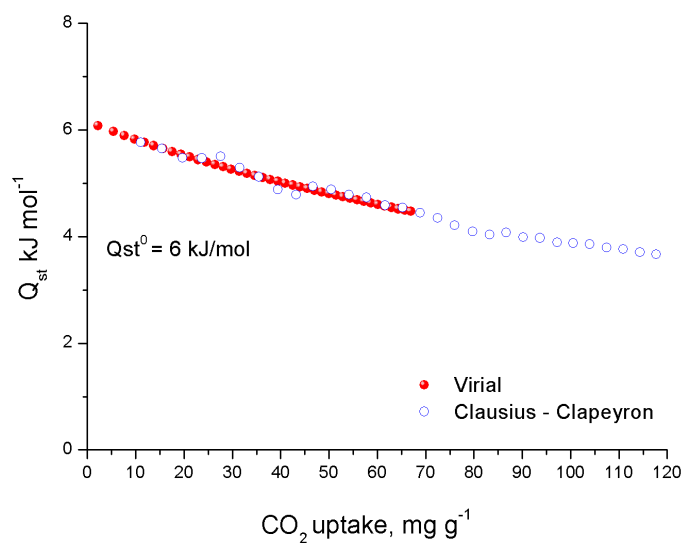


Figure 64. Calculated isosteric heat of adsorption for CO₂.

3.4 Synthesis of COF 5

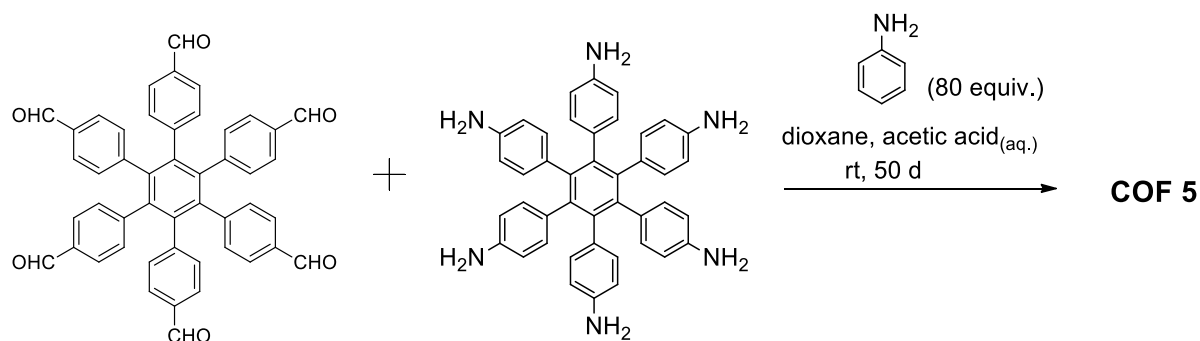
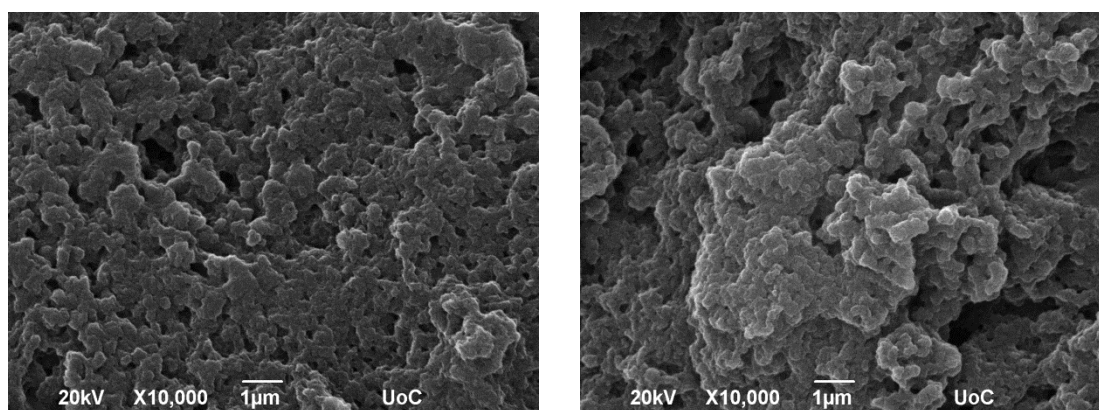


Figure 65. Synthesis of COF 5 with aniline.

A vial was charged with hexaldehyde (5.6 mg, 0.008 mmol), aniline (58 μ L, 80 eq) and 1 mL of 1,4-dioxane, then 0.2 mL of aqueous acetic acid (6 M) was added to the solution. [H₂N]₆HPB (5 mg, 0.008 mmol) dissolved in 1,4-dioxane (2 mL) was then added. The mixture was allowed to further stand at ambient temperature for 50 days to obtain a yellow precipitate (Figure 65).

The morphology of the final product was studied with the use of SEM (Figure 66). The figures that follow reveal the formation of relatively uniform, small, irregularly shaped, spongy particles, of size approximately 1 μ m.



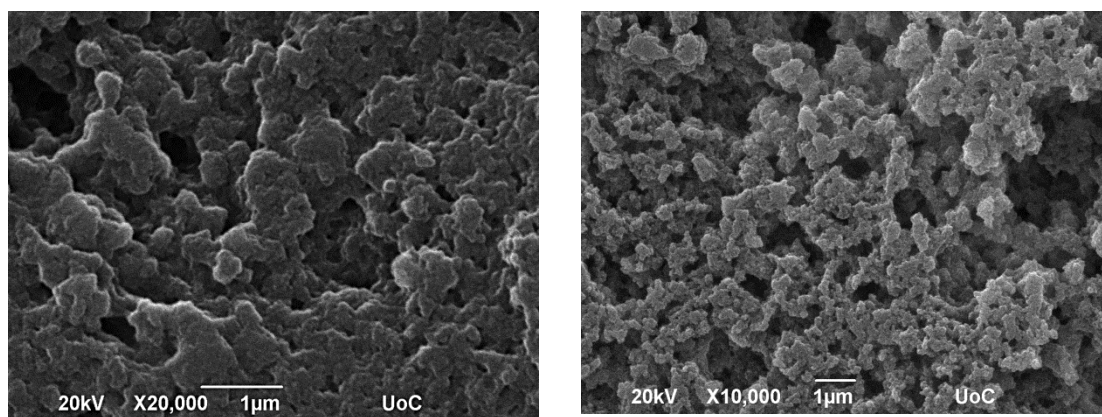


Figure 66. SEM images of COF 5.

3.4.1 Structural Characterization of COF 5

The solid was immersed in THF for six weeks. After that treatment the corresponding PXRD pattern shows the presence of a strong Bragg peak at 2.4° (36.3 \AA) angle followed by a weaker peak at 7.1° (12.3 \AA) 2θ position. (Figure 67)

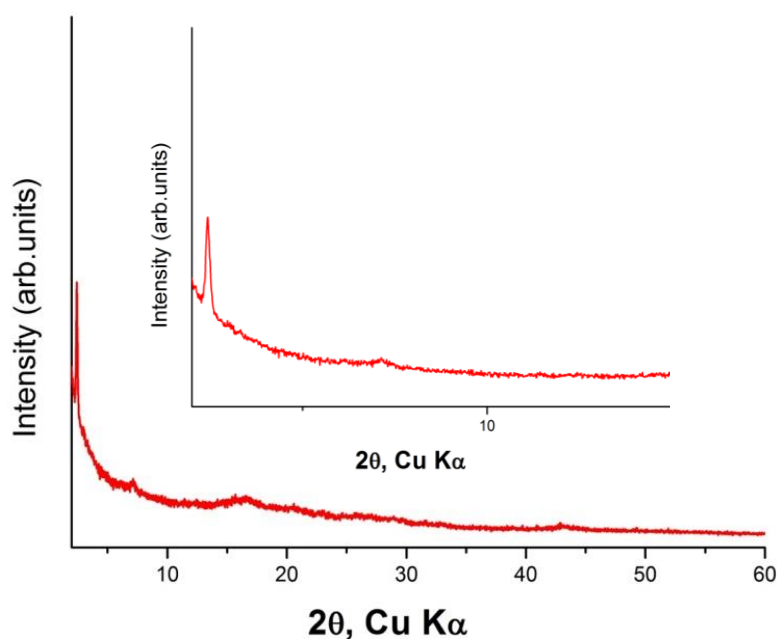


Figure 67. Experimental PXRD pattern of the COF 5.

3.4.2 Gas sorption properties

The material was activated after the copious exchanges of the solvents according to general procedures.

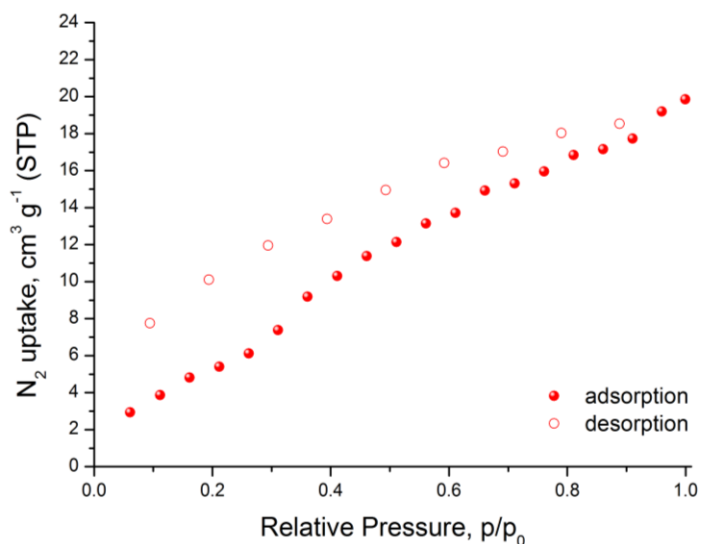


Figure 68. Nitrogen sorption isotherm of COF 5 recorded at 77 K.

The sample was activated under dynamic vacuum at 80 °C for 20 hours. A nitrogen sorption isotherm recorded at 77 K, confirmed the permanent porosity of COF 5 (Figure 68). The BET surface is 75 m² g⁻¹ and the total pore 0.14 cm³ g⁻¹ at p/p_0 0.99. The isotherm shows a gradual increase in N₂ uptake while the desorption curve shows hysteresis at low relative pressure. This behavior is consistent with a flexible material rather than a rigid framework solid. It could be related with the 2D nature of this COF and the fact that there are reduced π - π interactions between neighboring layers, because adjacent phenyl rings cannot be stacked one of the top of the other, see figure 69 [8].

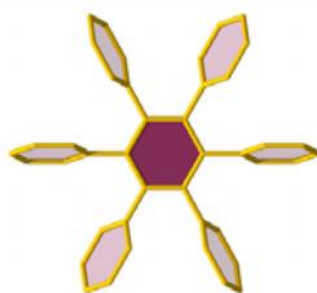


Figure 69. The vertical arrangement of the adjacent phenyl rings [8].

Regarding the gas sorption properties of this COF, we performed CO₂ sorption measurements at 273 K and 283 K up to 1 bar (Figure 70), The corresponding Q_{st} was calculated using both a Virial type and the Clausius-Clapeyron equation (Figure 71) and at zero coverage (Q_{st}⁰) is 18.7 kJ mol⁻¹. The CO₂ uptake at 273 K, 283 K and 1 bar is 150.7 cm³g⁻¹ and 139.6 cm³g⁻¹ respectively.

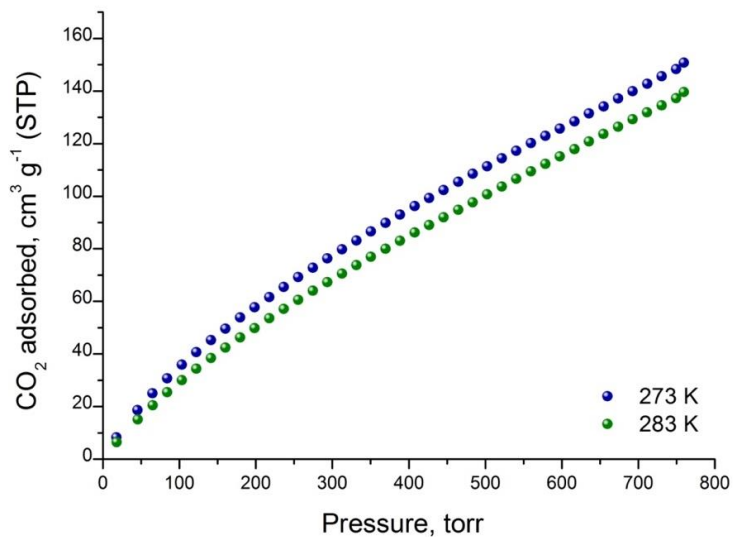


Figure 70. CO₂ sorption isotherms of COF 5 at the indicated temperatures, up to 1 bar.

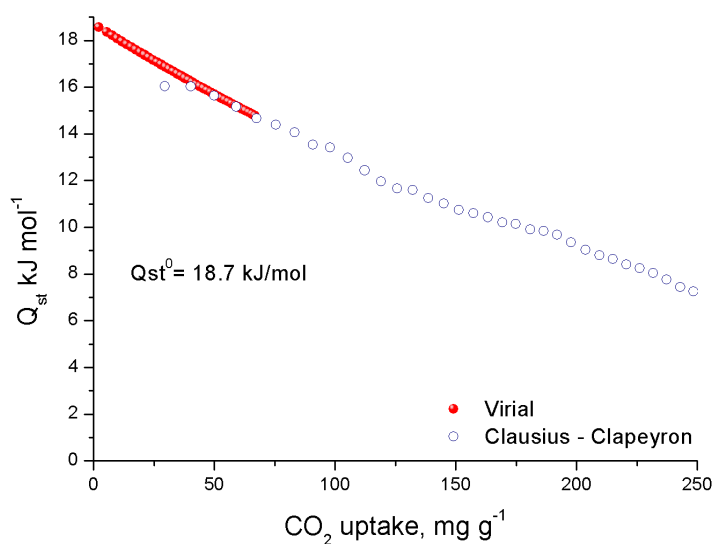


Figure 71. Calculated isosteric heat of adsorption for CO₂.

These values are very high and among the top performing COFs for CO₂ capture. For example, COF-JLU2 (Figure 72) displays a remarkable carbon dioxide uptake (up to 217 mg g⁻¹) at 273 K and 1 bar [9].

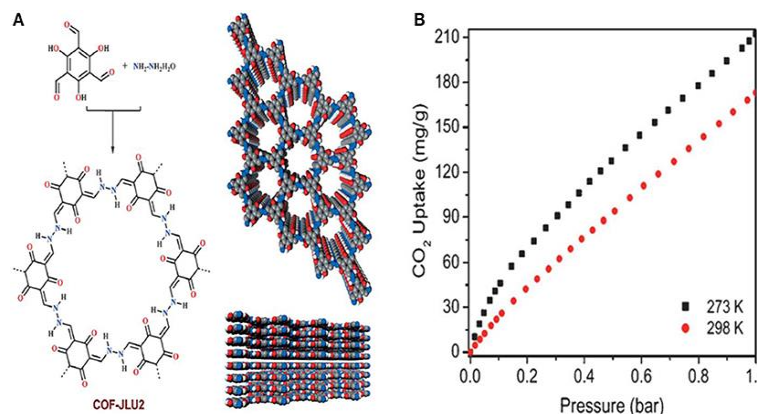
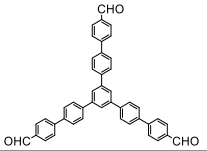
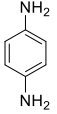
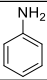
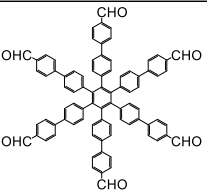
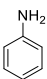
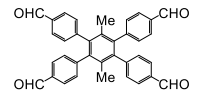
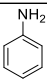
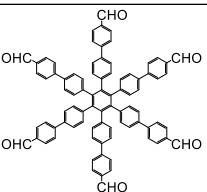
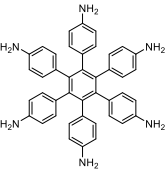
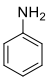
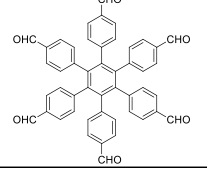


Figure 72. (A) Structure of COF-JLU2 and (B) the CO₂ adsorption isotherms of COF-JLU2 measured at both 273 and 298 K up to 1 bar pressure [9].

To the best of our knowledge, the synthesis of COFs with two hexagonal 6c-connected monomers is reported for the first time. We achieved to successfully connect the extended hexagonal hexabiphenyl benzene aldehyde with the hexagonal [H₂N]₆HPB bearing six amino groups (COF 4) and to connect the hexagonal hexaphenyl benzene aldehyde with the hexagonal [H₂N]₆HPB bearing six amino groups (COF 5).

All of these materials were not possible to be isolated as single crystalline COFs, despite all efforts, but we achieved to isolate them as polycrystalline materials.

In summary, the table below shows all the COFs that were synthesized including their properties and characteristics.

COFs	Monomers		Modulator	Crystallinity	BET	CO ₂ uptake
	Aldehydes	Amines				
1a			-	Good, hexagonal	250 m ² g ⁻¹	36.5 cm ³ g ⁻¹ (273 K) 16.2 cm ³ g ⁻¹ (298K)
1b				Good, lamellar	-	-
2a			-	Partial	-	-
2b				Disorder	105 m ² g ⁻¹	Measurement in progress
3a			-	Good	-	-
3b			Poor	-	-	
4				Disorder	190 m ² g ⁻¹	84.5 cm ³ g ⁻¹ (273 K) 75.8 cm ³ g ⁻¹ (298 K)
5					Disorder	75 m ² g ⁻¹

Bibliography

- [1] Smith, B. J.; Overholts, A. C.; Hwang, N. and Dichtel, W. R. *Chem. Commun.*, **2016**, 52, 3690-3693.
- [2] Dalapati S.; Addicoat M.; Jin S.; Sakurai T.; Gao J.; Xu H.; Irle S.; Seki S.; Jiang D. *Nat. Commun*, **2015**, p. 6:7786, 20155.
- [3] Ma, T.; Kapustin E.; Yin, S. X.; Liang, L.; Zhou, Z.; Niu J.; Li, L. H.; Wang, Y.; Su, J., Li, J.; Wang, X.; Wang, W. D.; Wang, W.; Sun, J.; Yaghi, O. M. *Science*, **2018**, 361, 6397, 48-52.
- [4] Li, Z.; Feng, X.; Zou, Y.; Zhang, Y.; Xia, H.; Liu, X.; Mu, Y. *Chem. Commun.* **2014**, 50, 13825.
- [5] Zou, L.; Yang, X.; Yuan, S.; Zhou, H. C. *CrystEngComm*, **2017**, 19, 4868-4871.
- [6] Huang, N.; Chen, X.; Krishna, R.; Jiang, D. *Angew. Chem. Int. Ed.* **2015**, 54(10), 2986-2990.
- [7] Alahakoon, S. B.; Thompson, C. M.; Nguyen, A. X.; Occhialini, G.; McCandless, G. T.; Smaldone, R. A. *Chem. Commun.* **2016**, 52, 2843-2845.
- [8] Alezi, D.; Spanopoulos, I.; Tsangarakis, C.; Shkurenko, A.; Adil, K.; Belmabkhout, Y.; O'Keeffe, M.; Eddaoudi, M. and Trikalitis, P. N. *J. Am. Chem. Soc.* **2016**, 138, 39, 12767-12770.
- [9] Li, Z.; Zhi, Y.; Feng, X.; Ding, X.; Zou, Y.; Liu, X. and Mu, Y. *Chem. Eur. J.* **2015**, 21, 12079-12084.

4. Summary, conclusions and outlook

The objective of this thesis was the design and synthesis of novel COFs based on imine bonds through the successful implementation of reticular chemistry and the study of selected gas-sorption properties, related to the energy and environmental sectors.

Four aldehydes and one amine of different geometry and size were designed and synthesized. The synthetic routes that were used result to as much as possible high yield of pure products with minimum steps.

The combination of these organic linkers with the linear p-phenylenediamine or with the [H₂N]₆HBC amine occurred with success. The resulting networks form strong bonds with new topologies and enhanced stability.

More specifically, we have synthesized successfully COF 1a resulting from the combination of a new trialdehyde and p-phenylenediamine as organic linkers. Its structure was characterized through PXRD experiments. The material was successfully activated and its gas sorption properties were studied. In particular, the new imine-based COF was studied for CO₂ storage by recording isotherms at low (1 bar) pressures. These studies revealed very good CO₂ storage properties, due to the large pore size in the mesopore range. Interestingly, the Q_{st} value is one of the highest reported in COF literature for CO₂ (29.5 kJ mol⁻¹).

Our research was continued with the synthesis of one expanded 6-c connected hexagonal organic linker. COF 2b was synthesized using aniline as a modulator and nitrogen sorption measurements confirmed its porosity.

We further investigated the possible nets that can occur from a rectangular linker, when combined with the linear p-phenylenediamine. Under solvothermal conditions COF 3a was synthesized and nitrogen sorption measurements confirmed its porosity.

Finally, we successfully synthesized two COFs with two hexagonal 6-c connected building blocks as monomers. To the best of our knowledge, these are the first COFs with this new topology. Both materials were structurally characterized through PXRD, successfully activated and their gas sorption properties were studied. More specifically, their CO₂ adsorption was evaluated, revealing a high CO₂ uptake, reaching 84.5 cm³ g⁻¹ and 75.8 cm³ g⁻¹ at 273 K and 298 K respectively, at 1 bar for COF 4 (Figure 63) and 150.7 cm³ g⁻¹ and 139.6 cm³ g⁻¹ at 273 K and 283 K respectively, at 1 bar for COF 5 (Figure 70).

On the other hand, we have to mention that these materials are polycrystalline despite our efforts to isolate them as single crystals. The activation of such kind of materials is surprisingly not straight forward and their yields are not very sufficient.

In summary, through this work we gained valuable knowledge as far as the chemistry and properties of imine-based COFs are concerned. These COFs belong to an important class of porous materials with very interesting properties, resulting from the combination of their enhanced chemical and thermal stability with the pore structure and their chemical composition. Our research open new directions in both material's design and applications, including gas storage. For example, it will be very important to evaluate the CH₄ uptake for the novel COF 4 and COF 5 and further exploratory work on this new type COFs needs to be performed.

Appendix 1

General methods and Instrumentation

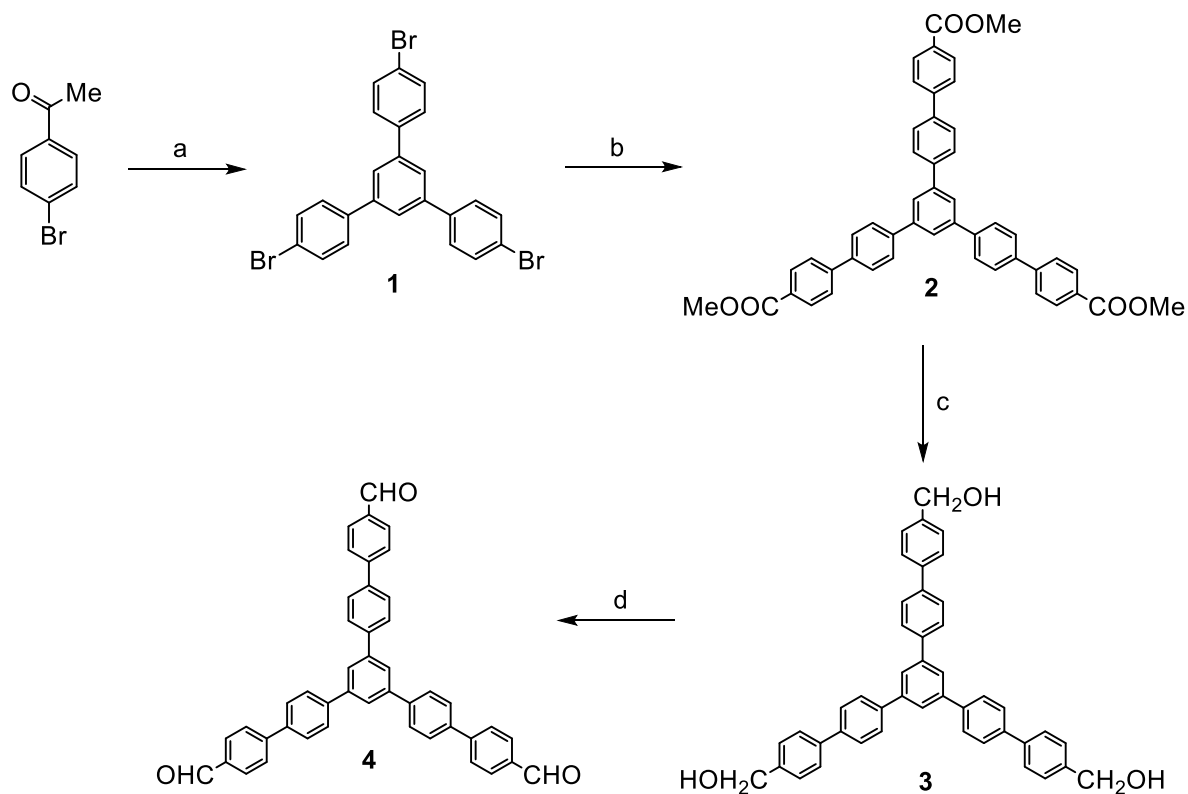
Starting Materials. All chemicals were purchased in the highest possible purity and used without further purification. The distillation of the THF solvent was occurred in the presence Na/benzophenone.

Powder X-Ray Diffraction (PXRD) Measurements. PXRD patterns were collected using a Panalytical X'pert Pro MPD System CuK α ($\lambda = 1.5418 \text{ \AA}$) radiation operated at 45 kV and 40 mA. A typical scan rate was 1.2 sec/step with a step size of 0.02 deg.

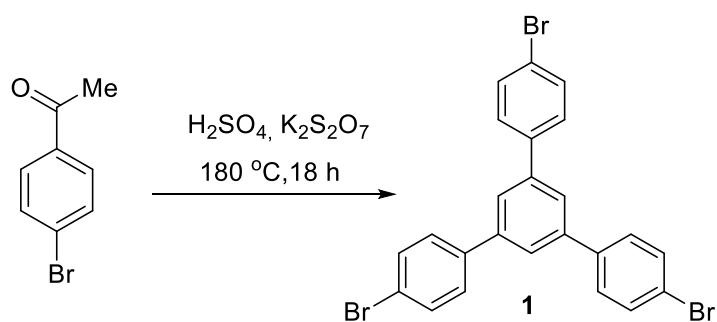
NMR data were obtained for ^1H at 500 MHz and for ^{13}C at 125 MHz at Bruker Avance-III-500 spectrometer.

Synthesis of organic linkers of Chapter 2 and 3

Synthesis of compound 4



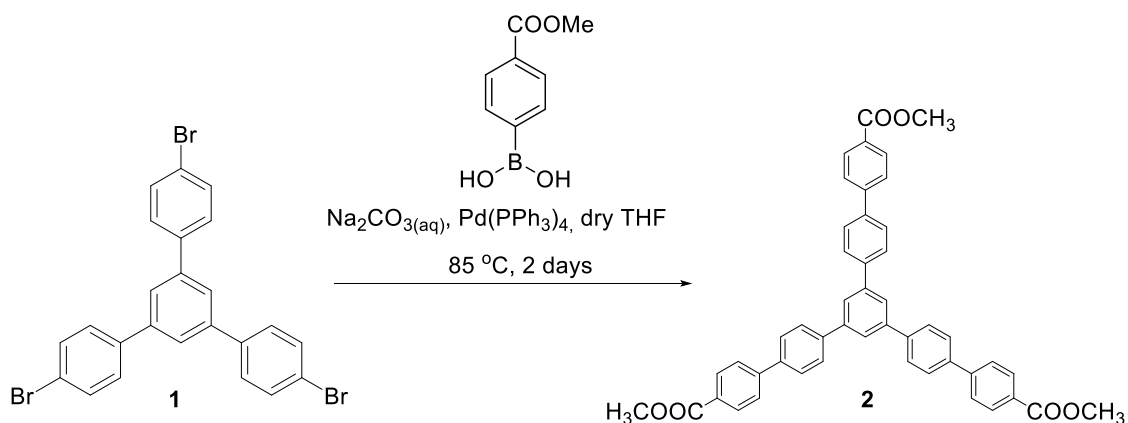
Reagents and conditions: (a) $K_2S_2O_7$ (1.17 equiv.), H_2SO_4 , 180 °C, 18 h; (b) 4-Methoxycarbonylphenylboronic acid (3.5 equiv.), aqueous Na_2CO_3 (2 M), $Pd(PPh_3)_4$ (4.3%), dry THF, Ar atmosphere, 85 °C, 2 d; (c) $LiAlH_4$ (3 equiv.), dry THF, Ar atmosphere, rt, 3 h; (d) IBX (3.3 equiv.), DMSO, rt, 30 min.



(1). In a round-bottom flask fuming H_2SO_4 , 98% (0.2 mL) was added in a mixture of solid 4-Bromoacetophenone (3 g, 15.07 mmol) and $K_2S_2O_7$ (4.5 g, 17.7 mmol). The reaction

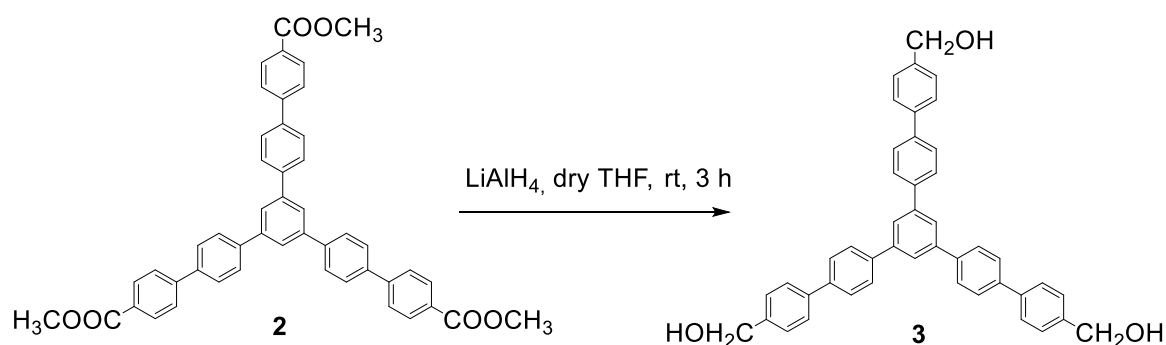
mixture was stirred and refluxed at 180 °C for 18 h. After cooling to rt, the solid in the round-bottom flask was pulverized and then EtOH (15 mL) was added. The reaction mixture was stirred and refluxed at 80 °C for another 2 h. After the reaction was completed, the mixture was filtered and washed with EtOH. The remaining solid was isolated, placed to another round-bottom flask and H₂O (15 mL) was added. The reaction mixture was stirred and refluxed at 95 °C for 1 h. The final product **1** was isolated by filtration and dried in an oven to obtain a dark yellow solid (2.4 g, 88% yield).

¹H NMR (500 MHz, CDCl₃): δ = 7.69 (s, 3H), 7.61 (d, *J*=8.6 Hz, 6H), 7.53 (d, *J*=8.6 Hz, 6H) ppm; ¹³C NMR (125 MHz, CDCl₃): δ = 141.5, 139.6, 132.0, 128.7, 125.0, 122.1 ppm.



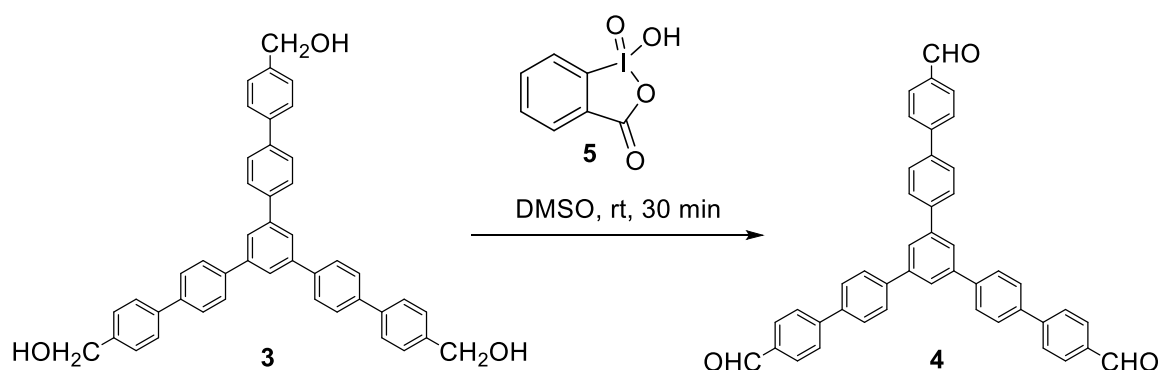
(2). Under argon atmosphere, compound **1** (0.5 g, 0.92 mmol), 4-methoxycarbonylphenylboronic acid (0.58 g, 3.22 mmol), dry THF (30 mL), aqueous Na₂CO₃ (10 mL, 2M) and Pd(PPh₃)₄ (50 mg, 0.04 mmol) were added into a two-neck flask. The reaction mixture was stirred and refluxed at 85 °C for 2 d. After cooling to rt, THF was removed under reduced pressure. The resultant mixture was collected by filtration, washed with H₂O and dried in an oven to obtain the product **2** as a pale brown powder. (0.48 g, 78% yield)

¹H NMR (500 MHz, CDCl₃): δ = 8.14 (d, *J*=8.4 Hz, 6H) , 7.89 (s, 3H) 7.82 (d, *J*=8.4 Hz, 6H), 7.76 (d, *J*=8.4 Hz, 6H), 7.73 (d, *J* = 8.4 Hz, 6H), 3.96 (s, 9H) ppm; ¹³C NMR (125 MHz, CDCl₃): δ = 166.9, 144.9, 141.8, 140.7, 139.2, 130.2, 129.0, 127.8, 127.7, 126.9, 125.1, 52.1 ppm.



(3). Under argon atmosphere LiAlH_4 (30 mg, 0.75 mmol) and dry THF (2.5 mL), were added into a two-neck flask. The mixture was kept at 0 °C. Compound **2** (100 mg, 0.14 mmol), dissolved in dry THF (2.5 mL), was added dropwise to the stirred mixture. The cooling bath was removed and then the reaction mixture was stirred at rt for 3 hours. After the reaction was completed, the mixture was kept at 0 °C and Rochelle salt (5 mL) and EtOAc (10 mL) was added. The mixture was stirred at rt for 30 min. The product **3** was extracted with EtOAc, the organic phase was dried over anhydrous MgSO_4 and then the solvent was removed under reduced pressure to provide the product **3** as a pale yellow solid (40 mg, 42% yield).

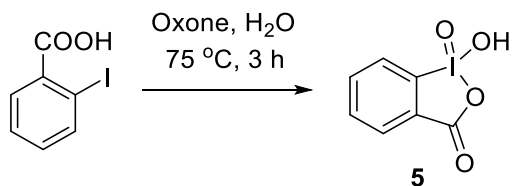
^1H NMR (500 MHz, DMSO-d_6): δ = 8.0-7.99 (m, 9H), 7.82 (d, $J=8.3$ Hz, 6H), 7.72 (d, $J=8.1$ Hz, 6H), 7.44 (d, $J=8.1$ Hz, 6H), 5.26 (t, $J=5.8$ Hz, 3H), 4.57 (d, $J=5.6$ Hz, 6H) ppm; ^{13}C NMR (125 MHz, DMSO-d_6): δ = 142.0, 141.3, 139.4, 139.0, 138.0, 127.8, 127.2, 127.1, 126.4, 124.2, 62.7 ppm.



(4). In a round-bottom flask 2-iodobenzoic acid (IBX 0.12 g, 0.42 mmol) was added in a mixture of compound **3** (80 mg, 0.128 mmol) and DMSO (4 mL). The reaction mixture was stirred at rt for 30 min. After the reaction was completed, H_2O was added and the product **4** was extracted with EtOAc. The combined organic layer was washed with aqueous

NaHCO₃ as well as with brine and dried over anhydrous MgSO₄. Then, the solvent was removed under reduced pressure to provide the product **4** as a pale yellow solid (69 mg, 87% yield).

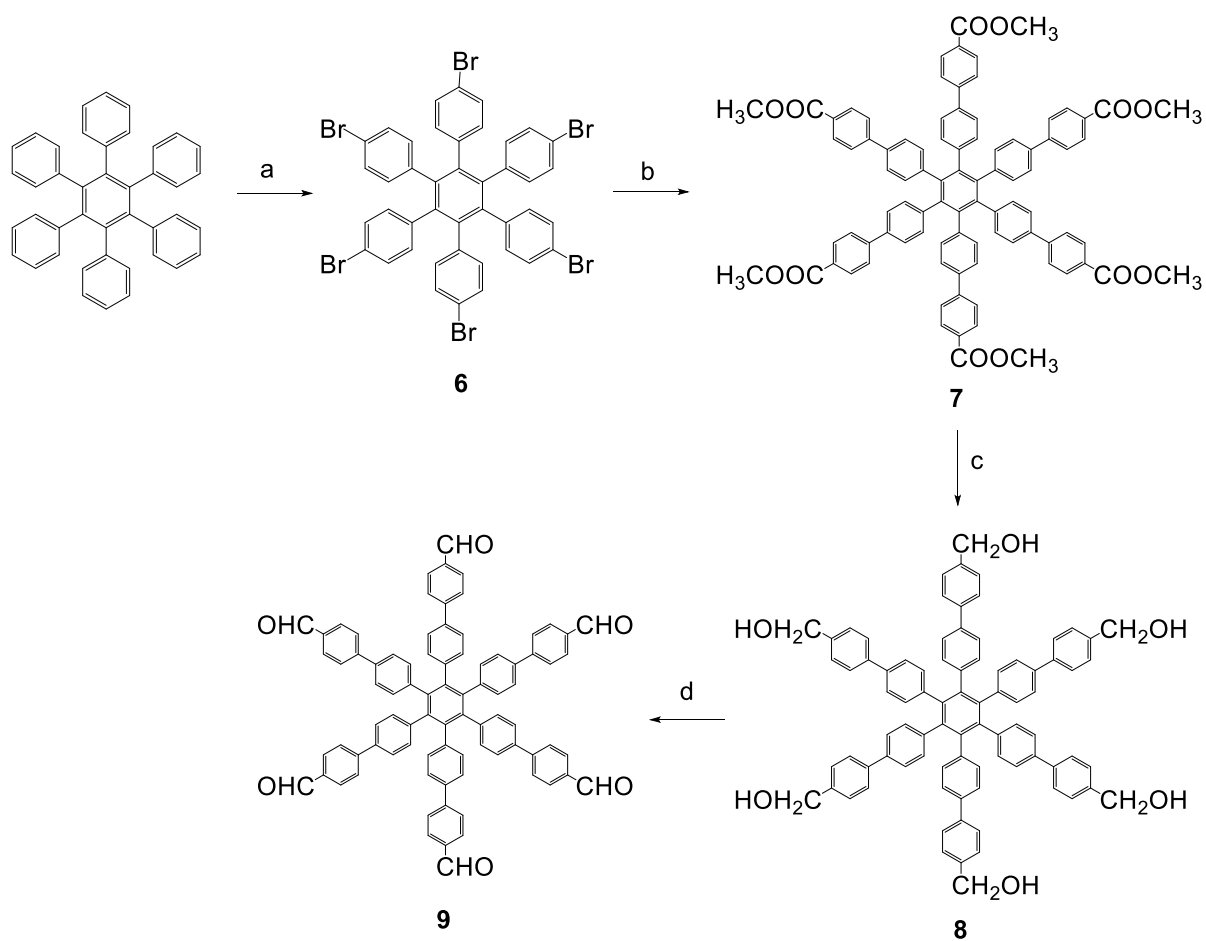
¹H NMR (500 MHz, CDCl₃): δ = 10.1 (s, 3H), 7.99 (d, *J*=8.3 Hz, 6H), 7.91 (s, 3H), 7.85 (t, *J*₁=8.3 Hz, *J*₂=8.0 Hz, 12H), 7.79 (d, *J*=8.4 Hz, 6H) ppm; ¹³C NMR (125 MHz, CDCl₃): δ = 191.9, 146.5, 141.8, 141.0, 139.0, 135.3, 130.4, 127.9 (2 C), 127.6, 125.3 ppm.



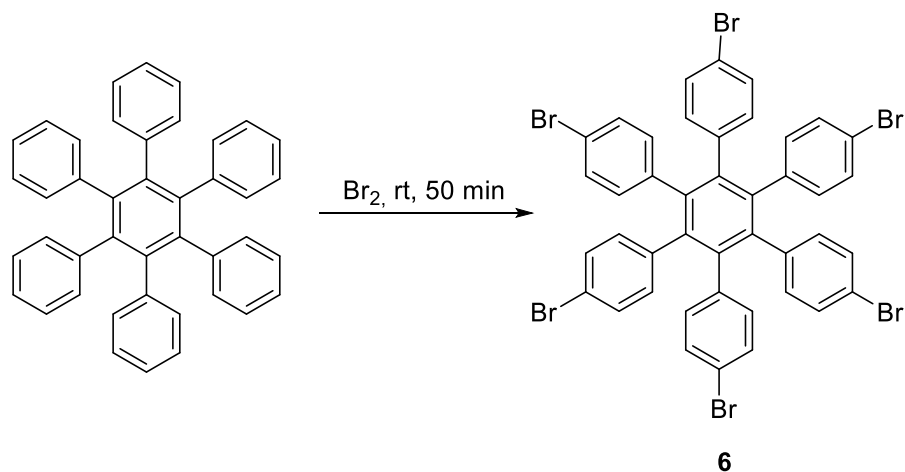
(IBX) (5). In a 250mL round-bottom flask 2-iodobenzoic acid (7 g, 0.028 mol) was added dropwise to a stirring mixture of oxone (potassium peroxymonosulfate) (26 g, 0.085 mmol) and H₂O (150 mL). The reaction mixture was stirred and refluxed at 75 °C for 3 h. After cooling to rt, the mixture was kept at 0 °C for 30 min. Then the mixture was filtered and washed with H₂O (3 x 50 mL) and acetone (1 x 25 mL). The resulting solid was dried in an oven to provide the product **5** as a white powder (6.650 g, 85% yield).

¹H NMR (500 MHz, DMSO-*d*₆): δ = 8.16 (d, *J*=7.9 Hz, 1H), 8.05 (d, *J*=7.9 Hz, 1H), 8.02 (t, *J*=7.4 Hz, 1H), 7.86 (t, *J*=7.4 Hz, 1H) ppm; ¹³C NMR (125 MHz, DMSO-*d*₆): δ = 167.6, 146.6, 133.5, 133.0, 131.5, 130.2 125.1 ppm.

Synthesis of compound 9

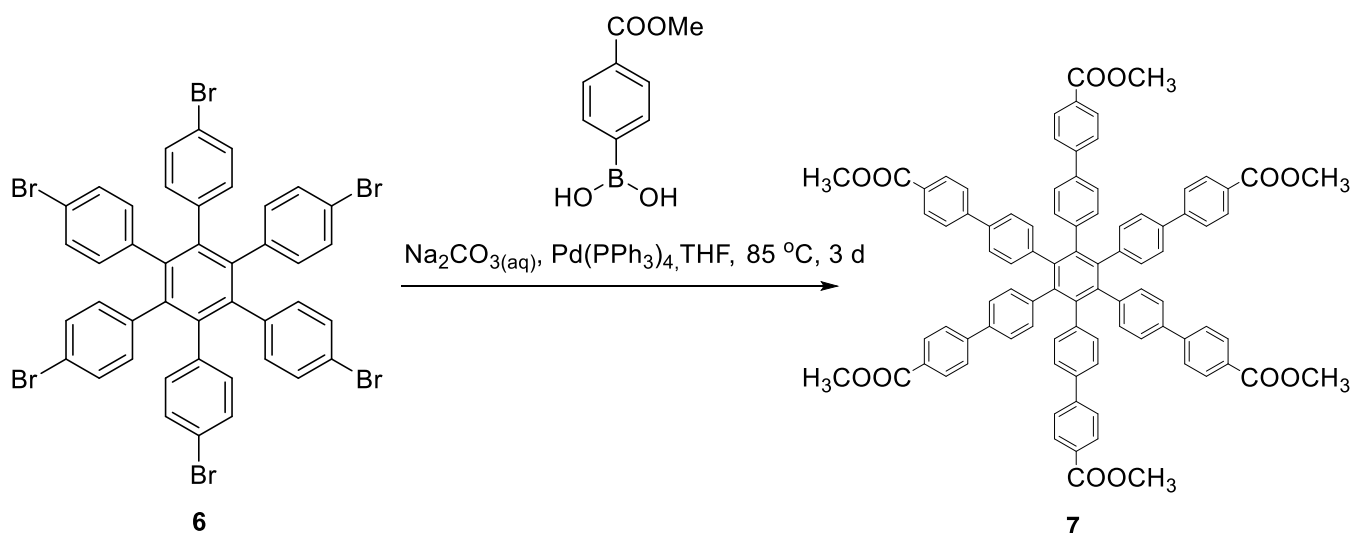


Reagents and conditions: (a) neat Br₂ (41 equiv.); (b) 4-Methoxycarbonylphenylboronic (7.4 equiv.), aqueous Na₂CO₃ (2 M), Pd(PPh₃)₄ (2.84 equiv.), dry THF, Ar atmosphere, 85 °C, 3d; (c) LiAlH₄ (35 equiv.), dry THF, Ar atmosphere, rt, 6 h; (d) IBX (5.9 equiv.), DMSO, rt, 1 h.



(6). In a 25 mL round bottom flask 1.0 g (1.9 mmol) hexaphenylbenzene and neat Br₂ (4 mL, 77.83 mmol) were added. The mixture was stirred at rt for 50 min. Then, chilled ethanol was added and the flask was kept at -20 °C for 16 h. The mixture was filtered and washed with chilled ethanol. The resulting solid was dried in an oven to provide product **6** as a white powder (1.836 g 96 % yield).

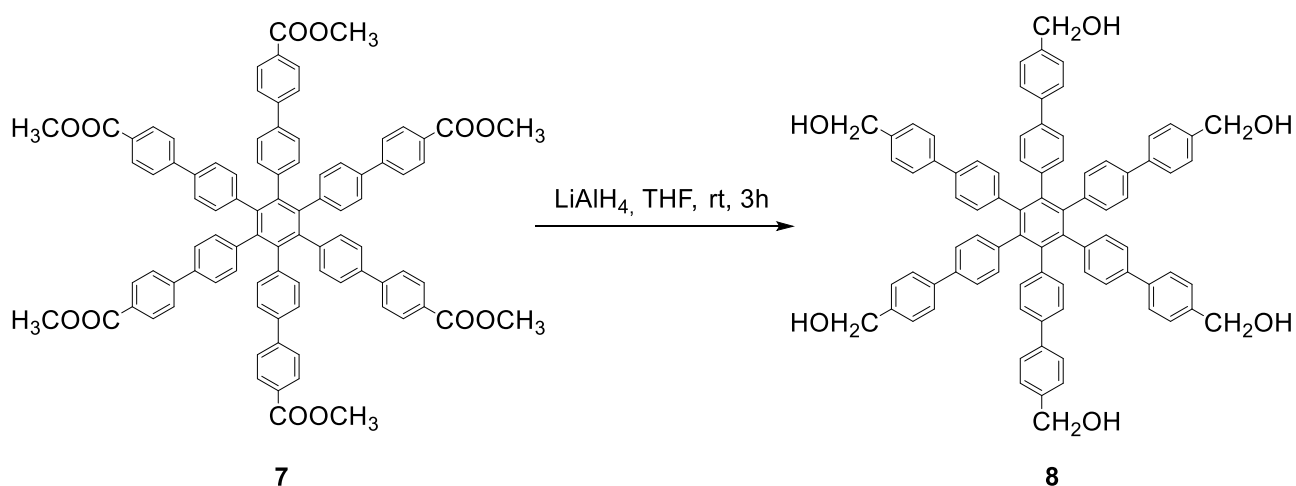
¹H NMR (500 MHz, CDCl₃): δ = 7.05 (d, *J*=8.3 Hz, 12H), 6.61 (d, *J*= 8.4 Hz, 12H) ppm; ¹³C NMR (125 MHz, CDCl₃): δ = 139.5, 138.4, 132.5, 130.4, 120.3 ppm.



(7). Under argon atmosphere, compound **6** (0.80 g, 0.79 mmol), 4-methoxycarbonylphenylboronic acid (1g, 5.6 mmol), dry THF (40 mL), aqueous Na₂CO₃ (15 mL, 2M) and Pd (PPh₃)₄ (50 mg, 0.04 mmol) were added into a two-neck flask. The reaction mixture was stirred and refluxed at 85 °C for 3 d. After cooling to rt, THF was removed

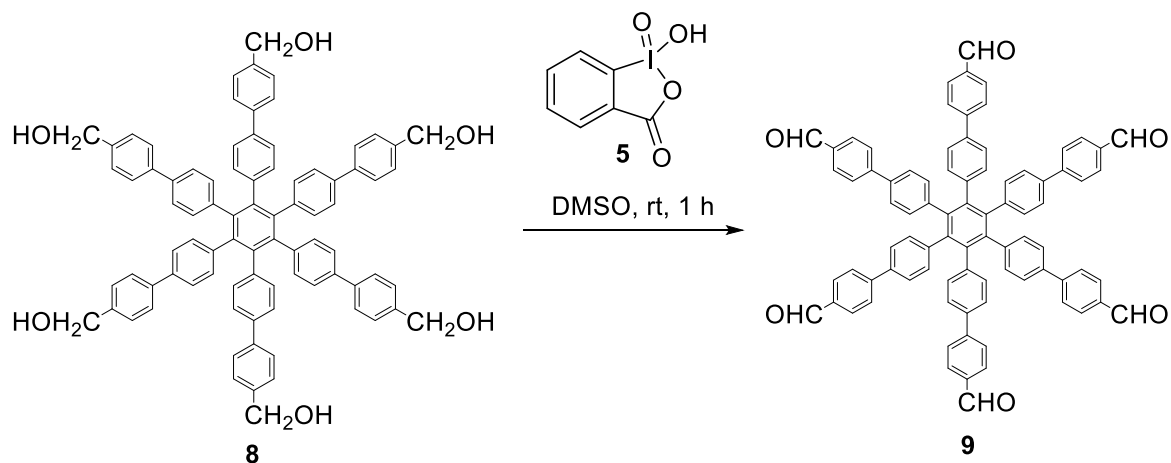
under reduced pressure. The resultant mixture was collected by filtration, washed with H₂O and dried in an oven to obtain the product **7** as a light grey powder (962 mg, 77 % yield).

¹H NMR (500 MHz, CDCl₃): δ = 7.97 (d, *J*=8.6 Hz, 12H), 7.48 (d, *J*=8.6 Hz, 12H), 7.21 (d, *J*=8.4 Hz, 12H), 7.0 (d, *J*=8.4 Hz, 12H), 3.89 (s, 18H) ppm; ¹³C NMR (125 MHz, CDCl₃): δ = 166.9, 144.9, 140.3, 140.1, 136.7, 131.9, 129.9, 128.6, 126.5, 125.7, 52.1 ppm.



(8). Under argon atmosphere, LiAlH₄ (60 mg, 1.58 mmol) and dry THF (2.5 mL), were added into a two-neck flask. The mixture was kept at 0 °C. Compound **7** (60 mg, 0.045 mmol), dissolved in dry THF (2.5 mL), was added dropwise to the stirred mixture. The cooling bath was removed and then the reaction mixture was stirred at rt for 6 h. After the reaction was completed, mixture was kept at 0 °C and Rochelle salt (5 mL) and EtOAc (10 mL) was added. The mixture was stirred at rt for 30 min. The product **8** was extracted with EtOAc, the organic phase was dried over anhydrous MgSO₄ and then the solvent was removed under reduced pressure to provide the product **8** as a pale yellow solid. (30 mg, 57% yield).

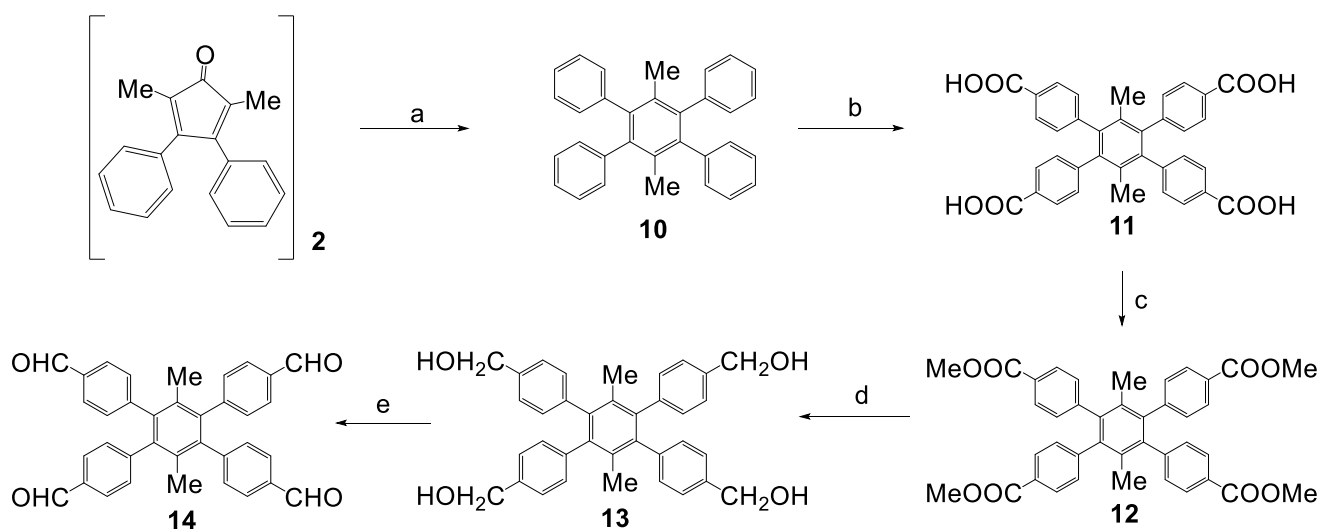
¹H NMR (500 MHz, DMSO-*d*₆): δ = 7.40 (d, *J*=7.6 Hz, 12H), 7.24 (d, *J*=7.4, 12H), 7.23 (d, *J*=7.9, 12H), 7.06 (d, *J*=7.5 Hz, 12H), 5.13 (t, *J*=5.4 Hz, 6H), 4.42 (d, *J*=5.2 Hz, 12H) ppm; ¹³C NMR (125 MHz, DMSO-*d*₆): δ = 141.6, 140.0, 139.3, 137.6, 136.5, 131.7, 126.9, 125.8, 124.5, 62.5 ppm.



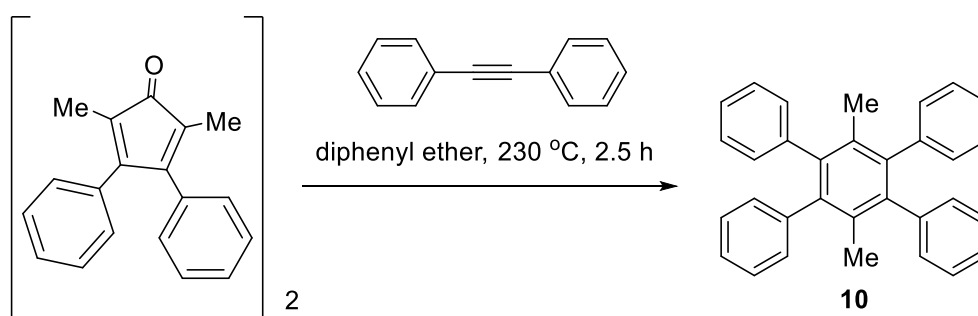
(9). In a round-bottom flask 2-iodobenzoyl peroxide (IBX) (57 mg, 0.2 mmol) was added in a mixture of compound **8** (40 mg, 0.034 mmol) and DMSO (3 mL). The reaction mixture was stirred at rt for 1 h. After the reaction was completed, H₂O was added and the product **9** was extracted 3 times with EtOAc. The combined organic layer was washed with aqueous NaHCO₃ as well as with brine and dried over anhydrous MgSO₄. Then the solvent was removed under reduced pressure to provide the product **9** as a pale yellow solid (32 mg, 81% yield).

¹H NMR (500 MHz, DMSO-*d*₆): δ = 9.94 (s, 6H), 7.82 (d, *J*=8.3 Hz, 12H), 7.71 (d, *J*=8.3 Hz, 12H), 7.42 (d, *J*=8.4 Hz, 12H), 7.16 (d, *J*=8.4 Hz, 12H) ppm; ¹³C NMR (125 MHz, CDCl₃): δ = 191.7, 146.3, 140.6, 140.1, 136.5, 135.0, 132.0, 130.1, 127.2, 125.8 ppm.

Synthesis of compound 14

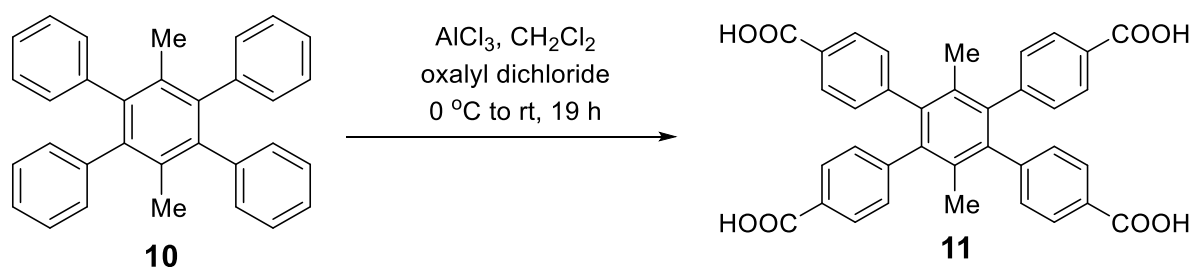


Reagents and conditions: (a) diphenylacetylene (2.9 equiv.), diphenyl ether, 230 °C, 2.5 h; (b) oxalyl chloride (13.6 equiv.), AlCl₃ anhydrous (9.4 equiv.), CH₂Cl₂, Ar atmosphere, 0 °C for 1.5 h, then rt, overnight; (c) H₂SO₄ 98%, MeOH, 80 °C, overnight; (d) LiAlH₄ (6 equiv.), dry THF, Ar atmosphere, rt, 4 h; (e) IBX (4 equiv.), DMSO, rt, 1 h.



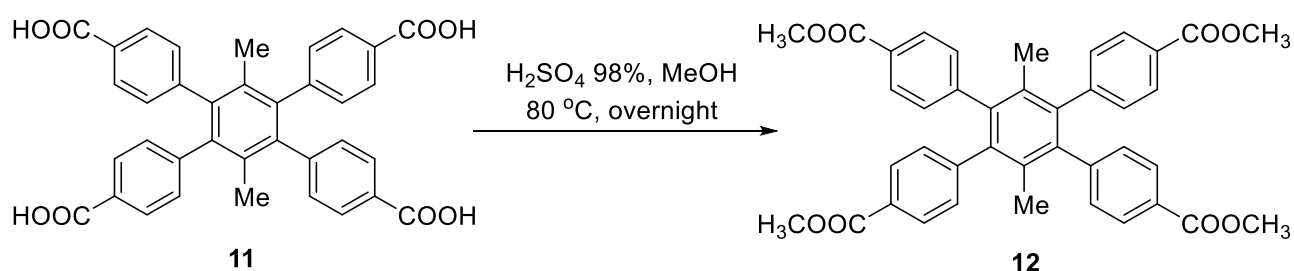
(10). In a 50 ml round bottom flask, a mixture of 2,5-dimethyl-3,4-diphenylcyclopentadienone dimer (1 g, 1.92 mmol) and diphenylacetylene (1 g, 5.61 mmol) in diphenyl ether (2.5 ml) was stirred and refluxed at 230 °C for 2.5 h. During this period of time, the mixture color changed to deep red and then faded to orange. Slow cooling at rt and then at 0 °C, crystals were formed after 30 min, which were collected by filtration, washed with hexane and dried in an oven, giving the product **10** as a white solid (1.22 g, 77% yield).

¹H NMR (500 MHz, CDCl₃): δ = 7.16-7.13 (m, 8H), 7.08-7.05 (m, 12H), 1.80 (s, 6H) ppm; ¹³C NMR (125 MHz, CDCl₃): δ = 141.4, 140.8, 131.3, 130.2, 127.4, 125.8, 19.6 ppm.



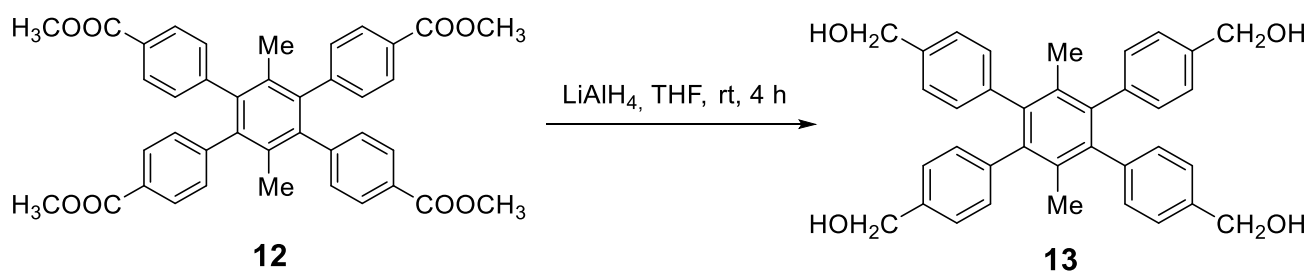
(11). Under argon atmosphere, compound **10** (1.06 g, 2.58 mmol) was dissolved in CH₂Cl₂ (20 mL) into a two-neck flask. The solution was cooled down at 0 °C and oxalyl chloride (2.5 ml, 25.8 mmol) and AlCl₃ (1.7 g, 12.7 mmol) were added. During the last addition, the color of the solution changed from brown to black. The mixture was stirred for 90 min at 0 °C and then additional AlCl₃ (1.5 g, 11.2 mmol) and CH₂Cl₂ (5 ml) were added. The mixture was stirred under argon at rt for 18 h. After this period of time the mixture was

transferred in a 50 ml beaker containing ice, where light yellow solid was precipitated. The mixture was acidified with HCl (3 M), until pH=3. The CH₂Cl₂ was evaporated under vacuum and the solid was collected by filtration, washed with H₂O and dried in an oven overnight to provide product **11** as a white solid (1.3 g, 2.22 mmol, 86 % yield). ¹H NMR (500 MHz, DMSO-d₆): δ = 7.74 (d, *J*=8.3 Hz, 8H), 7.22 (d, *J*=8.3 Hz, 8H), 1.67 (s, 6H) ppm; ¹³C NMR (125 MHz DMSO-d₆): δ = 167.1, 145.1, 139.8, 130.6 130.3, 128.8, 128.7 19.1 ppm.



(12). In a round-bottom flask fuming H₂SO₄ (98%, 3 mL) was added in a solution of compound **11** (300 mg, 0.51mmol) and MeOH (30 mL). The reaction solution was stirred and refluxed at 80 °C overnight. After the reaction was completed, the solvent was removed under reduced pressure to give a white solid. The solid was filtrated, washed with ice cold H₂O and dried in an oven to obtain the product **12** as a white powder (230 mg, 70% yield).

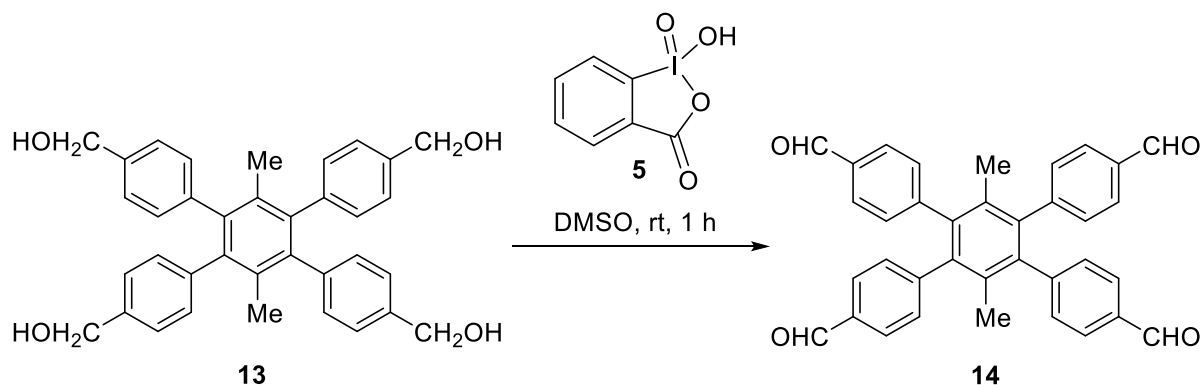
¹H NMR (500 MHz, CDCl₃): δ = 7.83 (d, *J*= 8.4 Hz, 8H), 7.12 (d, *J*=8.4 Hz, 8H), 3.86 (s, 12H), 1.74 (s, 6H) ppm; ¹³C NMR (125 MHz, CDCl₃): δ = 166.9, 145.6, 140.1, 131.0, 130.1, 129.1, 128.2, 52.0, 19.2 ppm.



(13). Under argon atmosphere LiAlH₄ (40 mg, 1.04 mmol) and dry THF (2.5 mL), were added into a two-neck flask. The mixture was kept at 0 °C. Compound **12** (100 mg, 0.155 mmol), dissolved in dry THF (2.5 mL), was added dropwise to the stirred mixture. The cooling bath was removed and then the reaction mixture was stirred at rt for 4 h. After the reaction was completed, the mixture was kept at 0 °C and Rochelle salt (5 mL) and EtOAc

(10 mL) was added. The mixture was stirred at rt for 30 min. The product **13** was extracted with EtOAc, dried over anhydrous MgSO₄ and then the solvent was removed under reduced pressure to give the product **13** as a pale yellow solid. (25 mg, 30% yield).

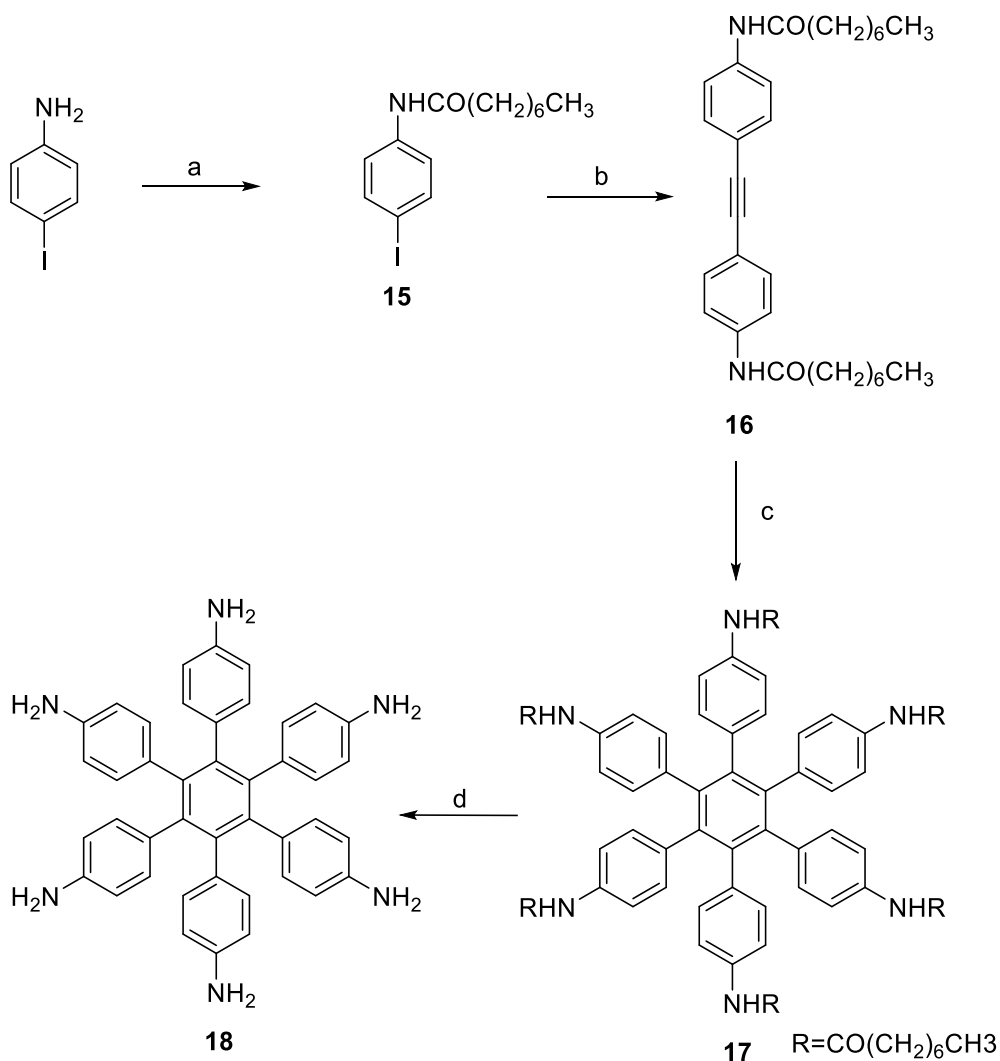
¹H NMR (500 MHz, DMSO-d₆): δ = 7.11 (d, *J* = 7.4 Hz, 8H), 7.03 (d, *J* = 7.3 Hz, 8H), 5.13 (t, *J* = 5.0 Hz, 4H), 4.39 (d, *J* = 5.3 Hz, 8H), 1.59 (s, 6H) ppm; ¹³C NMR (125 MHz, DMSO-d₆): δ = 140.2, 139.9, 139.5, 131.1, 129.6, 125.7, 62.6, 19.4 ppm.



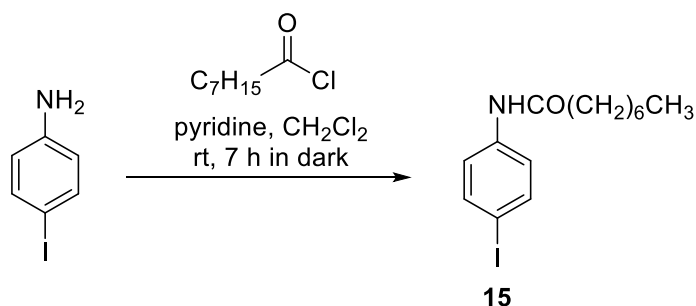
(14). In a round-bottom flask 2-iodobenzoyl chloride (IBX 68 mg, 0.24 mmol) was added in a mixture of compound **13** (30 mg, 0.056 mmol) and DMSO (3 mL). The reaction mixture was stirred at rt for 1 h. After the reaction was completed, H₂O was added and the product **14** was extracted 3 times with EtOAc. The combined organic layer was washed with aqueous NaHCO₃ as well as with brine and dried over anhydrous MgSO₄. Then, the solvent was removed under reduced pressure to provide the product **14** as a white solid. (23 mg, 79 % yield).

¹H NMR (500 MHz, CDCl₃): δ = 9.91 (s, 4H), 7.70 (d, *J* = 8.1 Hz, 8H), 7.23 (d, *J* = 8.1 Hz, 8H), 1.77 (s, 6H) ppm; ¹³C NMR (125 MHz, CDCl₃): δ = 191.8, 145.0, 140.1, 134.6, 131.1, 130.7, 129.3, 19.2 ppm.

Synthesis of compound 18

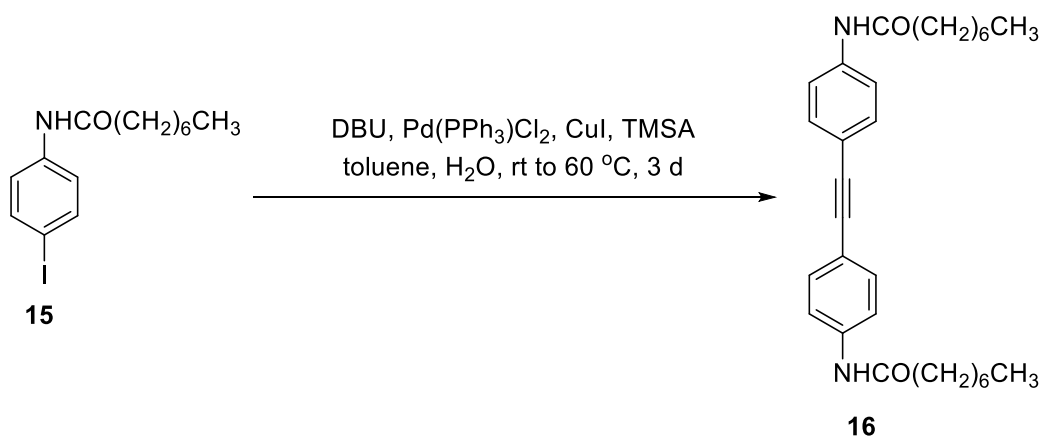


Reagents and conditions: (a) CH₃(CH₂)₆COCl (1.1 equiv.), pyridine (1.1 equiv.), rt, 17 h; (b) Pd(PPh₃)₂Cl₂ (6 mol%), CuI (10 mol%), DBU (6 equiv.), trimethylsilylacetylene (0.5 equiv.), toluene/ H₂O (30/1), 60 °C, 3 d; (c) Co₂(CO)₈ (11 mol%), dry dioxane, Ar atmosphere, 110 °C, 3 d; (d) HCl (6 M), 95 °C, 5 d and HCl (12 M), 90 °C, additional 6 d.



(15). A mixture of 4-iodoaniline (1 g, 4.5 mmol), dry CH_2Cl_2 (16 mL), and pyridine (0.5 mL, pre-treated with anhydrous MgSO_4) in a 100-mL round bottle flask was stirred in ice-cooled H_2O bath for 10 min and then octanoyl chloride (0.9 mL, 5.2 mmol) was added dropwise. The mixture was stirred in the dark at rt for 17 h. When the reaction was completed the solvent was removed under reduced pressure and hexane (20 mL) was added, to yield crystalline white solid. The solid was filtered, washed with hexane (2 mL x 3) and dissolved in CH_2Cl_2 (40 mL). The organic layers were washed with H_2O (20 mL x 2), then collected and dried over anhydrous Mg_2SO_4 . Then, the solvent was removed under reduced pressure to provide the product **15** as a white solid. (948 mg, 61 % yield).

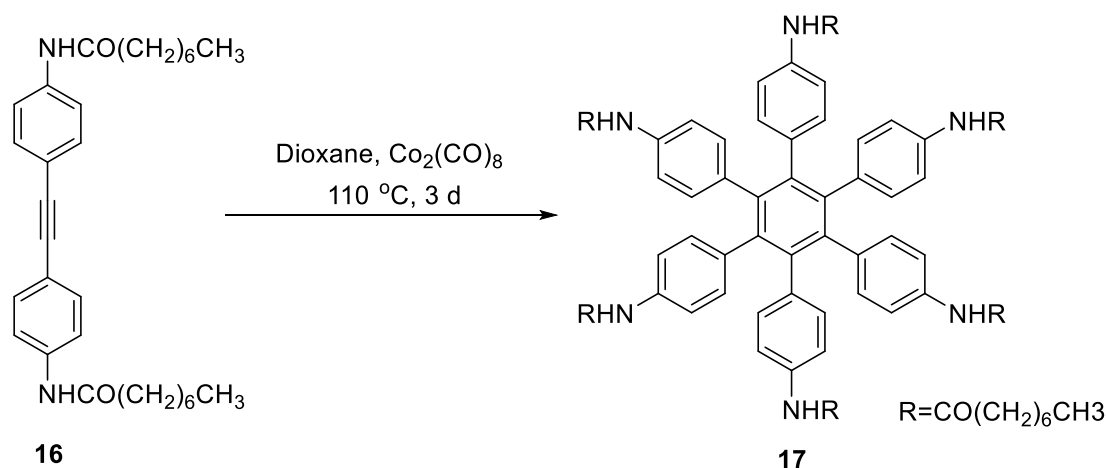
^1H NMR (500 MHz, CDCl_3): δ = 7.61 (d, $J=8.7$ Hz, 2H), 7.30 (d, $J=8.6$ Hz, 2H), 7.05 (brs, 1H), 2.34 (t, $J=7.5$ Hz, 2H), 1.74-1.68 (m, 2H), 1.36-1.25 (m, 8H), 0.88 (t, $J=6.8$ Hz, 3H) ppm; ^{13}C NMR (125 MHz, CDCl_3): δ = 171.5, 137.8, 137.7, 121.6, 87.2, 37.8, 31.6, 29.2, 29.0, 25.5, 22.6, 14.0 ppm.



(16). Under argon atmosphere a mixture of compound **15** (948 mg, 0.0027 mol), toluene (30 mL), H_2O (0.5 mL), and DBU (2.6 mL, 0.017 mol), in a 100-mL two-necked flask with condenser, was stirred and bubbled with argon for 45 min. Then, $\text{Pd(PPh}_3)_2\text{Cl}_2$

(0.120 g, 0.28 mmol, 6%) and CuI (0.056 g, 0.29 mmol, 10%) were added. Then, TMSA (0.2 mL, 1.42 mmol) was added dropwise, under Ar flow and the mixture was stirred at rt for 15 min and then heated at 60 °C for 3 d. After the reaction was completed, the mixture was cooled down to rt, and the obtained solid was collected and washed with CH₂Cl₂, CHCl₃, and H₂O. Then, the solid was dissolved in THF, and passed through celite. The solvent was evaporated under reduced pressure to provide product **16** as a white solid (300 mg, 30% yield).

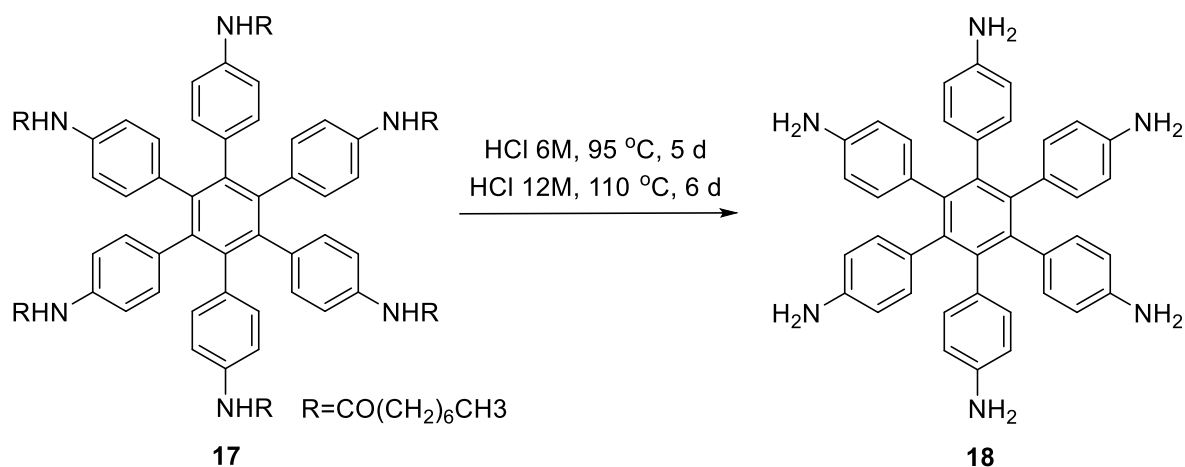
¹H NMR (500 Hz, DMSO-*d*₆): δ = 10.03 (s, 2H), 7.63 (d, *J*=8.7 Hz, 4H), 7.42 (d, *J*=8.7 Hz, 4H), 2.31 (t, *J* = 7.4 Hz, 4H), 1.59 (m, 4H), 1.29-1.23 (m, 16H), 0.86 (t, *J*=6.9 Hz, 6H) ppm; ¹³C NMR (125 Hz, DMSO-*d*₆): δ = 171.5, 139.6, 131.8, 118.9, 116.6, 88.6, 36.5, 31.2, 28.6, 28.5, 25.0, 22.1, 13.9 ppm.



(**17**). Compound **16** (150 mg, 0.325 mmol), dissolved in dioxane (7.5 mL), in a 100-mL two-necked flask with condenser, was bubbled with argon for 45 min and then Co₂(CO)₈ (13.5 mg) was added. After 10 min of Ar bubbling, the mixture was heated to reflux at 110 °C for 3 d. After the reaction was completed, the mixture was cooled to rt and Et₂O (40 mL) was added, providing a precipitate that was filtered and washed with Et₂O (25 mL x 3). Then, the residue was dissolved in a minimum volume of DMF (10 mL), filtered through a celite plug, in order to remove the Co₂(CO)₈ catalyst, and the solution was poured into H₂O (150 mL). The precipitate was collected via filtration, washed with H₂O, MeOH, and Et₂O, to provide product **17** as a white powder (90 mg, 80% yield).

¹H NMR (500 Mz, DMSO-*d*₆): δ = 9.54 (s, 6H), 7.09 (d, *J*=8.4 Hz, 12H), 6.71 (d, *J*=8.4 Hz, 12H), 2.16 (m, 12H), 1.23 (m, 60H), 0.85-0.82 (m, 18H) ppm; ¹³C NMR (125 Mz,

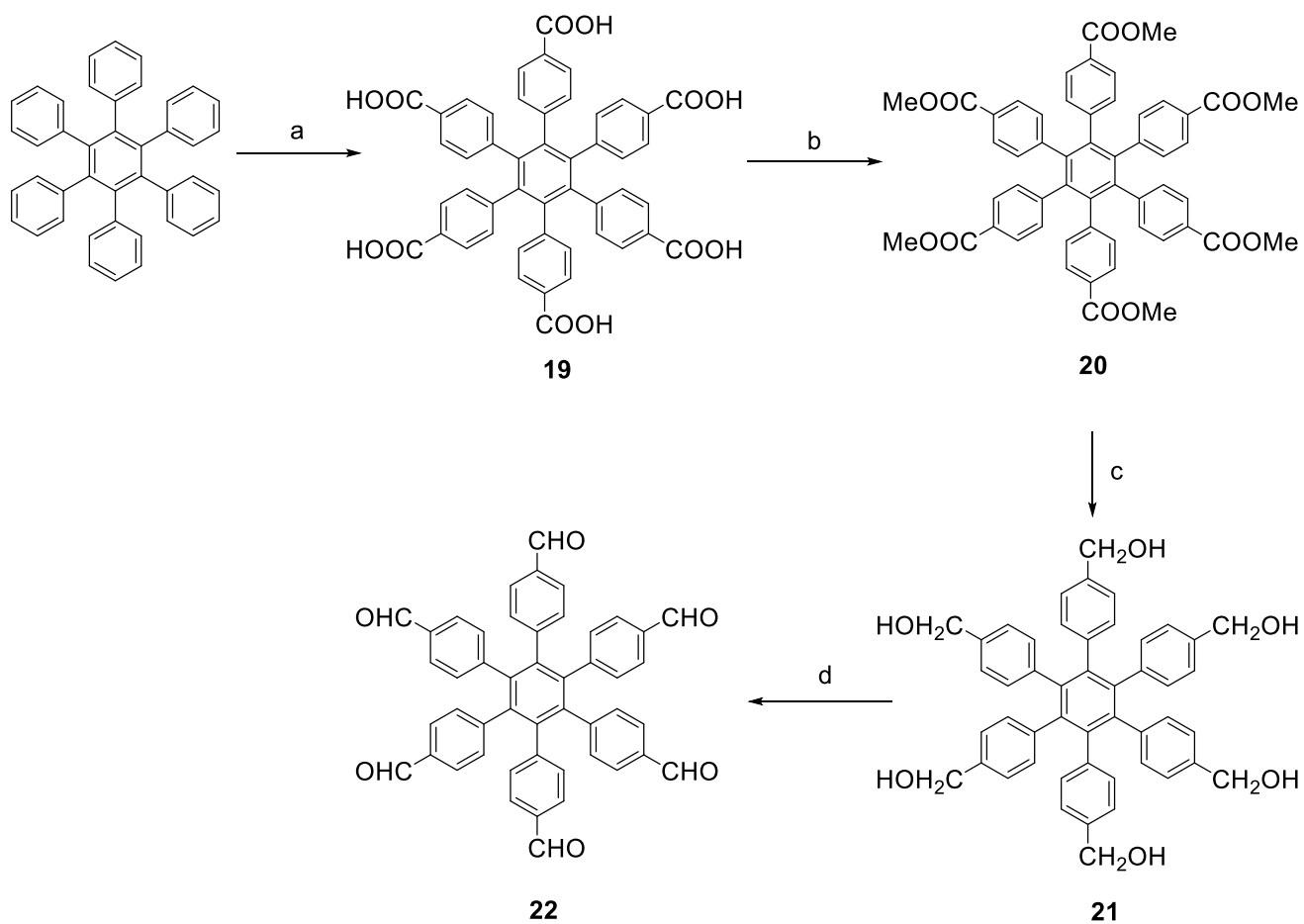
DMSO- d_6): $\delta = 170.9, 139.9, 136.4, 135.0, 131.0, 116.9, 36.4, 31.1, 28.7, 28.4, 24.9, 22.0, 13.9$ ppm.



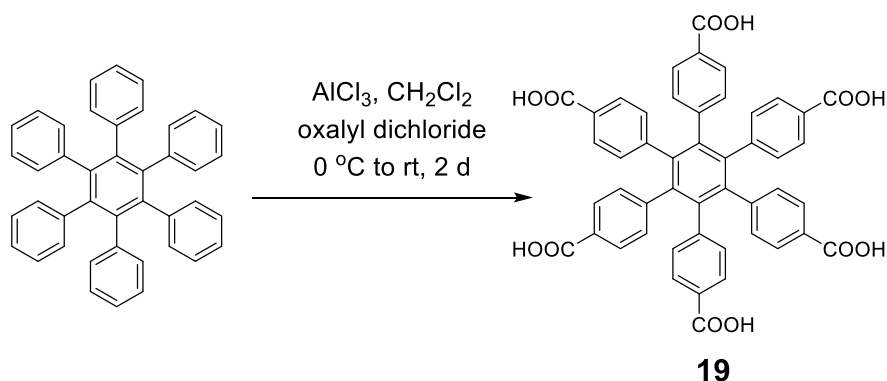
(18). A mixture of compound **17** (90 mg, 0.065 mmol) and aqueous HCl (6 mL, 6 M), in a 50-mL flask with condenser, under argon atmosphere, was stirred at 95 °C for 5 d. Then, aqueous HCl (3 mL, 12 M) was added and the reaction was heated to reflux at 110 °C for 6 days. After the reaction was completed, the mixture was cooled down to rt and was washed with Et₂O (25 mL x 2). The aqueous layers were neutralized with aqueous NaOH (6 M), at 0 °C. The resulting precipitate was collected and thoroughly washed with H₂O (25 mL x 3) and MeOH (5mL x 2). The solid was dried under high vacuum to provide product **18** as a yellow powder (32 mg, 78% yield).

¹H NMR (500 Mz, DMSO- d_6): $\delta = 6.35$ (d, $J=8.4$ Hz, 12H). 6.02 (d, $J=8.4$ Hz, 12H), 4.5 (s, 12H) ppm; ¹³C NMR (125 Mz, DMSO- d_6): $\delta = 145.1, 140.9, 131.5, 130.4, 112.6$ ppm.

Synthesis of compound 22

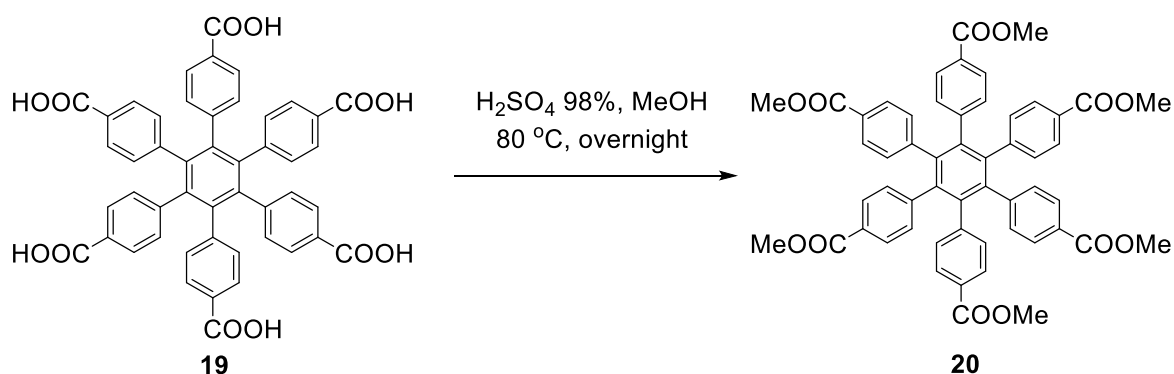


Reagents and conditions: (a) Oxalyl chloride (13.6 equiv.), AlCl₃ anhydrous (9.4 equiv.), CH₂Cl₂, Ar atmosphere, 0 °C, 90 min and then rt, 2 d; (b) H₂SO₄ 98%, MeOH, 80°C, overnight; (c) LiAlH₄ (10 equiv.), dry THF, Ar atmosphere, rt, 4 h; (d) IBX (6 equiv.) DMSO, rt, 1 h.



(19). Under argon atmosphere hexaphenylbenzene (100 mg, 0.19 mmol) was dissolved in CH_2Cl_2 (5 ml) into a two-neck flask. The solution was cooled down to 0 °C and oxalyl chloride (0.5 ml, 2.85 mmol) and AlCl_3 (202 mg, 1.52 mmol) were added. During the last addition, the color of the solution changed from brown to black. The mixture was stirred at 0 °C for 90 min and then additional AlCl_3 (178 mg, 1.34 mmol) and 1 ml CH_2Cl_2 were added. The mixture was stirred under argon atmosphere at rt for 2 days. Then, the mixture was transferred in a 25ml beaker containing ice and a light yellow solid was precipitated. The mixture was acidified with HCl (3 M), until pH=3. The CH_2Cl_2 was evaporated under vacuum and the remaining solid was collected by filtration, washed with H_2O and dried in an oven overnight, to provide the product **19** as a yellow solid (110 mg, 73 % yield).

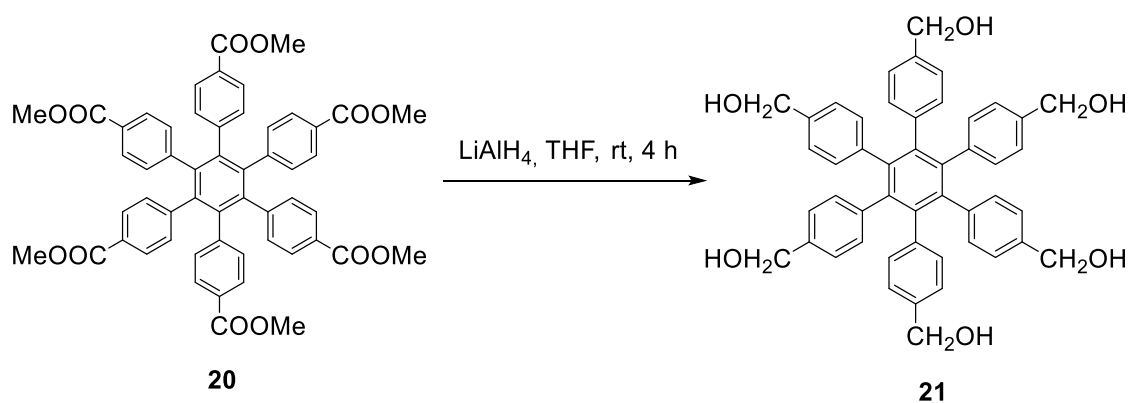
^1H NMR (500 MHz, DMSO-d_6): $\delta = 7.45$ (d, $J=8.1$ Hz, 12H), 7.04 (d, $J=8.1$ Hz, 12H) ppm; ^{13}C NMR (125 MHz DMSO-d_6): $\delta = 166.9, 143.7, 139.3, 131.1, 128.3, 127.9$ ppm.



(20). In a round-bottom flask, fuming H_2SO_4 , 98% (1 mL) was added in a solution of compound **19** (60 mg, 0.05 mmol) and MeOH (5 mL). The reaction mixture was stirred and refluxed at 80 °C overnight. After the reaction was completed, MeOH was evaporated under

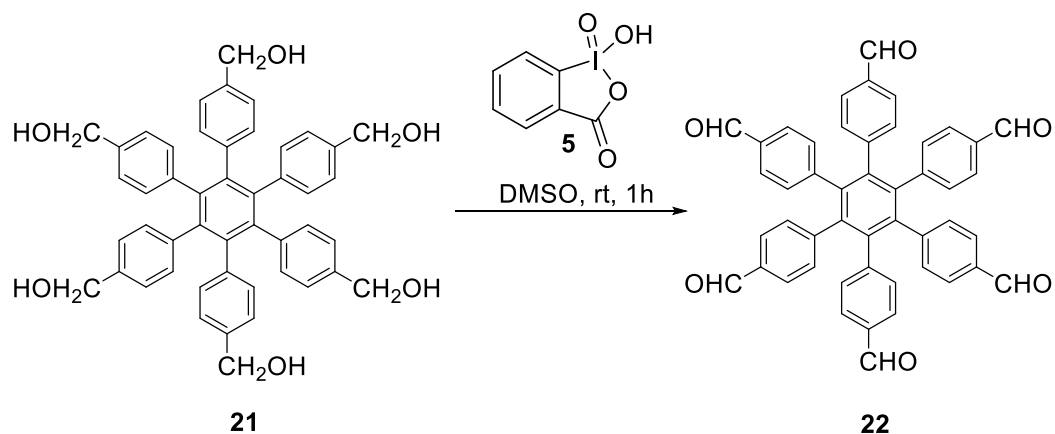
vacuum to give a white solid. The mixture was filtrated, washed with ice cold H₂O and dried in an oven to obtain product **20** as a white powder (40 mg, 78% yield).

¹H NMR (500 MHz, CDCl₃): δ = 7.55 (d, *J*=8.3 Hz, 12H), 6.87 (d, *J*=8.3 Hz, 12H), 3.80 (s, 18H) ppm; ¹³C NMR (125 MHz, CDCl₃): δ = 166.6, 144.0, 139.7, 131.0, 128.5, 127.8, 52.0 ppm.



(21). Under argon atmosphere, LiAlH₄ (60 mg, 1.5 mmol) and dry THF (2.5 mL), were added into a two-neck flask. The mixture was kept at 0 °C. Compound **20** (20 mg, 0.024 mmol), dissolved in dry THF (2.5 mL), was added dropwise to the stirred mixture. The cooling bath was removed and then the reaction mixture was stirred at rt for 4 h. After the reaction was completed, mixture was kept at 0 °C and Rochelle salt (5 mL) and EtOAc (10 mL) was added. The mixture was stirred at rt for 30 min. The product was extracted with EtOAc, dried over anhydrous MgSO₄ and the solvents were evaporated under vacuum to give product **21** as a white solid (10 mg, 58% yield).

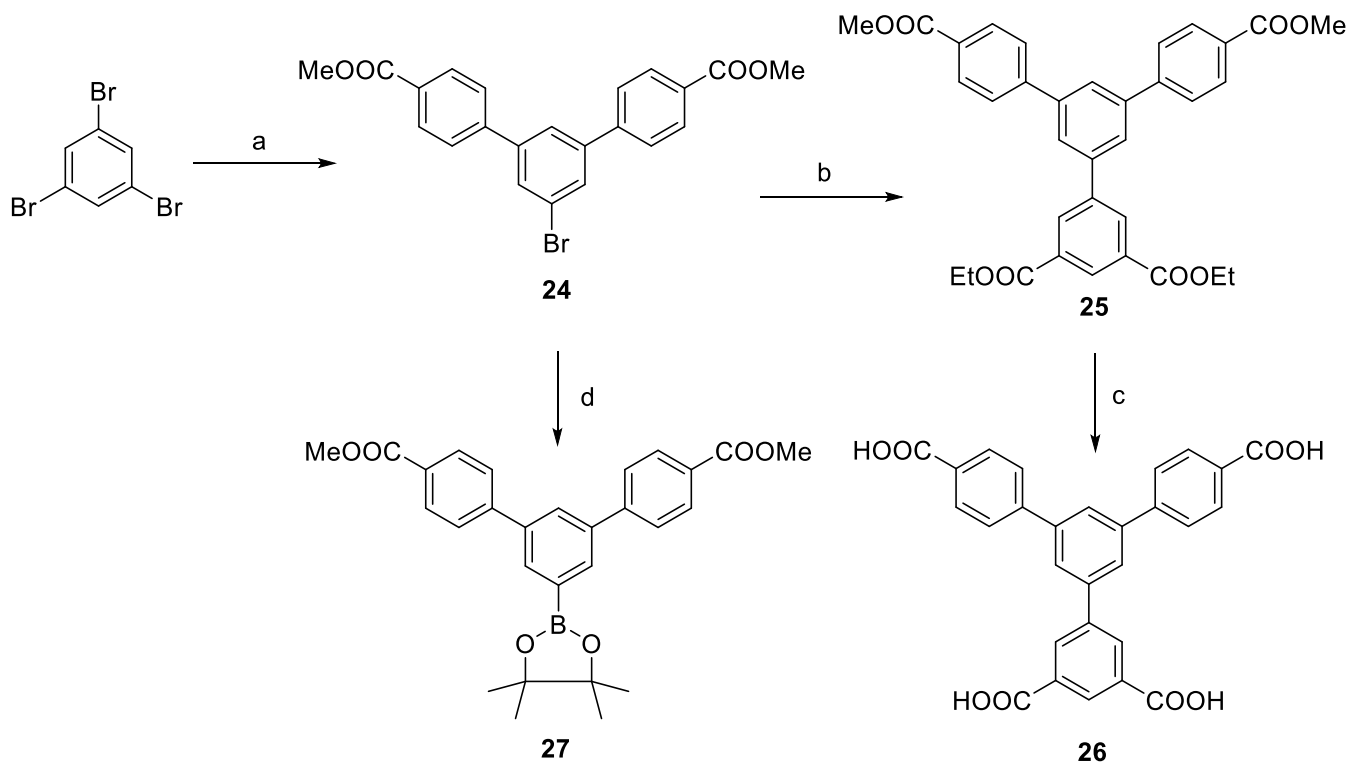
¹H NMR (500 MHz, DMSO-d₆): δ = 6.79 (d, *J*=8.2 Hz, 12H), 6.75 (d, *J*=8.2 Hz, 12H), 4.99 (t, *J*=5.8 Hz, 6H), 4.22 (d, *J*=5.6 Hz, 12H) ppm; ¹³C NMR (125 MHz, DMSO-d₆): δ = 140.0, 138.8, 138.6, 130.6, 124.3, 62.3 ppm.



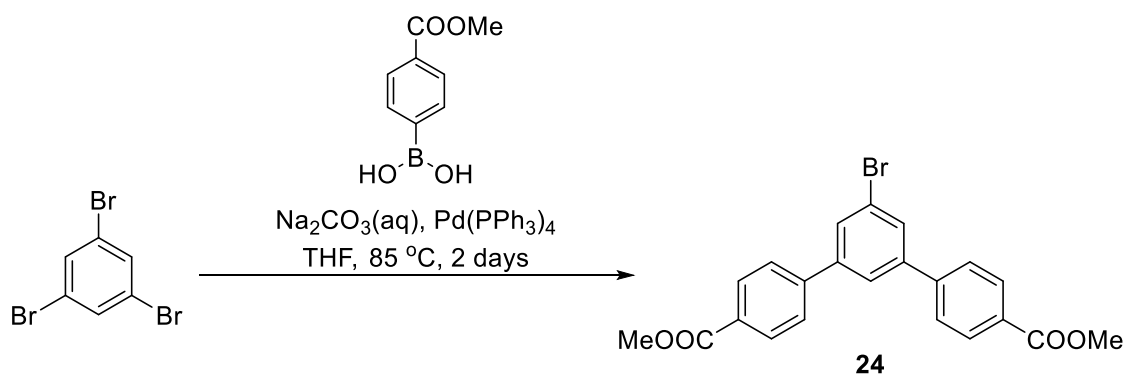
(22). In a round-bottom flask, 2-iodobenzoic acid (IBX) (47 mg, 0.168 mmol) was added in a mixture of compound **21** (20 mg, 0.028 mmol) dissolved in DMSO (3 mL). The mixture was stirred at rt for 1 h. After the reaction was completed, H₂O was added and the product was extracted with EtOAc. The combined organic layers were washed with aqueous NaHCO₃ as well as with brine and dried over anhydrous MgSO₄. Then the solvent was evaporated under vacuum to give product **22** as a white solid (12 mg, 61% yield).

¹H NMR (500 MHz, CDCl₃): δ = 9.77 (s, 6H), 7.43 (d, *J*=8.2 Hz, 12H), 7.01 (d, *J*=8.2 Hz, 12H) ppm; ¹³C NMR (125 MHz, CDCl₃): δ = 191.5, 145.1, 139.7, 134.3, 131.5, 128.7 ppm.

Synthesis of compounds 26 and 27

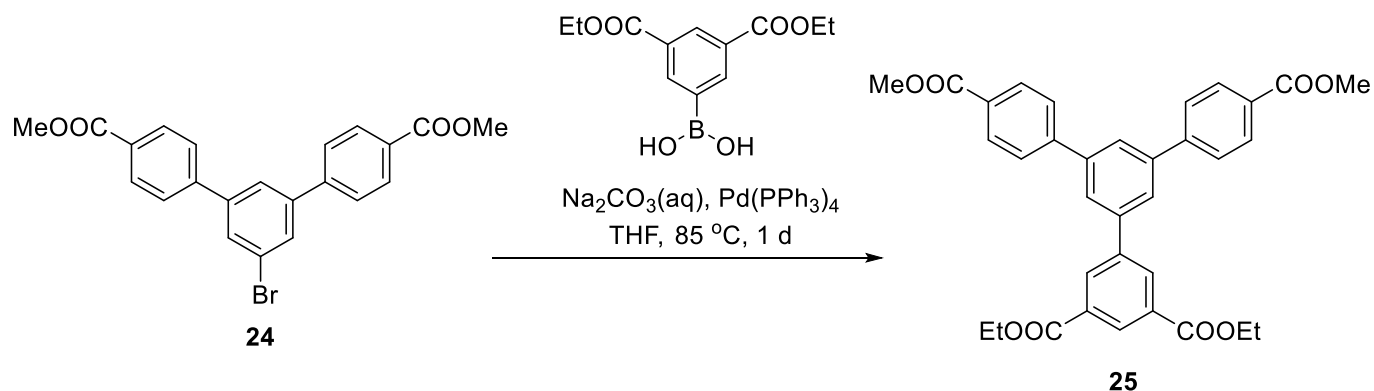


Reagents and conditions: (a) 4-Methoxycarbonylphenylboronic (2 equiv.), aqueous Na_2CO_3 (2 M), $\text{Pd}(\text{PPh}_3)_4$, dry THF, Ar atmosphere, 85 °C, 2d; (b) 3,5-bis(ethoxycarbonyl)phenylboronic acid (1 equiv.), Na_2CO_3 (2 M), $\text{Pd}(\text{PPh}_3)_4$ (3.6 equiv.), dry THF, Ar atmosphere, 85 °C, 1d; (c) THF, MeOH, aqueous NaOH (5 N), 85 °C, 1d; (d) bis(pinacolato)diboron (1.1 equiv.), $\text{Pd}(\text{dppf})\text{Cl}_2$ (10 equiv.), CH_3COOK (3 equiv.), dry DMF, Ar atmosphere 90 °C, 30 h.



(24). Under argon atmosphere, 1,3,5 tribromobenzene 4-methoxycarbonylphenylboronic acid (571 mg, 3.17 mmol), dry THF (40 mL), Na_2CO_3 (15 mL, 2 M) and $\text{Pd}(\text{PPh}_3)_4$ (80 mg, 0.04 mmol) were added into a two-neck flask. The reaction mixture was stirred and refluxed at 85 °C for 2 d. After cooling to rt, THF was removed under reduced pressure. The resultant crude solid was collected by filtration, washed with H_2O , dried in an oven and purified with a flash column chromatography (silica gel, petroleum ether EtOAc 10:1 \rightarrow 8:1) to afford product **24** as a white solid (270 mg, 40 % yield).

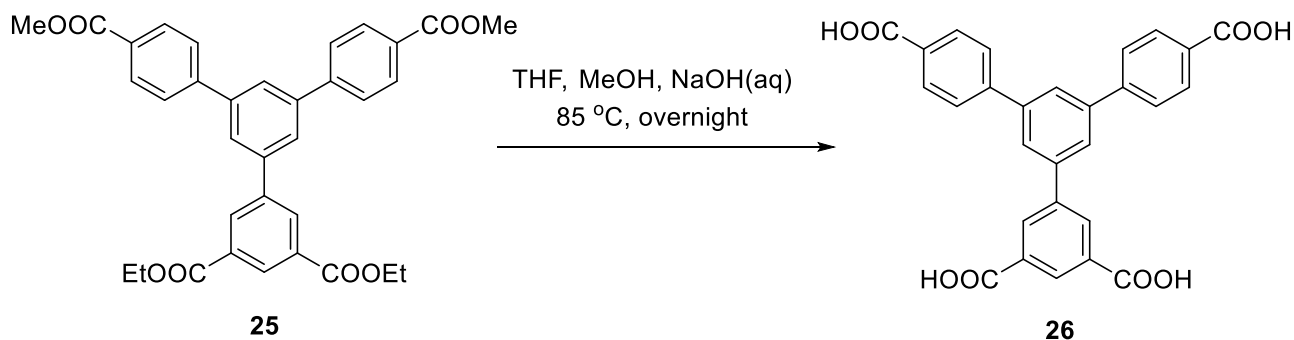
^1H NMR (500 MHz, CDCl_3): δ = 8.13 (d, $J=8.5$ Hz, 4H), 7.77 (d, $J=1.6$ Hz, 2H), 7.75(t, $J=1.6$ Hz, 1H), 7.68 (d, $J=8.5$ Hz, 4H), 3.96 (s, 6H) ppm; ^{13}C NMR (125 MHz, CDCl_3): δ = 166.7, 143.8, 142.7, 130.3, 129.8 (2C), 127.2, 125.0, 123.6, 52.2 ppm.



(25). Under argon atmosphere, compound **24**, 3,5-bis(ethoxycarbonyl)phenylboronic acid (174.5 mg, 0.66 mmol), THF (30 mL), Na_2CO_3 (10 mL, 2 M) and $\text{Pd}(\text{PPh}_3)_4$ (30 mg, 0.015 mmol) were added into a two-neck flask. The reaction mixture was stirred and refluxed at 85 °C for 1 d. After cooling to rt, THF was removed under reduced pressure. The resultant crude solid was collected by filtration, washed with H_2O , dried in an oven and purified with a

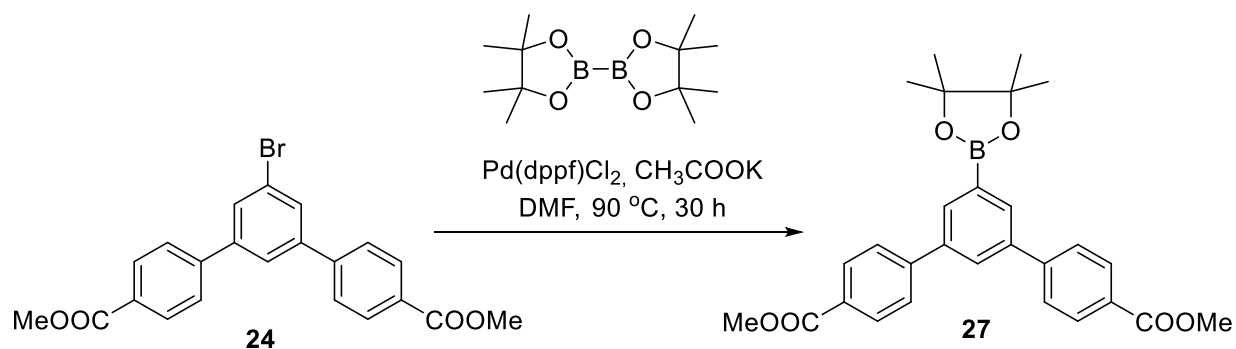
flash column chromatography (silica gel, petroleum ether EtOAc 10:1 → 4:1) to afford product **25** as a white solid (160 mg, 64 % yield).

^1H NMR (500 MHz, CDCl_3): δ = 8.71 (t, $J=1.5$ Hz, 1H), 8.52 (d, $J=1.5$ Hz, 2H), 8.16 (d, $J=8.4$ Hz, 4H), 7.87 (s, 3H), 7.77 (d, $J=8.4$ Hz, 4H), 4.46 (q, $J=7.1$ Hz, 4H), 3.96 (s, 6H), 1.45 (t, $J=7.1$ Hz, 6H) ppm; ^{13}C NMR (125 MHz, CDCl_3): δ = 166.8, 165.7, 144.8, 141.7, 141.3, 140.8, 132.3, 131.7, 130.2, 129.7, 129.5, 127.3, 126.1, 125.9, 61.6, 52.2, 14.3 ppm.



(26). In a round bottom flask, THF (5 mL), MeOH (5 mL) and aqueous NaOH (5 mL, 5 N) were added to compound **25** (100 mg, 0.18 mmol). The reaction mixture was stirred and refluxed at 85 °C overnight. After the reaction was completed, MeOH and THF were evaporated under vacuum. The residual mixture was acidified with HCl (3 M), until pH=3. Then the mixture was filtrated, washed with H_2O and dried in an oven to obtain the product **26** as a white powder (75 mg, 86% yield).

^1H NMR (500 MHz, DMSO-d_6): δ = 8.56 (d, $J=1.3$ Hz, 2H), 8.52 (t, $J=1.6$ Hz, 1H), 8.09 (m, 11H) ppm; ^{13}C NMR (125 MHz, DMSO-d_6): δ = 167.2, 166.6, 143.8, 140.9 140.8 (2C), 140.4, 132.3, 132.0, 130.1, 129.9, 127.5, 127.4, 125.6 ppm.

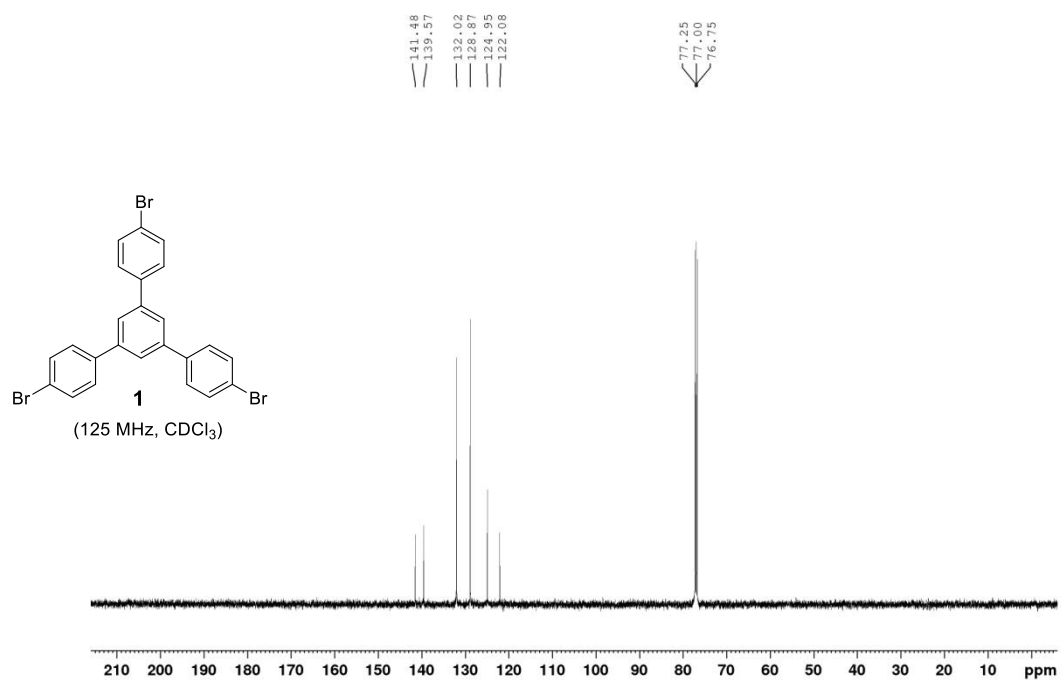
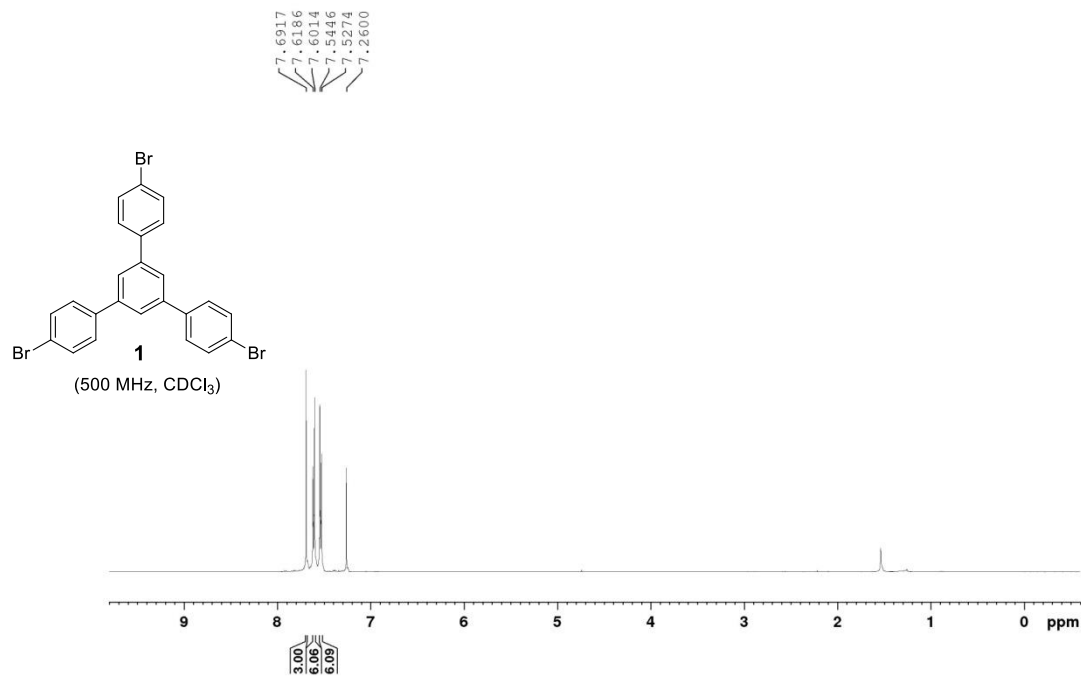


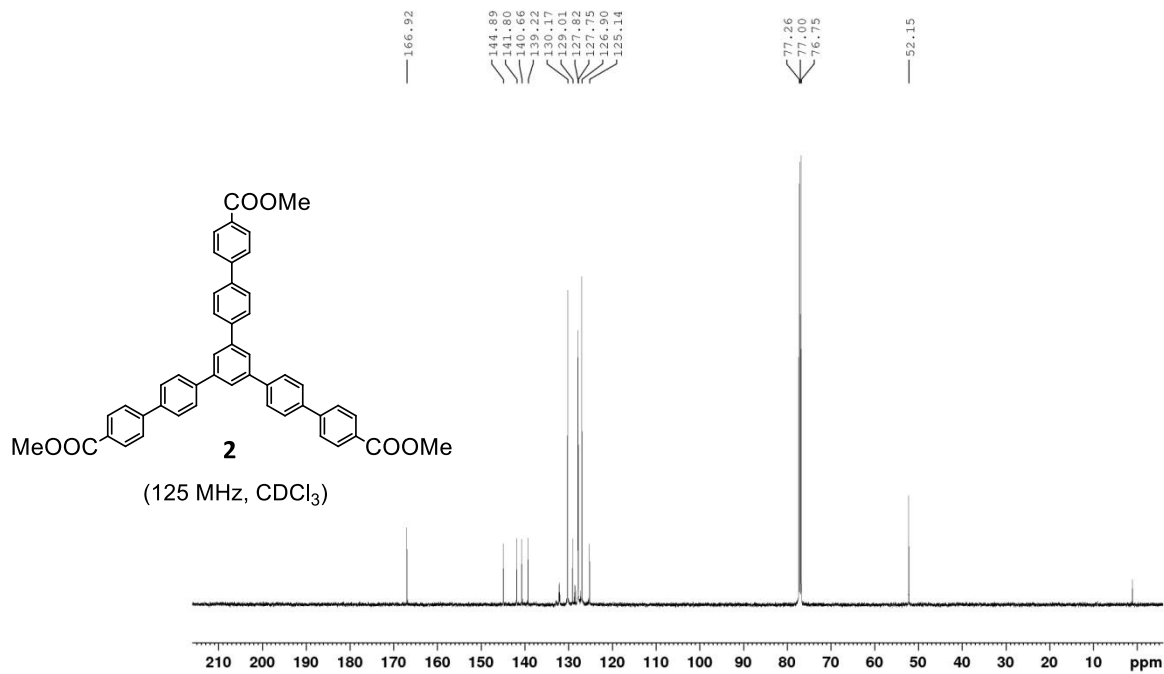
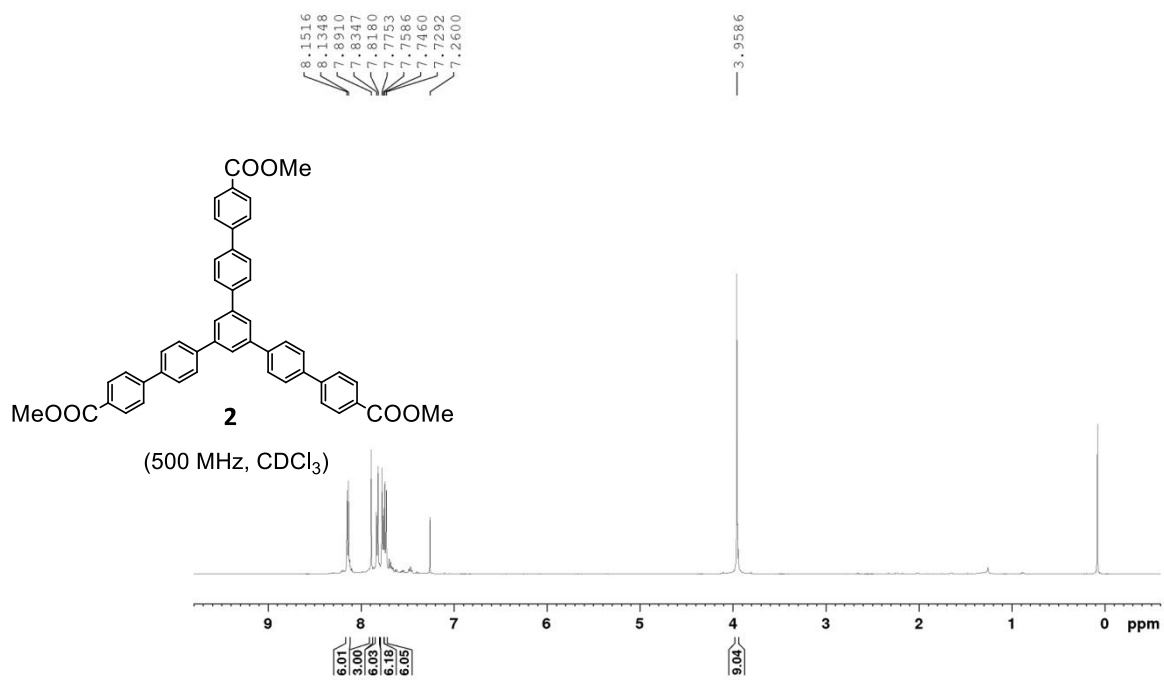
(27) In a two-neck bottom flask, compound **24** (150 mg, 0.350 mmol), bis(pinacolato)diboron (97.7 mg, 0.39 mmol), [1,1'-bis(diphenylphosphino)ferrocene]-dichloropalladium (II) (25.6 mg, 0.035 mmol) and CH₃COOK (103 mg, 1.05 mmol) were added. After, degassed dry DMF (5 ml) was added and the solution was stirred under argon atmosphere at 90 °C for 30 h. The reaction mixture was poured into H₂O and extracted with EtOAc. The solvent was removed under reduced pressure and the crude solid was purified with column chromatography (silica gel, petroleum ether EtOAc 10:1 → 4:1) to afford product **24** as a white solid (10 mg, 6 % yield).

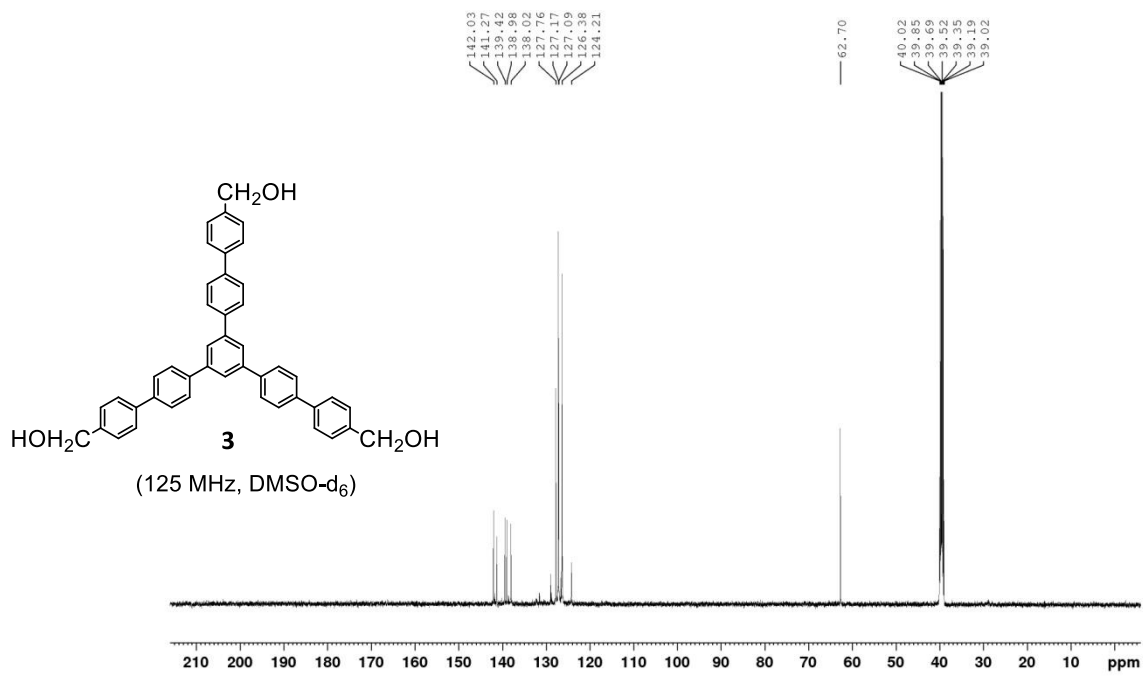
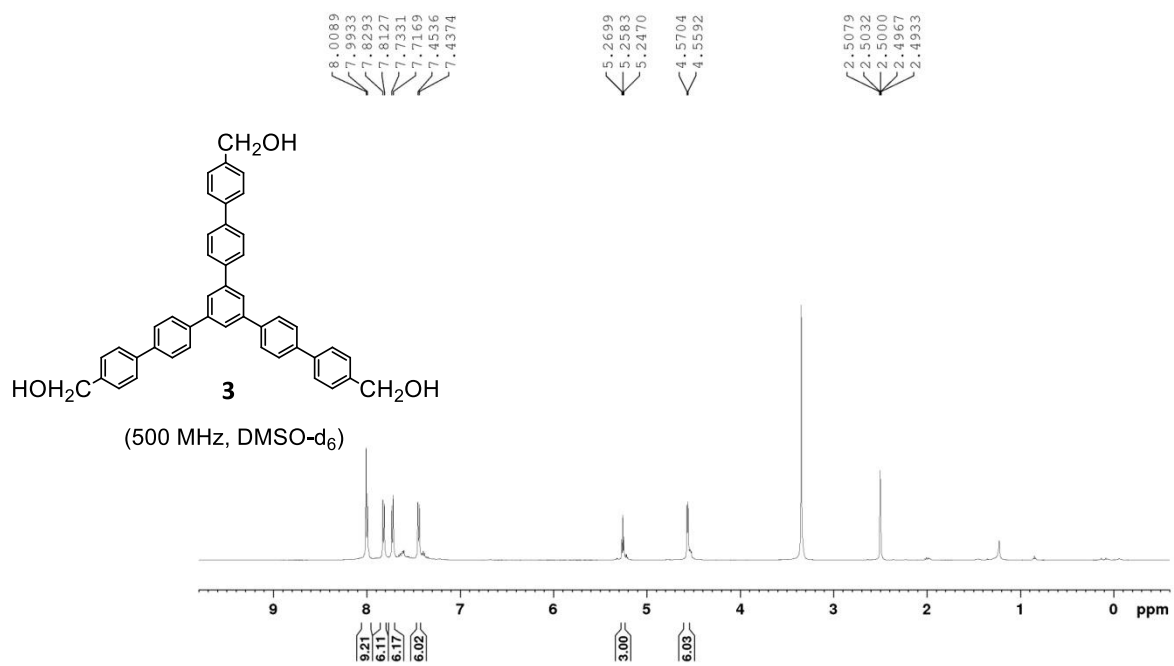
¹H NMR (500 MHz, CDCl₃): δ = 8.12 (d, *J*=8.4 Hz, 4H), 7.68 (d, *J*=8.4 Hz, 4H), 7.4 (t, *J*=1.4 Hz, 1H), 7.13 (d, *J*=1.4 Hz, 2H), 3.95 (s, 6H), 1.27 (s, 12H) ppm; ¹³C NMR (125 MHz, CDCl₃): δ = 167.0, 145.1, 142.3, 130.1, 129.3, 127.1, 118.8, 114.1, 83.2, 52.2, 24.8 ppm; ¹¹B NMR (160.4 MHz, CDCl₃): δ = 22.45 ppm.

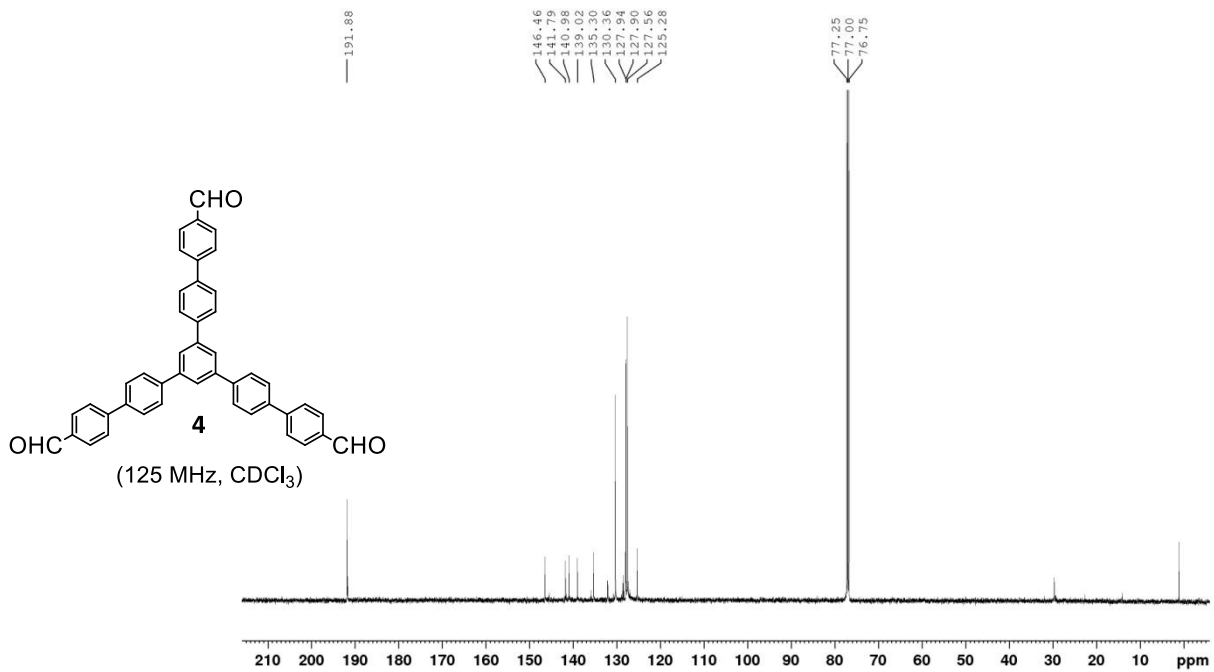
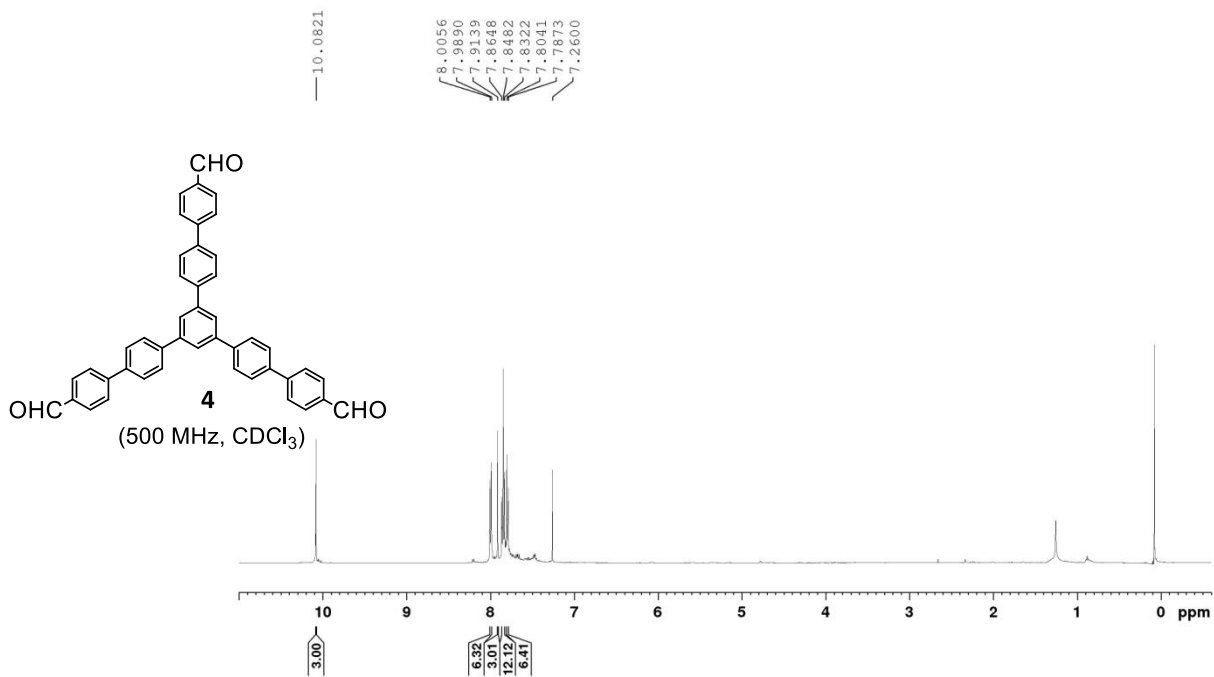
Appendix 2

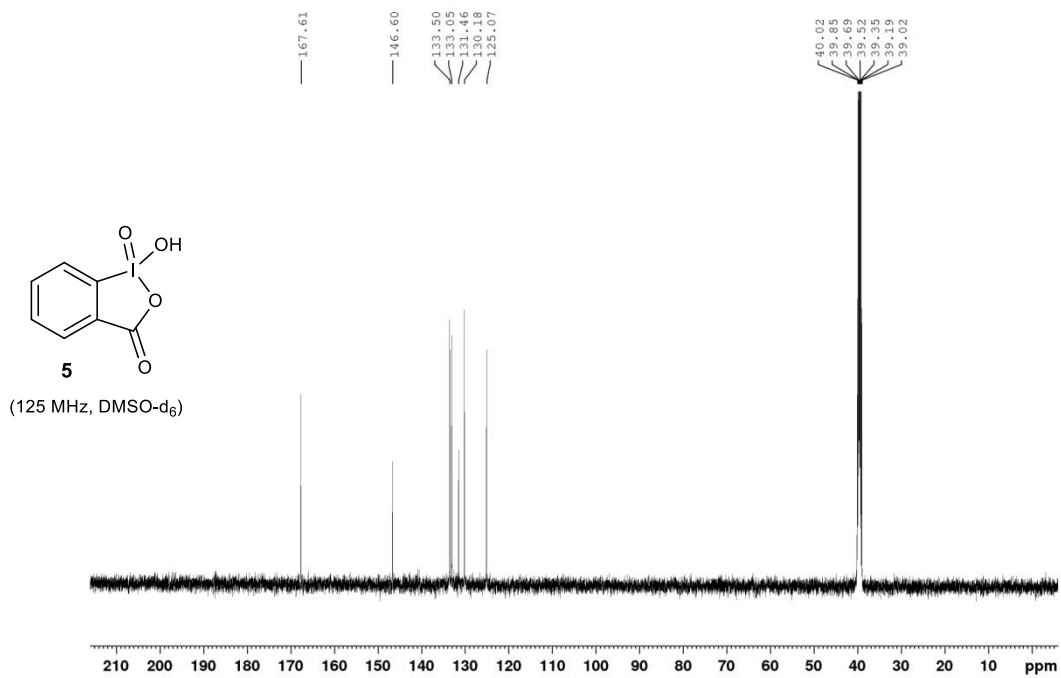
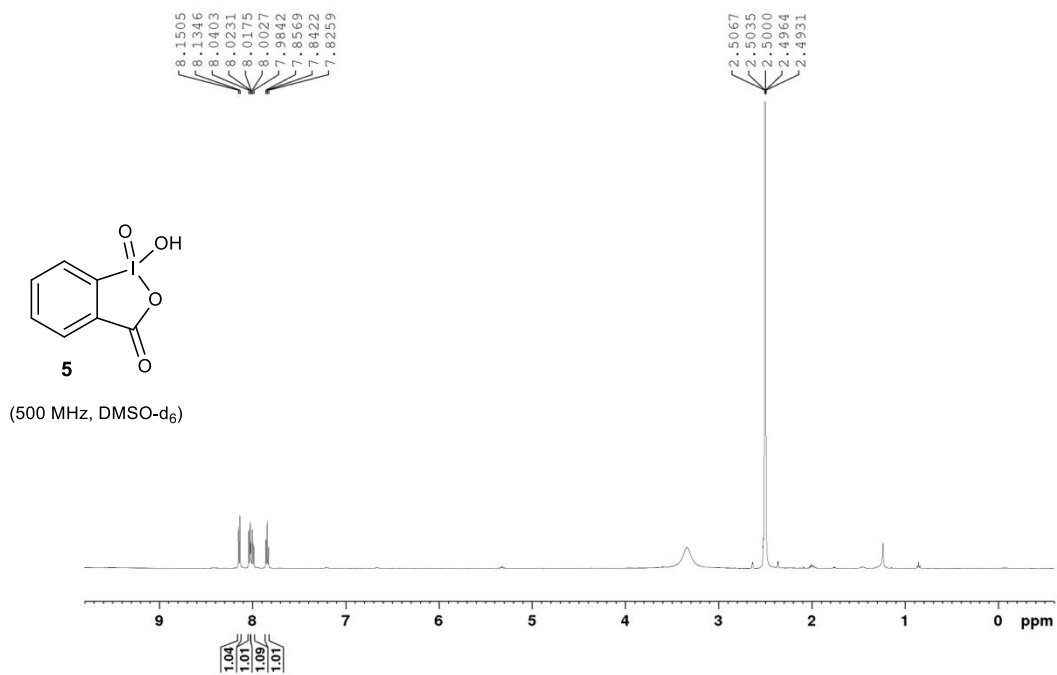
Copies of ^1H and ^{13}C NMR spectra

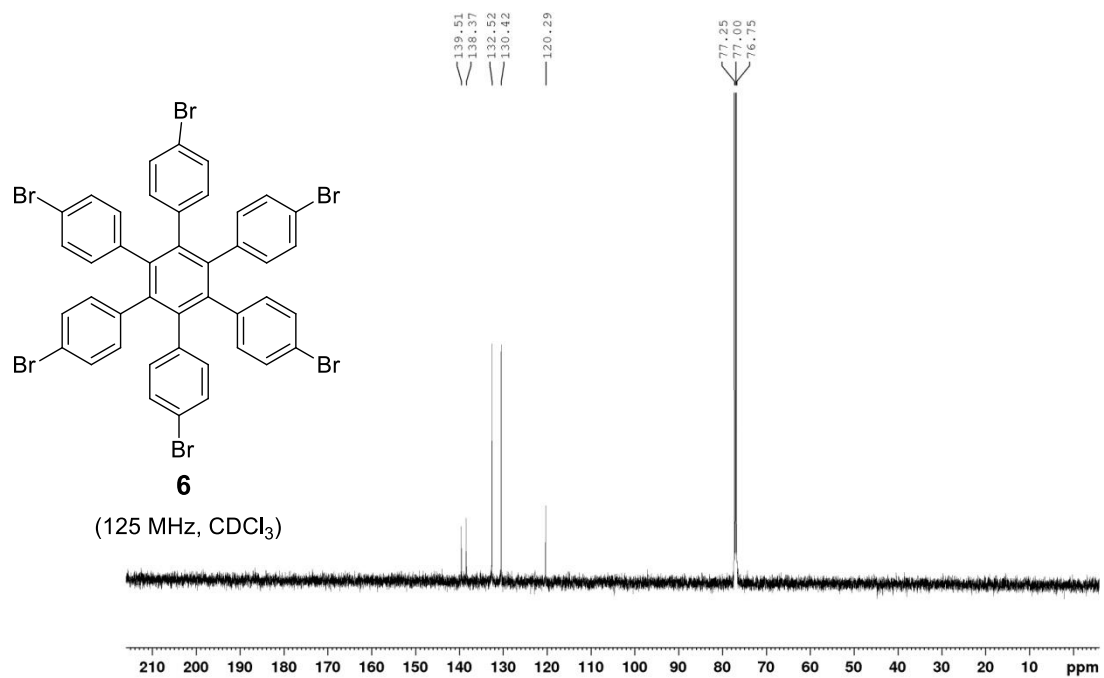
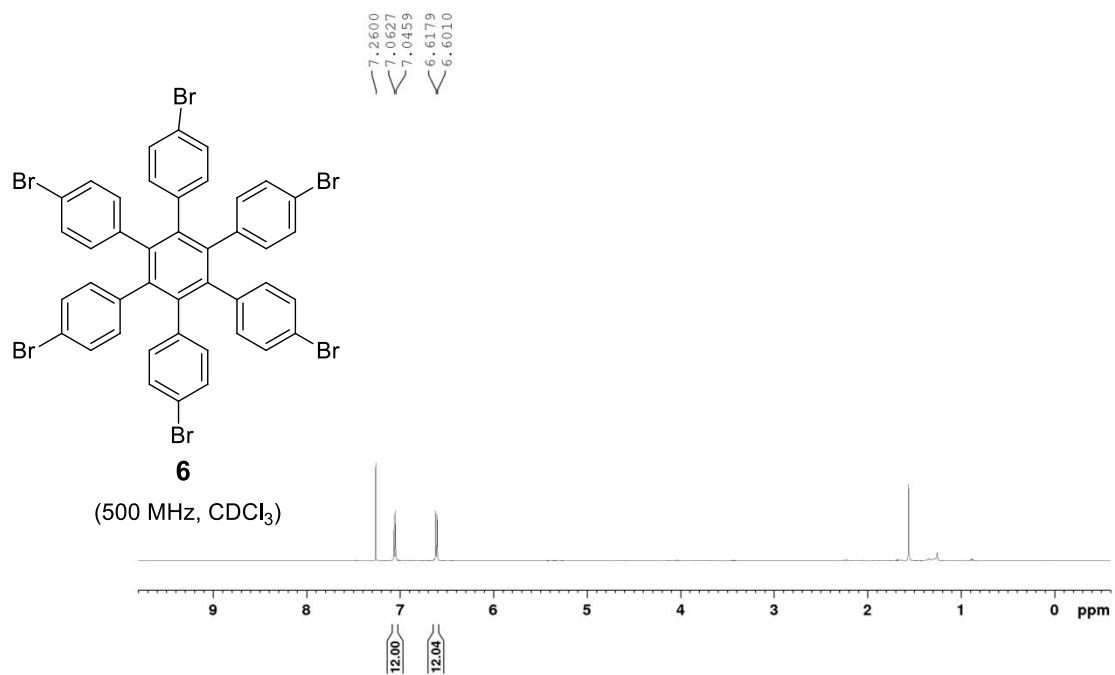


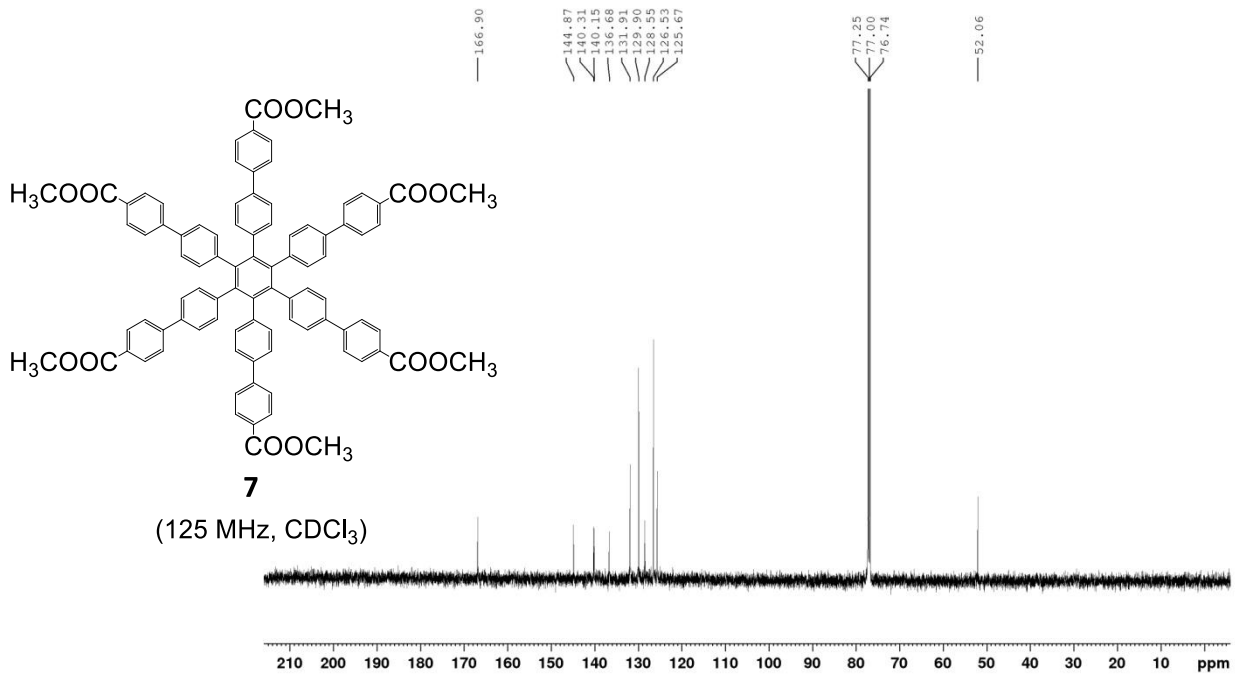
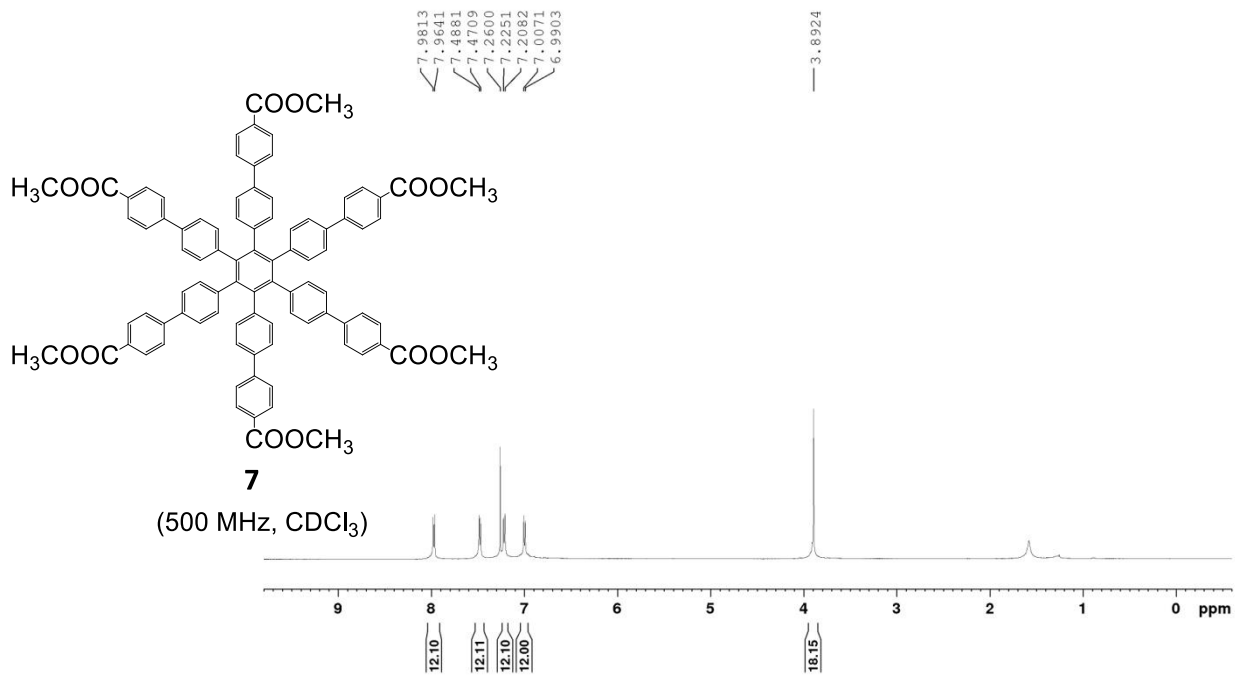


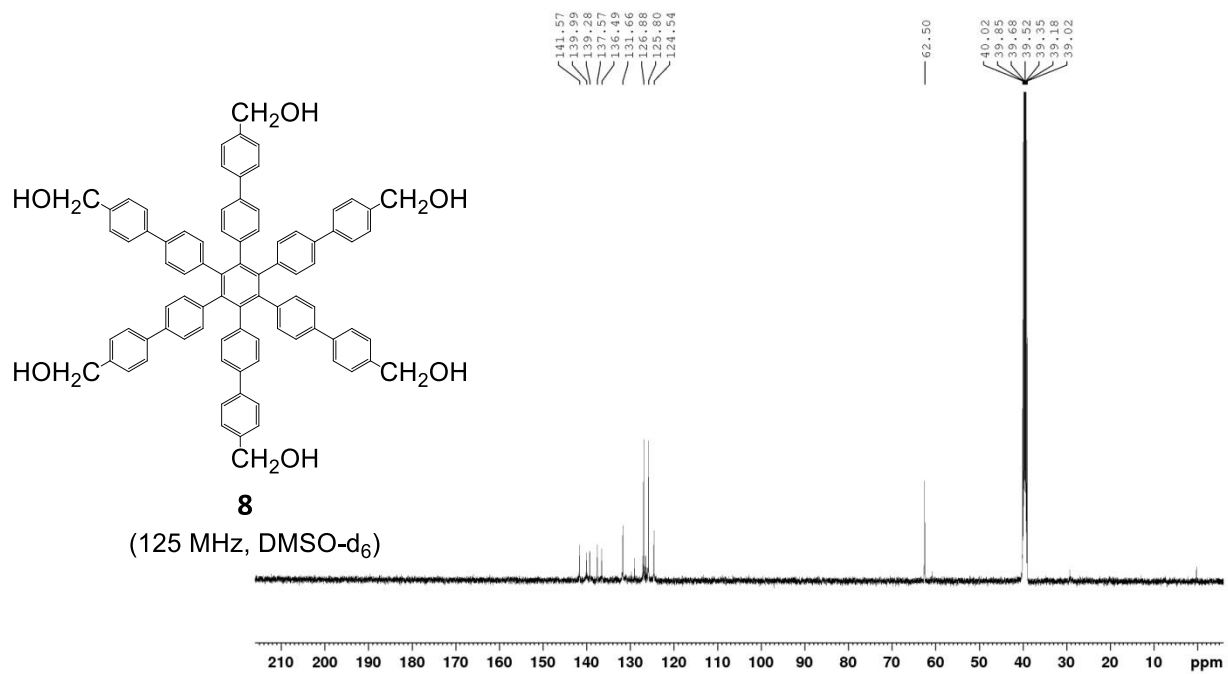
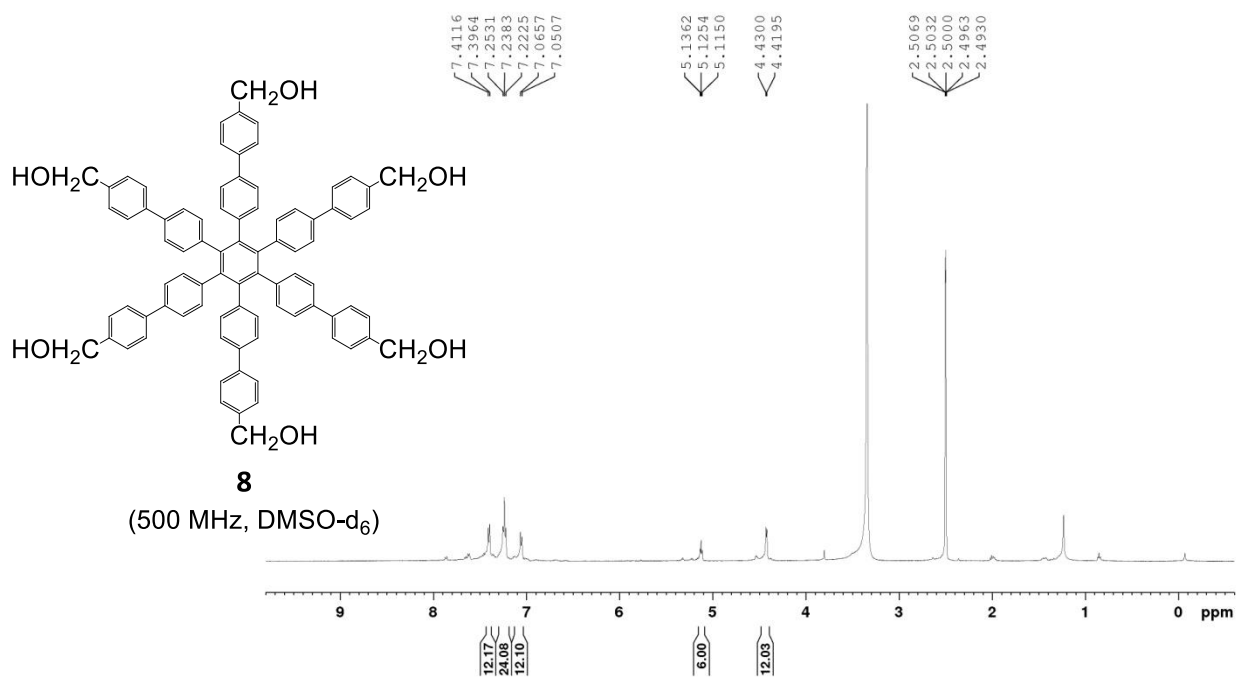


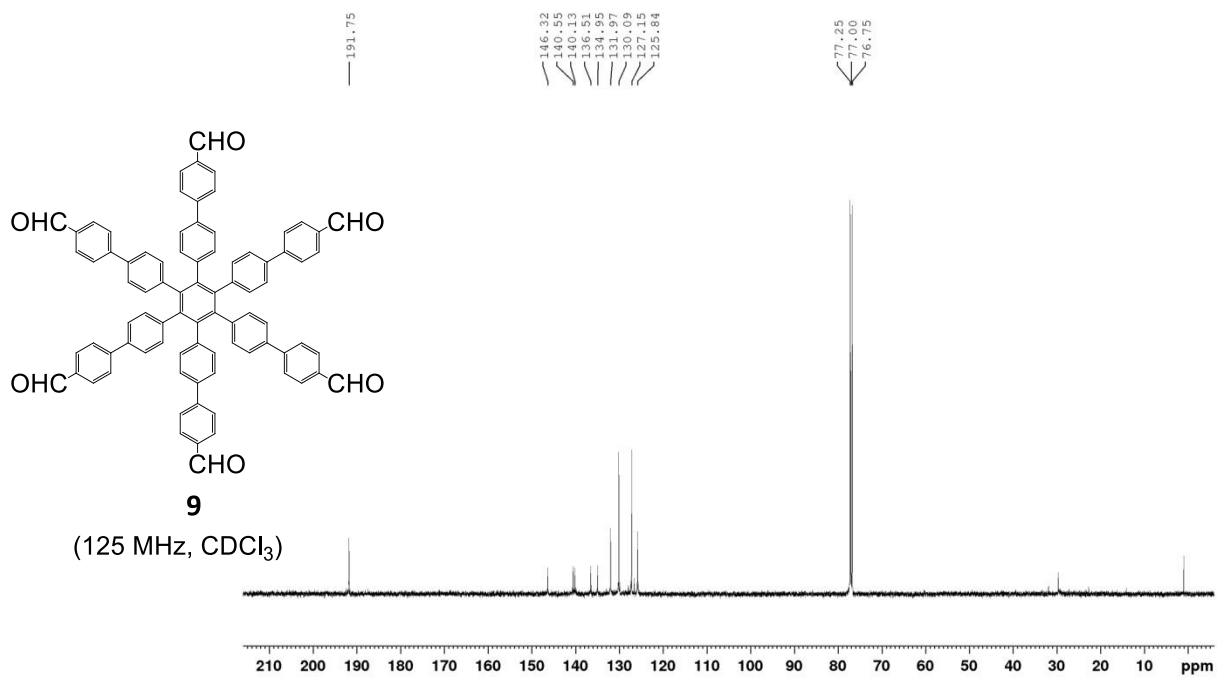
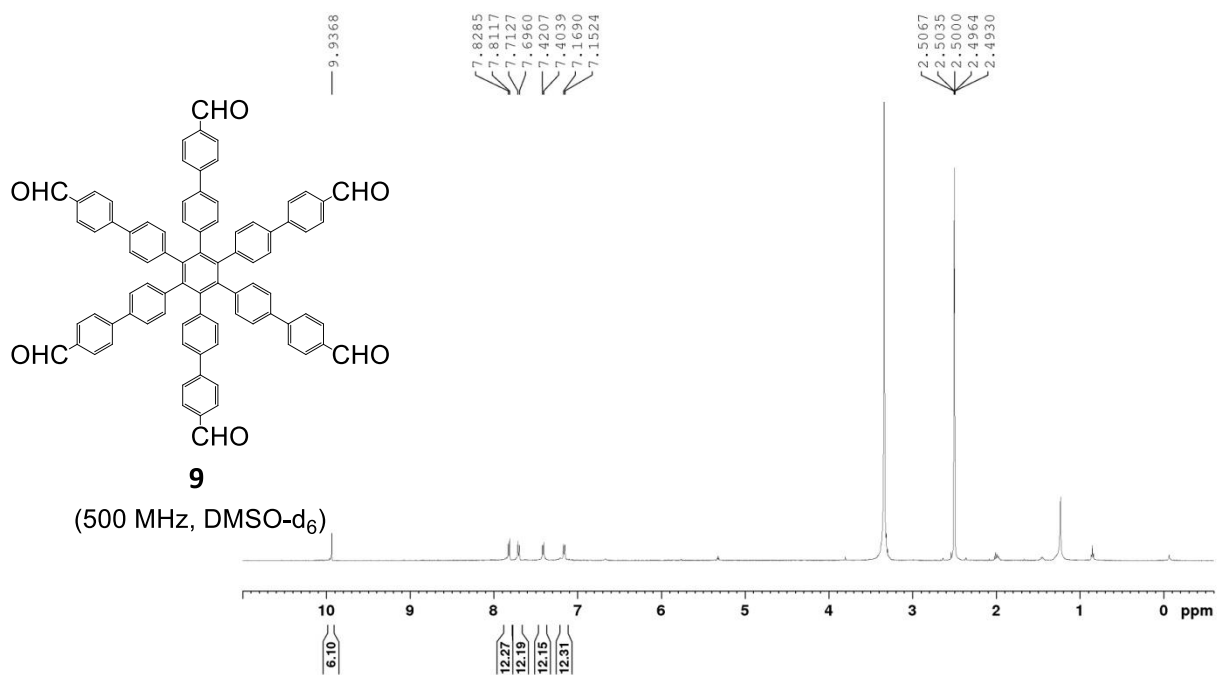


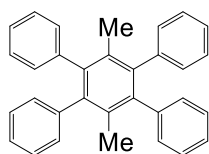






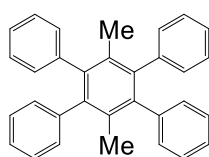
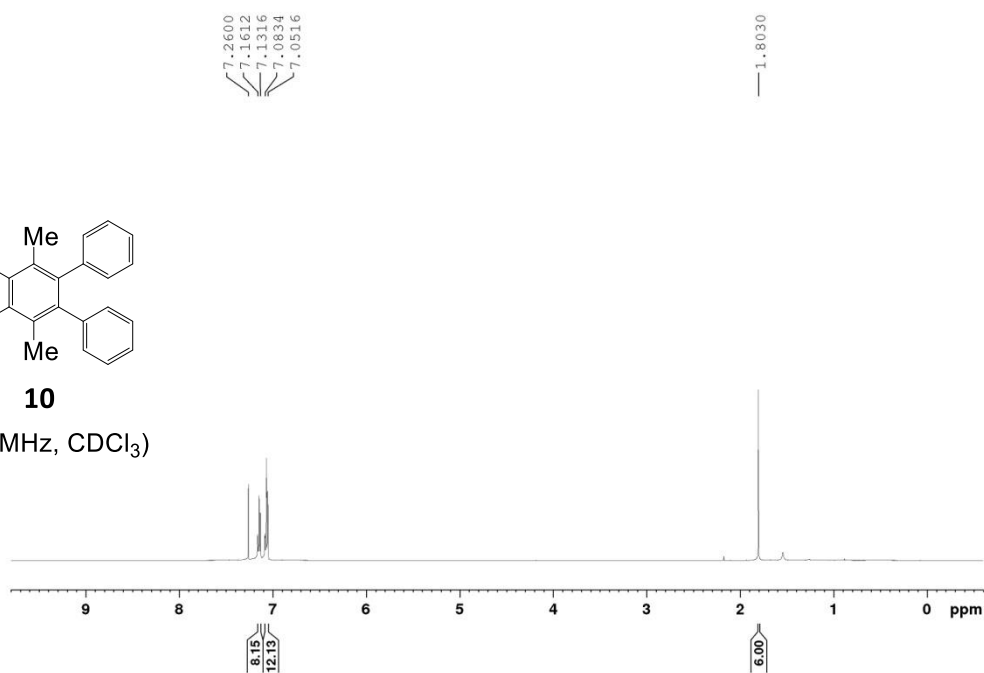






10

(500 MHz, CDCl₃)



10

(125 MHz, CDCl₃)

